공학박사학위논문

Numerical Simulation of Dynamic Soil-Pile-Structure Interactive Behavior Observed in Centrifuge Tests

원심모형시험에서 관측된 지반-말뚝-구조물 동적 상호작용의 수치 모델링

2014년 2월

서울대학교 대학원

건설환경공학부

권 선 용

Numerical Simulation of Dynamic Soil-Pile-Structure Interactive Behavior Observed in Centrifuge Tests

지도 교수 김 명 모

이 논문을 공학박사 학위논문으로 제출함

2013 년 12 월

서울대학교 대학원

건설환경공학부

권 선 용

권선용의 공학박사 학위논문을 인준함

2013 년 12 월

위 원 장 _____ 정 충 기 _____ (인)

부위원장 _____ 김 명 모 _____ (인)

위 원 _____ 박 준 범 _____ (인)

위 원 _____ 황 대 진 _____ (인)

위 원 _____ 김 성 환 _____ (인)

Abstract

Numerical Simulation of Dynamic Soil-Pile-Structure Interactive Behavior Observed in Centrifuge Tests

Kwon, Sun Yong

Department of Civil & Environmental Engineering

The Graduate School

Seoul National University

Being able to predict the dynamic behavior of the pile foundations used in many civil structures is a very important matter because it widely affects the performance of the entire structure. Several methods are used to evaluate the seismic behavior of such piles, including site investigation, physical model tests, and numerical modeling. The effectiveness of numerical modeling has recently become more important in light of the time-consuming, procedurally complex, and expensive nature of physical model tests. Most previous research which simulated the seismic behavior of piles using the numerical modeling method adopted a simplified approach which is relatively easy to apply but can lead to inaccurate results due to the many assumptions such an approach requires. On the other hand, three-dimensional continuum modeling is a computationally complex and time consuming process but is the most

direct approach and able to obtain reliable and accurate results. Therefore, in this study, three-dimensional continuum modeling is used to evaluate dynamic soil-pile structure interaction under earthquake loading.

First, three-dimensional dynamic numerical modeling based on the finite difference method was carried out to simulate the dynamic behavior of a soil-pile-structure system in dry sand observed in dynamic centrifuge model tests performed by Yoo (2013). The three-dimensional numerical model was formulated in a time domain to effectively simulate the nonlinear behavior of soil using the commercial finite difference code, FLAC3D. As a modeling methodology, the Mohr-Coulomb model was adopted as a soil constitutive model. Soil nonlinearity was considered by adopting a hysteretic damping which can simulate the nonlinear reduction of soil shear modulus according to shear strain. An interface model which can simulate slip and separation between soil and piles was used and the stiffness of the interface material was determined with consideration given to the nonlinear relation of soil by means of a user-defined FISH function. A simplified continuum modeling method was adopted as a boundary condition. In this method, the soil medium was divided into a near field and a far field, the latter of which is not affected by soil-pile-structure interaction (SPSI). The mesh was created only for the near field to reduce the computing time. A far-field response was applied as a boundary condition at the boundary of the near field.

Calibration of the proposed modeling method was carried out to minimize error and increase the reliability of the results generated by the numerical simulation. The results of a centrifuge test were used to demonstrate the capability of the model to reliably analyze a pile foundation

under earthquake loading. The peak bending moment and maximum lateral pile displacement along the depth obtained from centrifuge tests and the numerical model showed good agreement for various input conditions. Validation of the proposed modeling method was performed using the test results from other cases to verify the applicability of the numerical model. The dynamic pile responses produced by the numerical simulation also showed good agreement with the test results in various conditions. Based on the calibration and validation process, the applicability of the proposed modeling method for various conditions was verified.

A parametric study for various conditions was performed to investigate the dynamic behavior of a pile foundation by varying the weight of the superstructure, relative density, pile length, and pile head fixity. Parametric studies demonstrated which parameters have a considerable affect on the dynamic behavior of a pile foundation in dry soil deposits.

A three-dimensional numerical simulation of dynamic SPSI in a liquefiable condition was also carried out. In order to simulate the development of pore water pressure according to shear deformation of the soil for the liquefied state, the Finn model was adopted. The Finn model is one of the models that adopt an effective stress method so that the liquefaction at each location can be directly recorded in real time. The Finn model was combined with the standard Mohr-Coulomb criteria used in the dry condition.

The calibration of the proposed modeling method was carried out by comparing the results with those of the centrifuge test performed by Wilson (1998). The excess pore pressure ratio, pile bending moment, and pile head displacement-time histories calculated by the numerical model agreed

reasonably well with the test results. The validation of the proposed method was later performed using the test results from another case. The calculated dynamic pile responses also show generally good agreement with measured pile responses of another case. Based on the calibration and validation procedure, it was confirmed that the proposed modeling method can properly simulate the dynamic behavior of a soil-pile system in liquefiable soil deposits.

A parametric study was carried out to provide better insight into the dynamic behavior of pile foundations embedded in liquefiable sand under varying frequencies of input excitation, thicknesses of the liquefiable layer, relative densities, and weights of the superstructure. Parametric studies demonstrated which parameters have a considerable effect on the dynamic behavior of a pile foundation in liquefiable soil deposits. Moreover, the results obtained from parametric studies confirmed availability and applicability of the proposed numerical model comparing with the results from previous researches.

Keywords : Numerical simulation, Dynamic soil-pile-structure interaction, Centrifuge tests, FDM, Liquefaction

Student Number : 2008-21012

TABLE OF CONTENTS

LIST OF TABLES

LIST OF FIGURES

1. Introduction

1.1 Background

Being able to predict the dynamic behavior of the pile foundations used in many civil structures is a very important matter because it widely affects the performance of the entire structure. Therefore, many geotechnical engineers have tried to estimate the seismic response of piles, and several methods have been used to predict dynamic pile performance. However, the dynamic analysis of a soil-pile system is a very complicated procedure, different from static cases, and is affected by many factors such as soil nonlinearity and dynamic soil-pile interaction. Such analysis is typically carried out by one of three means: a site investigation, a physical model test, and numerical modeling.

A site investigation is a relatively primitive and direct approach which primarily involves observing the distribution of the failure patterns and the settlement, lateral displacement, and buckling of piles. During the Niigata earthquake of 1964, the piles supporting many superstructures failed due to excessive lateral displacement and buckling induced by the liquefaction of the surrounding soils. According to Hamada (1983), the ground vicinity of a four-story building moved approximately 1.1 m, and the maximum lateral displacement of concrete piles with a diameter of 35 cm and a length of 6 m to 9 m was around 70 cm. According to Ishihara (1997), numerous piles suffered multiple cracks, with the greatest damage being at a depth of approximately 8

to 14 m, which corresponds to the depth of the interface zone between the liquefied fill deposit and the underlying silty soil layer. Mori et al. (1993) conducted an excavation survey and internal inspection of the damaged piles of a silo which suffered severe damage due to the Hokkaido Nansei-Oki Earthquake of 1993 and concluded that damage usually occurs at three different locations: at the pile head (for fixed-head piles), at a depth of 1 m to 3 m below the pile cap (for free-head piles) and at the interface of the liquefied and non-liquefied layers. These findings have been confirmed in several other studies including Shamoto et al. (1996), Onishi et al. (1996), and Tachikawa et al. (1998).

Physical model tests include 1 g shaking table tests and dynamic centrifuge tests of soil-pile-structure systems in which the seismic response of a soil-pile system and dynamic SPSI interaction are investigated. Boulanger et al. (1999) conducted a series of centrifuge tests on single piles in order to observe the p-y behavior of piles embedded in dry sands. Wilson (1998) performed centrifuge tests on single piles and groups of piles embedded in liquefying sands. The centrifuge test results indicated that the p-y curves were highly time-dependent in liquefiable soils; the lateral resistance on the pile decreased by increasing pore water pressure; and that there was very little lateral resistance on the pile even under large relative displacements. Furthermore, Yao et al. (2004) used large shaking table tests to conclude that the transient state prior to soil liquefaction was important in the design of piles because the dynamic earth pressure showed a peak response during this state. Other researchers such as Abdoun and Dobry (2002), Bhattacharya et al. (2004), Suzuki et al. (2005), Tamura and Tokimatsu (2005), Dungca et al.

(2006), Han (2006), Yang (2009), Yang et al. (2011) and Yoo (2013) have also investigated the seismic behavior of pile foundations using physical model tests.

The effectiveness of numerical modeling has recently become more important in light of the time-consuming, procedurally complex, and expensive nature of physical model tests. Most researchers and designers prefer to use simplified approaches such as one-dimensional Winkler methods for the dynamic analysis of pile foundations because two- and three-dimensional continuum modeling are computationally complex and time-consuming procedures. Matlock et al. (1978), Kagawa and Kraft (1980), Novak and Sheta (1980), and Nogami et al. (1992) have developed such methods. Kagawa (1992), Yao and Nogami (1994), Fujii et al. (1998) and Liyanapathriana and Polous (2005) developed this method to take into account the liquefaction of the surrounding soil during the process of analysis. Miwa et al. (2005), Chang et al. (2007), Tahghighi and Konagai (2007), and Liyanapathriana and Polous (2009) have all shown that the one-dimensional methods are capable of predicting the maximum lateral displacement and the peak bending moment of piles with relative accuracy. However, such approaches make numerous assumptions and are not able to simulate the prototype accurately because it is difficult to estimate accurate values for the spring and dashpot coefficients, which change considerably over time. Finn and Fujita (2002), Klar and Frydman (2004), Oka et al. (2004), Martin and Chen (2005), Uzuoka et al. (2007), Cheng and Jeremic (2009), Comodromos et al. (2009), Kim (2011) and Kim et al. (2012) used three-dimensional models in order to simulate the dynamic behavior of piles, each of whose

models possess varying degrees of accuracy and certainty in the predictions they generate. However, little research has been done using a three-dimensional continuum model, with some of the previous research done using such a model having been calibrated only for a 1 g shaking table test which is unable to reproduce field-confining pressure under prototype conditions. Therefore, calibration for centrifuge tests is needed to increase the reliability of the numerical model. Furthermore, in some of these studies which treated liquefaction related problems, a fully coupled formulation (a u-P or u-P-U formulation) has been employed to address liquefaction-related problems, while in others an uncoupled formulation, in which the soil skeleton displacements and pore water pressure generation are computed separately, has been used. According to these studies, three-dimensional continuum modeling is able to simulate most of the phenomena which have been observed in the field more accurately than simplified approaches can and reliably draws the dynamic response of piles directly in the time domain. Therefore, three-dimensional continuum model which can properly simulate dynamic soil-pile-structure interaction for both dry and liquefiable condition is necessary. For liquefiable condition, development of pore water pressure according to the shear deformation of soil element has to be directly captured by proper model considering liquefaction in real time to obtain reliable results.

For the present study, a numerical simulation of the dynamic SPSI for dry and liquefiable conditions observed in centrifuge tests was carried out. A commercial FDM code, FLAC3D, was used for the numerical simulation tool and appropriate modeling methodologies were proposed for a soil-pile system embedded in dry and liquefiable soil deposits. The calibration and validation

of the proposed modeling method was performed by comparing the computed results with centrifuge test results. Based on the verification of the applicability of the proposed model, a parametric study for various conditions was carried out to investigate the dynamic behavior of the piles. For dry soil, parametric studies were performed varying the weight of the superstructure, length of the piles, relative density, and pile head fixity. For liquefiable soil, parametric studies were performed varying the frequency of the input excitation, thickness of the liquefiable layer, relative density, and weight of the superstructure. The results obtained from parametric studies confirmed availability and applicability of the proposed numerical model comparing with the results from previous researches.

1.2 Objectives

The specific objectives of this study are to:

(i) Establish a modeling methodology and validate by comparing internal pile responses both in dry and liquefiable soil deposits

(ii) Investigate the dynamic behavior of piles for various conditions via parametric studies

For the modeling methodology, the nonlinear behavior of soil under strong earthquake loading was considered, slip and separation between the soil and piles were simulated properly. Simplified continuum modeling was adopted as a boundary condition to reduce the calculation time while maintaining accuracy. The generation of excess pore pressure due to shear deformation of the soil element during liquefaction was directly captured in

real time.

Verification of the proposed model was performed by comparing computed internal pile responses with measured pile responses. Through the process of calibrating and validating the proposed modeling method, the applicability of the numerical model for various cases was verified and important dynamic characteristics of a soil-pile system under earthquake loading were captured and discussed.

Based on a validation of the numerical model, parametric studies for various conditions were carried out to investigate the dynamic behavior of pile foundations. In the dry soil condition, a parametric study was conducted while varying the weight of the superstructure, pile length, relative density, and pile head fixity to investigate the dynamic behavior of the piles. In the liquefiable soil condition, a parametric study was conducted while varying the frequency of input excitation, thickness of the liquefiable layer, relative density, and weight of the superstructure. From the parametric study for various conditions, the influence of many parameters on the seismic behavior of the soil-pile system could be established, providing insight into the dynamic behavior of piles embedded in dry and liquefiable soil deposits. And availability and applicability of the proposed numerical were confirmed comparing with the results from previous researches.

1.3 Dissertation organization

The dissertation consists of five chapters:

Chapter 1. Introduction – includes the background, research objectives and an organizational summary of the dissertation.

Chapter 2. Literature Review – Case histories about pile foundation damage due to earthquakes are reviewed for dry and liquefiable conditions. Previous studies on the numerical analysis of simplified approaches and three-dimensional continuum modeling for pile analysis in dry soil deposits are presented. Previous studies on the numerical analysis of pile foundations embedded in liquefiable soil deposits are discussed as well.

Chapter 3. Numerical Simulation for Dry Soil Deposits – First, a description of the test apparatus, materials, and test program for the centrifuge tests for the dry condition which is used as exact results of the prototype is given. This chapter also includes an explanation of the modeling methodology used for a numerical simulation of dynamic SPSI in dry soil deposits. A soil constitutive model, damping model, interface model, boundary condition, and pile model are presented for the given soil-pile system. The calibration and validation results of the proposed model generated by comparing computed results with measured

results are then presented. Based on the verification of the proposed numerical model, the results of the parametric studies for various conditions while varying the weight of the superstructure, pile length, relative density, and pile head fixity are presented.

Chapter 4. Numerical Simulation for Liquefiable Soil Deposits – This chapter includes a description of the test apparatus, material, and test program used for the centrifuge test for the liquefiable condition which is used as exact results of the prototype. A consideration of modeling methodology as it relates to liquefaction phenomena is presented and the formulation of a relationship between the development of excess pore pressure and shear deformation of soil is explained. The calibration and validation results of the proposed model generated by comparing the computed results with the measured results are then presented. Finally, the results of the parametric studies for various conditions while varying the frequency of input excitation, thickness of liquefiable layer, relative density, and weight of the superstructure are presented.

Chapter 5. Conclusions and recommendations – are presented.

2. Literature Review

2.1 Introduction

Many researchers have tried to predict and investigate failure pattern and seismic behavior of pile foundations under strong earthquake. Site investigation, a.k.a. field observation is the representative and direct approach for investigating failure pattern and damage of pile. It mainly investigates the distribution of the failure pattern, settlement, lateral displacement of piles, etc. However, this is somewhat passive approach which is carried out after damage occurs already. If dynamic behavior of pile foundation is predicted and proper seismic design is conducted, massive damage from strong earthquake can be prevented. There are several approaches to predict seismic behavior of pile foundations, which are physical model tests and numerical modeling. According to advance of computing devices such as PC, effectiveness of numerical modeling tools becomes more important and prominent nowadays in the light of potential disadvantages of physical model tests. Therefore in this chapter, literature reviews are focused on previous researches about numerical simulation for dynamic pile behavior. And previous researches about several field observations are reviewed also to identify general failure pattern and damage in the field.

2.2 Case histories of pile damage under earthquakes

Pile foundation damage has been a major issue which causes structure failure after the earthquakes. In the recent few decades the strong earthquakes occur and cause the severe damage of pile foundations such as the 1991 Costa Rica, 1994 Northridge, the 1995 Kobe, the 1999 Chi-Chi, the 2001 Seattle, 2010 Chile, 2011 East-Japan Earthquake, etc. In this section, previous literatures about the case histories for pile damage under strong earthquakes are reviewed.

Priestley et al. (1991) studied extensive damages of pile foundation occurred during the Costa Rica Earthquake, 1991. Bridges over the rivers Vizcaya, Bananito, Estero Negro and La Estrella partially or completely collapsed. Several aspects seemed to have a responsibility of the damage. Pile lengths were probably inadequate and not founded on firm and stable materials.

Hamada (1992) reported severe pile damages during the Niigata earthquake, 1964. Severe damages to concrete piles of the foundation of a building in Niigata City were found by the excavation of the ground for construction twenty five years after the 1964 Niigata Earthquake. Figure 2.1 shows schematic drawing of the damage to two piles and their deformations. The pile of No. 2 was perfectly broken at the depth of about 2m from the top of the pile and also many horizontal bending cracks were observed at the lower elevation of the pile. On the other hand, in the case of the pile of No.1 bending cracks were observed only at the upper elevation. Figure 2.2 shows the soil condition in the neighborhood of the damaged building and the

estimated liquefied soil layer. The pile of No.2 was penetrated about 2 m into non-liquefiable layer under the estimated liquefied layer, while the penetration of the pile of No.1 into the underlying non-liquefiable layer is much shallower compared with that of the pile of No.2. It can be guessed that the damage at the lower elevation resulted from this difference of the penetration depth into the non-liquefiable layer. The ground surface nearby the building displaced 1 to 2 meters as shown in Figure 2.2. The numerals at the top of the vectors are the magnitude of the horizontal displacements. The ground in the southern-west side in front of the building moved about 1.5 m towards the building, while and the ground displacement reduced to about 50cm in the northern - east area behind the building.

Mori et al. (1994) conducted an excavation survey and internal inspection of the damaged piles of a silo which suffered severe damage due to the Hokkaido Nansei-Oki Earthquake, 1993. The investigation revealed that all the pile heads were damaged up to a depth of 3m, which made it easy to understand the peculiarity that enabled the failure of the pile heads to be classified in two patterns. The failure patterns of the pile heads are illustrated in Figure 2.3; one is shear failure or bending shear failure at pile head (Type A) with large shear deformation and the other is bending failure at a depth of 1 to 3m below sound pile top (Type B) with large tilting. The failure patterns and deformations of the 5 piles that had distinct failure are shown in Figure 2.4, attached with the soil profile of the site. This figure clearly shows that the piles after failure deformed largely at a depth corresponding to the bottom of reclaimed layer or the top of old sea bottom at the depth of around 7m. Damage to the piles along the depth is summarized in Figure 2.5. Damaged

portions of the piles were at three different locations: at the pile head, a depth of 1 to 3m below the pile cap, and at the depth corresponding to the bottom of the reclaimed layer. The first two locations mean the breakage points of Type-A and Type-B piles as mentioned earlier.

Ishihara (2004) reported the observations from detailed field survey of the ground and inspection of the damage to the piles. In this paper, a well-documented case study from the 1995 Kobe Earthquake highlighting the performance of pile foundations undergoing lateral spreading in liquefied deposits has been presented. Results of ground surveying and field inspection of pile depicting the damage features were also presented. It may seen in Figure 2.6 that the piles developed multiple cracks and suffered largest damage at a depth of approximately 8 to 14m, which corresponds to the depth of the interface zone between the liquefied fill deposit and underlying silty soil layer.

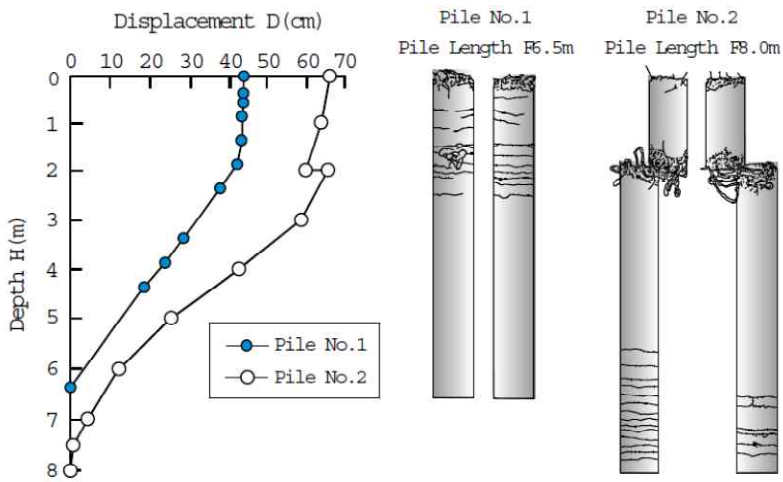

Figure 2.1 Damage to foundation piles and deformation (Hamada et al., 1992)

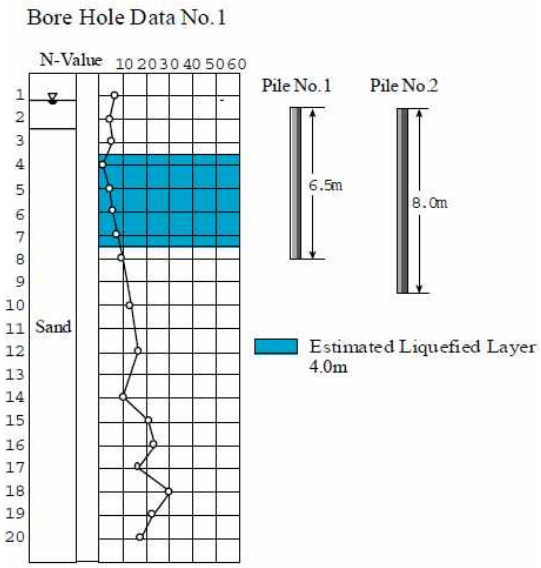

Figure 2.2 Soil condition and estimated liquefied soil building
(Hamada et al., 1992)

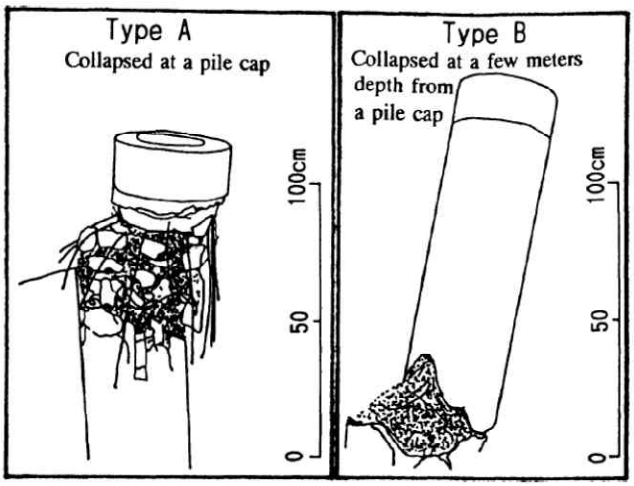

Figure 2.3 Faliure patterns of damaged pile heads (Mori et al., 1994)

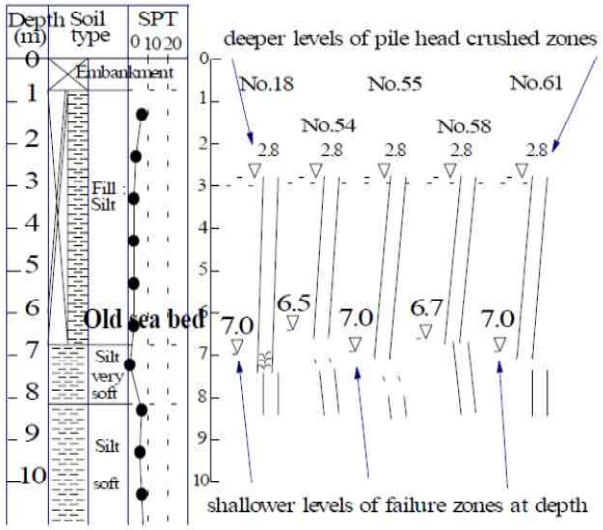

Figure 2.4 Pile failure at depth of old sea bottom (Mori et al., 1994)

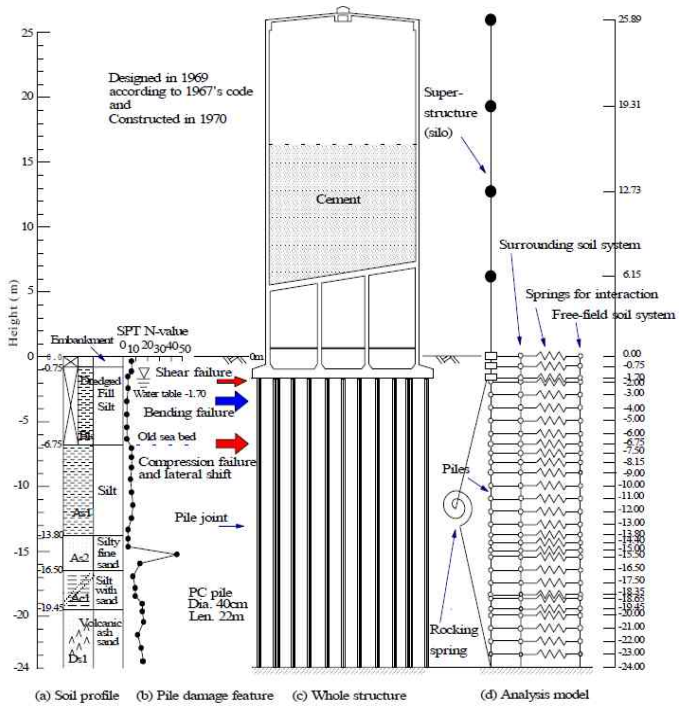

Figure 2.5 Soil profile, pile damage portions, silo-pile structure and analysis model (Mori et al., 1994)

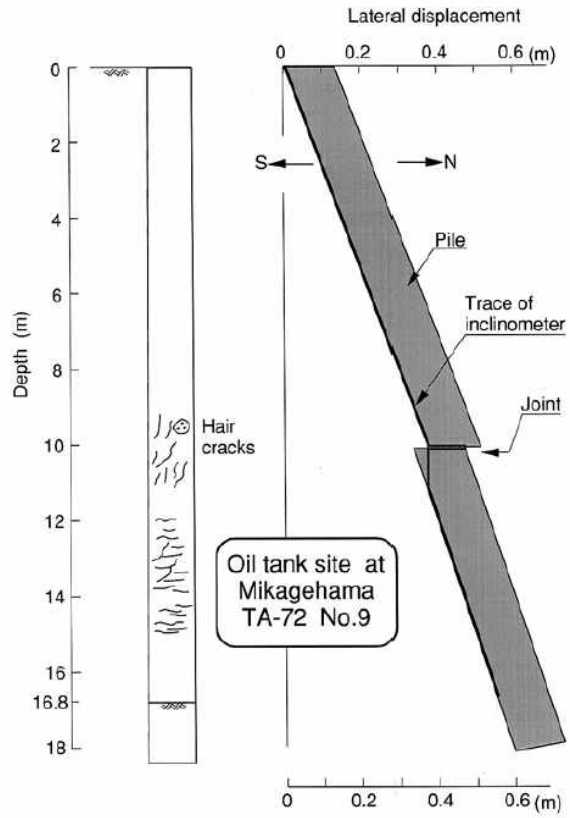

Figure 2.6 Lateral displacement and observed cracks on the inside wall of Pile No.2 (Ishihara et al. 2004)

2.3 Numerical modeling for dynamic behavior of piles

Numerical modeling tools have become more widely used according to advance of computing devices nowadays. However, application of numerical model for dynamic problem is still a challenge to geotechnical engineers. It is much more complex than numerical modeling for static problems because it has many parameters that affect on seismic behavior sensitively and

nonlinearity has to be considered for adequate simulation under strong earthquakes. Therefore, most of the researchers used simplified model to estimate dynamic pile behavior conveniently. However, this kind of approach can draw inaccurate results due to many assumptions by simplify. In recent, several studies have been carried out by three-dimensional continuum model for numerical modeling tools. This is time consuming and complex to apply, but most direct and straightforward method which can obtain reliable results if appropriate model is adopted and proper calibration is accomplished. In this section, previous researches which adopted simplified approach to predict dynamic SPSI are reviewed firstly. And other researches which used three-dimensional modeling are presented afterward.

Novak (1974) tried to solve a soil-pile problem by assuming a plane strain soil reaction, which could be interpreted as a Winkler foundation model with frequency dependent coefficients. A number of design chart and tables for the dynamic pile head stiffness and damping of piles are proposed in this paper. Novak and Aboul-Ella (1978) extended Novak's plane strain approach to layered soil and obtained the satisfactory results for higher frequencies. Gazetas et al. (1993) proposed a Winkler foundation model with much simpler stiffness and damping coefficients as following equation.

$$k_x = 1.2E_s \tag{2.1}$$

$$c_x = 1.6\rho_s v_s d\left(\frac{\omega d}{v_s}\right)^{-1/4} + 2\beta_s \frac{k_x}{\omega} \tag{2.2}$$

where E_s is the soil modulus, V_s is the mass density of soil, β_s is the hysteretic material damping ratio of the soil, d is the pile diameter, and ω is the angular frequency of the excitation. These coefficients are much simpler

than those which Novak proposed.

Dobry et al. (1982) carried out the parametric study and those parameters were then adjusted by calibration compared to the pile head response obtained in the FEM. Those parameters of Winkler stiffness were calculated by the following equation.

$$\frac{\pi}{64} E_p d^4 \frac{d^4 y(z)}{dz^4} + \delta E_s y(z) = 0 \tag{2.3}$$

General solution for equation 2.3 for a fixed head boundary condition and infinitely long pile can be induced in the following equation.

$$k_h = d E_s \sqrt[4]{\frac{\pi}{16} \frac{E_p}{E_s} \delta^3} \tag{2.4}$$

Value of δ was obtained as equation 2.5 by equating the pile head stiffness in the Winkler model and the FEM.

$$\delta = 1.67 \left(\frac{E_p}{E_s}\right)^{-0.053} \tag{2.5}$$

Kavvadas and Gazetas (1993) revised the value of δ as equation 2.6 by equating the results of the Winkler model and FEM in terms of the maximum bending moment at the natural frequency.

$$\delta = \frac{3}{1-\upsilon_s{}^2} \left(\frac{E_p}{E_s}\right)^{1/8} \left(\frac{L}{d}\right)^{1/8} \tag{2.6}$$

where υ_s is Poisson's ratio of soil.

Makris and Gazetas (1992) evaluated simplified methods for axial and lateral dynamic response for pile group using dynamic Winkler model as Figure 2.7. The procedure for a simplified Winkler foundation is as follows.

(Step 1) Motion of the foundation without superstructure is obtained, which means the kinematic effect.

(Step 2) Dynamic impedances of the oscillations in all directions of the foundation are obtained.

(Step 3) Seismic response of the superstructure on the springs and dashpots of step 2 subjected at the motion of step 1.

Gazetas and Mylonakis (1998) proposed the procedure of numerical modeling using the principle of superposition as shown in Figure 2.8.

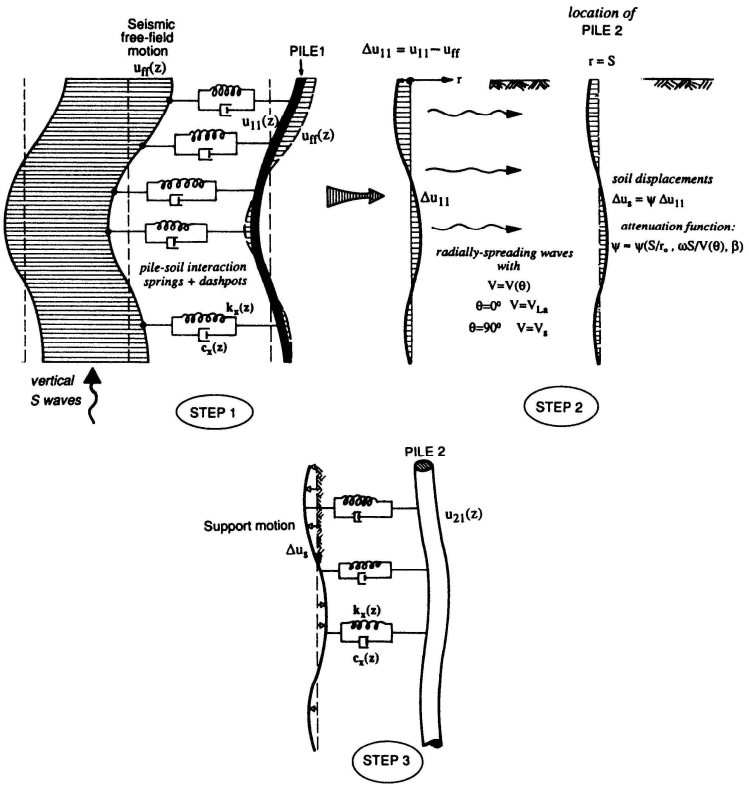

Figure 2.7 Schematic of three step procedure for computing pile-soil-pile interaction (Makris and Gazetas, 1992)

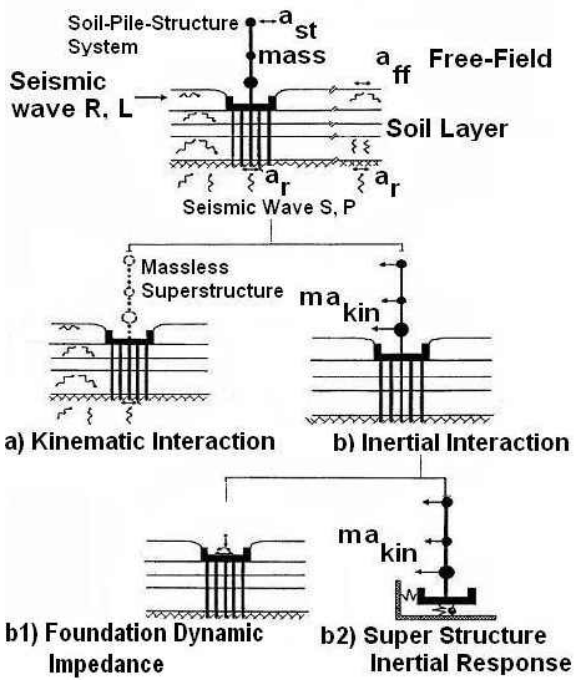

Figure 2.8 Schematic of superposition for SPSI problems
(Gazetas and Mylonakis, 1998)

Liyanapathirana & Poulos (2005) presented the one-dimensional numerical model which was developted for the analysis of piles founded in liquefying soil. This was based on the finite element method and involves two stages. First, an effective stress based free-field ground response analysis was carried out to determine the external soil movement and the degradation of soil stiffness and strength due to pore pressure generation. Second, a seismic analysis of the pile was carried out by applying computed ground displacements dynamically to the pile. For the method, a computer program based on the C language has been developed and the ability of the method to simulate pile behavior in liquefying soil has been demonstrated by comparing

with centrifuge tests performed by Wilson (1998). Figure 2.9 shows the measured and computed pore pressure distribution close to the surface of the soil deposits, the superstructure acceleration. In the numerical model, dilative bevavior of the soil is not included. At present, it can model only pore pressure generation due to cyclic loading and dissipation within the soil due to vertical drainge. Therefore the sharp pore pressure decreases observed during the experiment cannot be modeled using the numerical model but the maximum pore pressure generated during the earthquake loading can be modeled and is in general agreement with the centrifuge test.

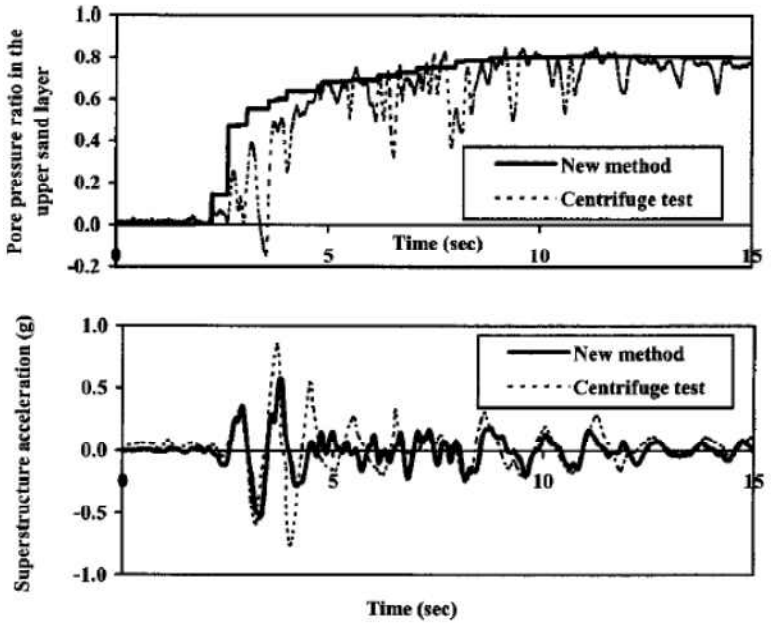

Figure 2.9 Comparison of time histories of pore pressure in upper sand layer, superstructure acceleration with centrifuge test by Wilson et al. (1998) (Liyanapathirana & Poulos, 2005)

The finite element method, a.k.a. FEM is one of the most popular approaches to simulate soil nonlinear behavior and non-homogeneity. However, this method requires a very large two- or three-dimensional meshes and techniques to consider the appropriate damping mechanism. And this method has been rarely applied in practice because it is very complicated to analyze and time consuming. Nevertheless, FEM is potentially one of the most powerful means to estimate dynamic SPSI. This is capable of carrying out SPSI analysis of a single piles and pile groups in a coupled manner without additional site response analysis and independent computation of superstructure responses. In FEM, whole system including soil, piles, and superstructure etc., can be considered and analyzed simultaneously.

Blaney et al. (1976) carried out the finite element analysis with a consistent boundary matrix to represent the free field and derived dynamic pile stiffness coefficients as a function of dimensionless frequencies. Desai and Appel (1973) presented a three-dimensional finite element solution with interface elements for the laterally loaded pile. Kuhlemeyer (1979) studied efficient static and dynamic solutions for lateral soil-pile elastic responses. Dobry et al.(1982) performed parametric studies of dynamic response of head loaded single piles in uniform soil using Blaney's method and proposed revised pile stiffness and damping coefficients as a function of E_s and E_p. Lewis and Gonzalez (1985) compared field test results of drilled piers to results from three-dimensional FEM that included nonlinear soil response and soil-pile gapping. Trochanis et al. (1988) studied nonlinear monotonic and cyclic soil-pile responses in both lateral and axial modes with a three-dimensional FEM, integrating slippage and gapping at the soil-pile interface.

Wong et al. (1989) analyzed soil-drilled shaft interaction with a specially developed three-dimensional thin layer interface element. Brown and Shie (1991) used a three-dimensional FEM to study group effects on modification of *p-y* curves. Cai et al. (1995) studied a three-dimensional nonlinear FEM consisting of sub-structured solutions of the superstructure and soil-pile systems. Wu and Finn (1997a; 1997b) presented a quasi-3D finite element formulation for the nonlinear dynamic analysis of pile foundations. Dynamic nonlinear analysis of pile groups in the time domain is performed using the quasi-three-dimensional finite element method which greatly reduces the computational time for the direct analysis of pile groups. Computed and measured bending moments envelope along the pile at the instant of peak pile cap displacement is shown in Figure 2.6. The computed bending moments agree reasonably well with the measured bending moments, especially in the range of peak bending moments.

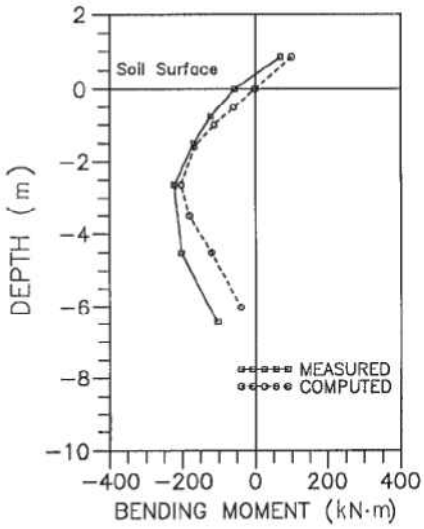

Figure 2.10 Comparison between measured and computed bending moments (Wu and Finn, 1997a)

Wu and Finn also carried out dynamic elastic analysis of pile foundations using FEM in the frequency domain. The computed lateral interaction factors for stiffness and damping were compared to those by Kaynia and Kausel (1982), and there was a good agreement, as shown in Figure 2. 11. Zhang et al. (2008) presented a two-dimensional advanced nonlinear finite element model of an actual bridge and its responses to seismic input motions using OpenSees. Rahmani and Pak (2012) analyzed dynamic behavior of pile foundations under cyclic loading in liquefiable soils using OpenSees also.

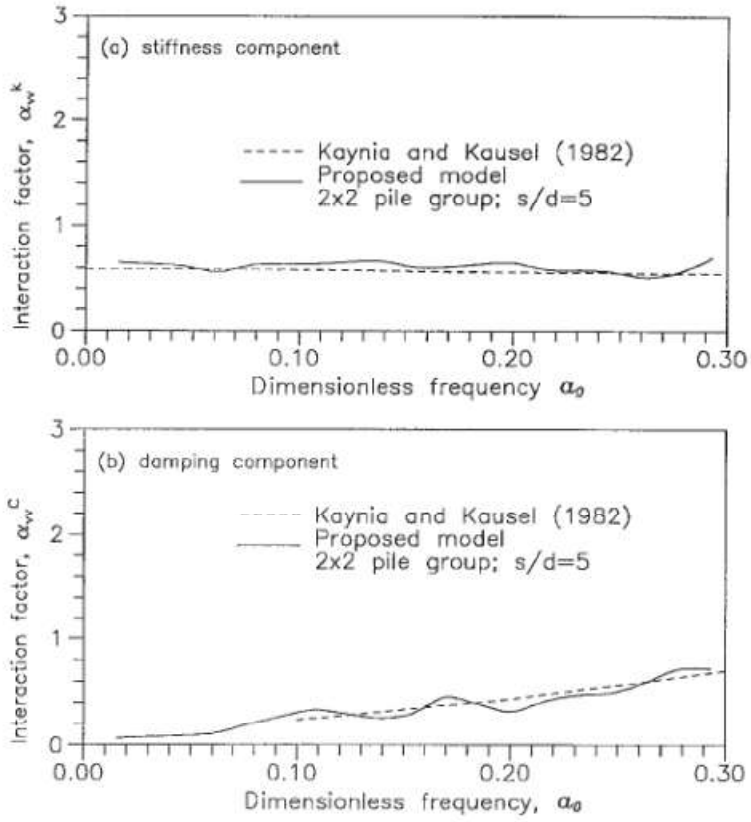

Figure 2.11 Comparison of dynamic interaction factors (E_p/E_s = 1000) (Kaynia and Kausel, 1982)

The finite difference method, a.k.a. FDM, is perhaps the oldest numerical technique used for the solution of sets of differential equations. In FDM, the mixed discretization scheme (Marti and Cundall, 1982) is often used for accurate modeling of plastic behavior of material. This scheme is treated to be physically more justifiable than the reduced integration scheme commonly used with FEM. An explicit solution scheme is often used for FDM in contrast to the implicit methods commonly used with FEM. In explicit calculation, no iteration process is necessary when computing stresses from strains in an element, even if, the constitutive law is wildly nonlinear. In an implicit method, every element communicates with every other element during one solution step, so several cycles of iteration are necessary before compatibility and equilibrium are obtained. Overall, explicit methods are best for ill-behaved systems such as nonlinear, large-strain, physical instability problems.

Reese (1977) presented the document for the computer program COM622, which solves deflection and bending moment of a pile under lateral loading as a function of depth. Calculations are performed on a finite difference model of the pile, and the soil is represented by a series of nonlinear *p-y* curves. Polous (1994) proposed an approximate method of numerical analysis of piled-raft foundations in which the raft is modeled as a thin plate and the piles as interacting springs of appropriate stiffness.

Several programs based on the FDM are developed such as COM624P, ALLPILE, LPILE, and FLAC. Among those, FLAC is one of the popular programs in geotechnical engineering. FLAC3D is a three-dimensional explicit finite-difference program for engineering mechanics computation.

Klar and Frydman (2002) carried out three-dimensional analysis of

lateral pile responses using FLAC2D. A generalized Winkler model and a coupled model are presented in this study. In the coupled model, the pile is represented by beam elements and the soil by an interacting plane strain system. They verified their approach for the simple cases of dynamic loading of piles in homogenous, visco-elastic material. Fig. 2.12 shows the basic calculation cycle of the procedure. The technique is based on discretization of the 3D soil continuum into a series of horizontal layers, each represented by a 2D boundary value problem (BVP). A cavity is inserted in each layer to model the pile cross section. In addition, a separate grid, consisting of a series of connected, unsupported beam elements representing the pile, is defined. The calculation procedure advances in time, and develops the interaction between the two systems through transfer of velocities and forces from pile (beam) nodes to BVP grid points, and vice versa. In each calculation time step, the equations of motion of the pile are solved, and pile node velocities are applied to the corresponding cavity boundary nodes. Resulting forces acting on the cavity perimeter are calculated, and applied to appropriate pile nodes. These forces are then used to solve again the pile's equations of motion in the next time step. The coupled model, used in the present investigation, includes shear springs and dashpots joining every layer node to the corresponding nodes of the layer above and below.

Several verification problems for a single pile and pile groups in a homogeneous soil layer modeled as a viscoelastic material were solved and compared to known solutions in order to assess the reliability of the models. Good agreement was observed between results of the present analyses and existing solutions (Figure 2.13).

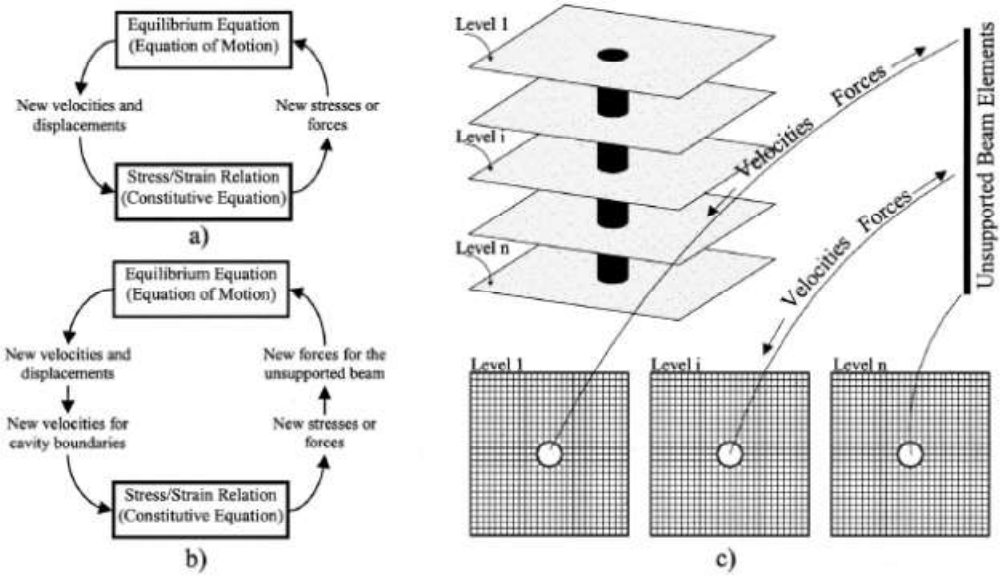

Figure 2.12 Analysis procedure (a) FLAC's original calculation cycle (b) Modified calculation cycle (c) Sub-grids and beam interaction (Klar and Frydman, 2002)

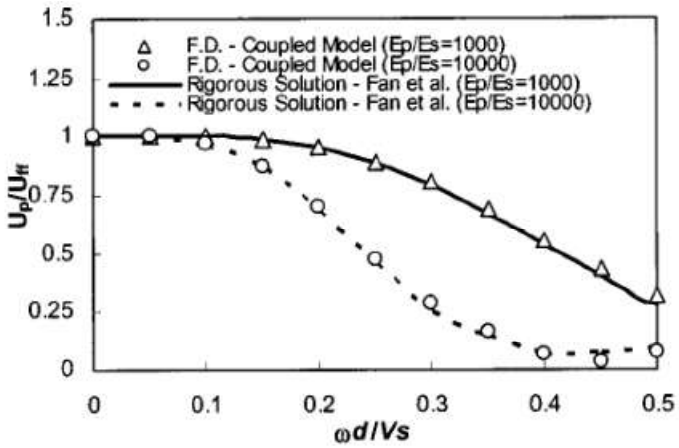

Figure 2.13 Comparison of Kinematic seismic response with the rigorous solution of Fan et al. (1991) (Klar and Frydman, 2002)

Comodromos (2003) applied three-dimensional finite difference analysis (FDA) to evaluate the response of free-head pile groups. Based on the results of a full-scale pile load test, he firstly applied back analysis techniques using the p–y method and a three-dimensional FDA to verify and adjust the soil parameters. A parametric 3D analysis was then performed and the results have been compared to those of the pile test. The effect of the soil–pile interaction was then estimated for various group configurations. Finally, a relationship was proposed allowing the establishment of load–deflection curves limited for free-head pile groups.

Martin and Chen (2005) estimated the response of piles caused by an embankment slope in a translational failure mode, induced by a weak soil layer or a liquefied layer beneath the embankment by the FLAC3D. Case histories calibrated by Chen and Poulos (1997) were used to verify the accuracy of numerical tools used for simulating pile response under lateral soil movement. Figure 2.14 plots the results for developed bending moment, indicating the trend of the pile response is similar to observed values.

Kim (2011) evaluated modeling methodology for dynamic SPSI observed in 1g shaking table tests and centrifuge tests. FLAC3D was used for modeling tools and soil nonlinearity, slip and separation at soil-pile interface was considered for accurate prediction of pile performance. Calibration of the various modeling parameters was carried out and results obtained from proposed model were compared to test results. Pile internal responses from numerical model showed good agreement for the results from 1g shaking table tests. However results from numerical analysis consistently underestimate results obtained from dynamic centrifuge tests because

calibration was performed only for 1g shaking table tests (Figure 2.15).

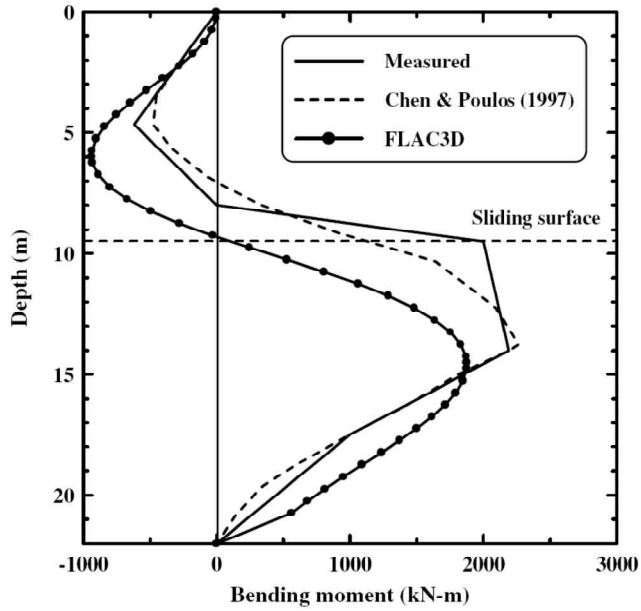

Figure 2.14 Comparison of distribution of bending moment (Martin and Chen, 2005)

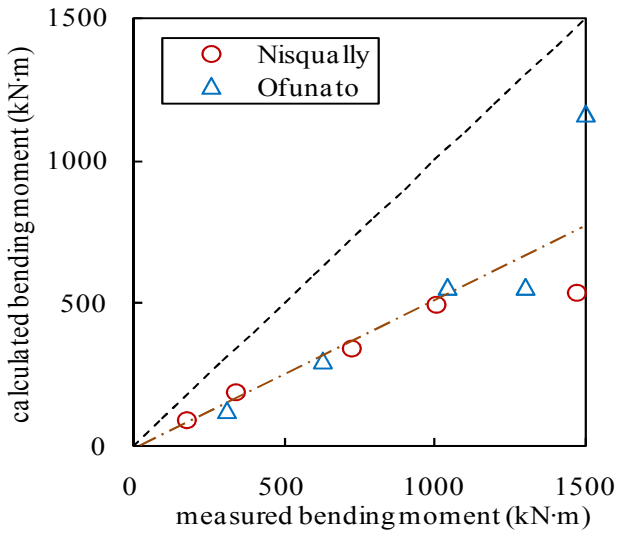

Figure 2.15 Comparison between calculated and measured peak bending moment (Kim, 2011)

3. Numerical Simulation for Dry Soil Deposits

3.1 Introduction

In this chapter, three-dimensional continuum model to simulate dynamic soil-pile-structure interactive behavior observed in centrifuge tests is proposed. At first, dynamic centrifuge test (Yoo, 2013) which is used as exact solution for prototype is introduced. Experiment was conducted for various input conditions, both for sinusoidal waves and real earthquake events. The finite difference code, FLAC3D was used in this study to model the dynamic soil-pile-structure interaction problem. Various modeling parameters which were properly calibrated for centrifuge model tests are explained. Calibration and validation procedure are introduced afterward. Calibration of the proposed modeling method was performed using results from test case of pile with a diameter of 1m and thickness of 0.04m. Pile internal responses obtained from numerical model were compared to those of experiment. Validation of the proposed modeling method was performed using results from test case of pile with a diameter of 0.72m and thickness of 0.04m. Applicability of the numerical model was estimated by comparing computed values with measured results.

Parametric study for various conditions was conducted in order to understand the effect of several variables on the dynamic pile behavior. In this study, weight of superstructure, relative density, pile length, pile head fixity was considered and detailed discussions are presented.

3.2 Dynamic centrifuge tests

In this dissertation, a series of centrifuge tests performed to evaluate the dynamic soil-pile-structure interactive behavior using the shaking table on the 5m radius KOCED centrifuge at the Korea Advanced Institute of Science and Technology is introduced (Yoo, 2013). Tests were conducted with different pile diameters and various input motions. Test apparatus, test materials, and test programs will be introduced.

3.2.1 Description of the centrifuge and model layouts (Yoo, 2013)

3.2.1.1 Centrifuge facility

The dynamic centrifuge model tests were conducted on the Korea Construction Engineering Development Collaboratory Program (KOCED), Geo-Centrifuge at the KAIST. Figure 3.1 shows the perspective views of centrifuge machine having a radius of 5 m and comprises a balanced arm with dual swing platforms. Shaking table is installed on the basket and input the excitation. Performance specification of the centrifuge machine is summarized in Table 3.1. This centrifuge has a maximum capacity of 240 g-tones and a maximum acceleration of 130 g. All the tests were performed at a centrifugal acceleration of 40g.

Figure 3.1 Perspective view of KOCED Geo-Centrifuge

Table 3.1 Performance specification of KOCED Geo-Centrifuge

Specifications	Centrifuge
Radius	5 m
Maximum capacity	240g-tons
Maximum payload	2,400 kg up to 100g
Maximum acceleration	130g @ 13,00kg playload
Payload dimension	1.2 m × 1.2 m × 1.2 m

3.2.1.2 Shaking table (Kim et al., 2013)

The centrifuge facility was equipped with an electro-hydraulic servo type earthquake simulator capable of shaking in the horizontally biaxial directions. The earthquake simulator at KAIST was initially operated in January of 2010 and has been actively used to simulate seismic problems of a various geotechnical structures and soil-structure systems in Korea. A self-balanced electro-hydraulic earthquake simulator is mounted on the centrifuge, which has an effective radius of 5 m and a maximum capacity of 240 g-tons. The

earthquake simulator is currently a unique apparatus capable of modeling seismic problems on centrifuge in Korea. It is designed to operate at up to centrifugal acceleration of 100 gc and the base shaking acceleration can be exerted to a maximum value of 20 gh with a maximum payload of 700 kg, which corresponds to 0.5 gh in prototype scale at 40gc centrifugal acceleration. The main specifications and general view of the earthquake simulator at KAIST are shown in Table 3.2 and Figure 3.2, respectively.

Table 3.2 Performance specification of the shaking table at KOCED Geo-Centrifuge

Specifications	Centrifuge
Payload moving mass	700 kg
Centrifuge Acc. range	10g ~ 100g
Frequency response	40 Hz ~ 300 Hz
Maximum acceleration	20g
Payload dimension	0.67 m× 0.67 m × 0.67 m

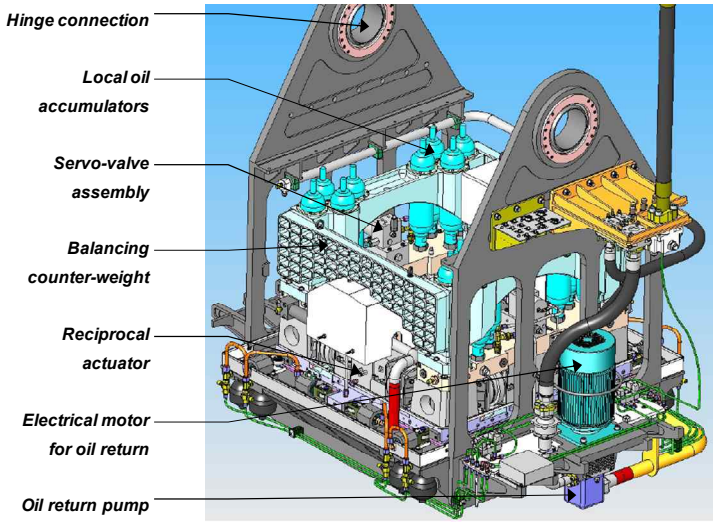

(a) Schematic view of shaking table

(b) Shaking table

Figure 3.2 Shaking table at KOCED Geo-Centrifuge

3.2.1.3 Equivalent shear box (Lee et al., 2011)

The model container used for the centrifuge tests in this dissertation is an Equivalent Shear Beam, a.k.a. ESB, box as shown in figure 3.3. The ESB model container at KAIST was formed by stacking 10 light-weight aluminum alloy rectangular frames on a base plate to create internal dimensions of 490 mm × 490 mm × 630 mm and external dimensions of 650 mm × 650 mm × 650 mm in length, width, and height, respectively. A relatively large wall thickness of 80 mm is applied so as to avoid any lateral bulging and to maintain uniform stress conditions against lateral soil pressures exerted by deep soil models under maximum 100 gc centrifugal acceleration. Each frame is 60 mm in height and is separated by inside ball bearings and rubber spacing layers. The ball bearing system permits single-axis movement parallel to the longitudinal axis of the container during base shaking and makes the dynamic stiffness of the rubber layers constant independent of the levels of centrifugal acceleration. A total of 9 rubber layers having roughly about 3 mm thickness each lead to discrete step-like deflection of the end walls. The rubber layers ensure sealing of the model container and shearing behaviors of the frames and inside soil models. The design concept is that the deflection of each frame matches that of the soil column at the middle of the frame. The increase in discrete deflection would cause discontinuity in the shear strain of soil near the end walls, but shear sheets attached on the end walls reduce this effect.

Figure 3.3 Elastic shear beam box

3.2.1.4 Model pile

Three kinds of model piles were used for dynamic centrifuge tests. These piles were fabricated with a close-ended aluminum pipe with 2.5cm, 2.2cm, and 1.8cm external diameters and a 0.1cm wall thickness. The embedment depth of piles was 57cm and they were installed to be longer than the infinite depth. All tests were carried out at a centrifugal acceleration of 40g which is same with scaling factor of centrifuge test. Therefore, the three model piles simulated the prototype piles with 72cm, 88cm and 100cm diameters, and the embedment depth of the prototype piles was 22.8m. The properties of piles are summarized in Table 3.3.

A model pile was prepared by scaling the dimension down as much as

the scaling factor, n (= 40), equal to the centrifugal gravity. There is an identical limitation with 1g shaking table test; the satisfaction of the similitude law for the diameter and elastic modulus could be obtained with the satisfaction for the flexural rigidity because the selection of material is limited. Consequently only the flexural rigidity, which governs the lateral behavior of pile foundation, was considered by adjusting diameter and thickness of hollow circular section.

A model pile was fixed to the bottom of soil container because prototype pile is embedded in weathered rock. Eight pairs of strain gauges were attached at opposite surface of pile in the bending plane along the pile (0cm, 5.1 cm, 10.3 cm, 18cm, 28.2 cm, 38.5 cm, and 49 cm) to measure the strain, which results from the bending moments. The surcharge mass was 1.4 kg.

Table 3.3 Properties of the model piles

	Model 1	Model 2	Model 3
Scaling relation	40	40	40
Diameter of pile (cm)	1.8(72*)	2.2(88*)	2.5(100*)
Thickness of pile (cm)	0.1(4*)	0.1(4*)	0.1(4*)
Flexural rigidity (kg•cm4)	133889 (3.43E+11*)	252080 (6.45E+11*)	376083 (9.63E+11*)
Embedment depth (cm)	57 (2280*)	57 (2280*)	57 (2280*)
Concentrated surcharge mass (kg)	1.4 (8960*)	1.4 (8960*)	1.4 (8960*)

*Prototype scale

3.2.1.5 Model soil

Jumunjin sand (USCS classification = SP) was used in centrifuge tests to estimate dynamic behavior of pile foundations in dry soil deposits. Grain size distribution curve of this soil is shown in Figure 3.4 and the properties are summarized in Table 3.4

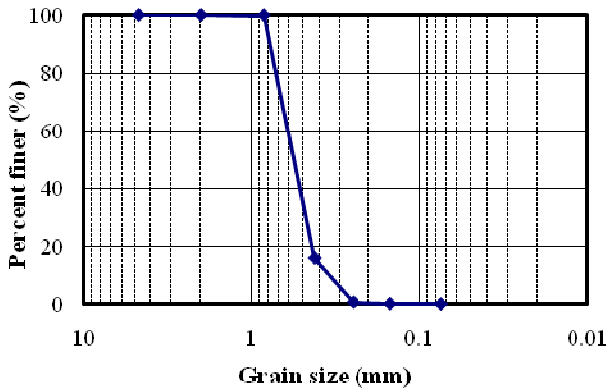

Figure 3.4 Grain size distribution

Table 3.4 Properties of Jumunjin sand

USCS	D_{10} (mm)	D_{50} (mm)	Cu	Gs	$\gamma_{d,max}$ (t/m^3)	$\gamma_{d,min}$ (t/m^3)
SP-SM	0.08	0.17	2.32	2.65	1.64	1.29

Dry sand layer for the centrifuge tests was prepared uniformly by sand raining machine. Before model preparation, the model pile was preinstalled by fixing it at the base of the ESB container. Dry sand was poured into the ESB model container from a sand raining system at a constant falling height of 80

cm over the surface of the sand deposit to provide a fairly uniform specimen with the desired relative density. Different relative densities were achieved by varying the opening size and the traveling rate of the sand raining system. The height of sand drop and the opening size was determined by trial and error.

3.2.1.6 Test Program

The layout and instrumentation of dynamic centrifuge test is shown in Figure 3.5. The model piles were fixed at the bottom of the ESB box in order to simulate the rock socketed pile and concentrated surcharge mass of 1.5kg was located 11cm above the subsurface. Eight pairs of strain gages were attached on both sides of the pile. Eight accelerometers were installed in the soil at the same depth as each strain gauges to calculate the displacement of soil and one accelerometer was attached to the pile head to measure the acceleration of the pile head.

After the completion of model fabrication, seismic loading was applied at a 40g condition. Both sinusoidal waves and real earthquake events were used as a input excitations. Sinusoidal wave is useful because adjustment of loading amplitude and frequency is not difficult. The loading amplitude of the input sine wave ranged from 0.05g to 0.4g and the frequency was from 1,2,3Hz in the prototype scale. Figure 3.6 shows the acceleration-time history, having maximum acceleration of 0.4g and frequency of 1Hz. Real earthquake events such as Ofunato earthquake and Nisqually earthquake were scaled into

various earthquake events having different amplitude of base input accelerations (0.06g, 0.13g, 0.25g, 0.36g, 0.51g). Figure 3.7 and 3.8 show the acceleration-time history, having maximum acceleration of 0.51g, of the base input for Ofunato earthquake and Nisqually earthquake, respectively.

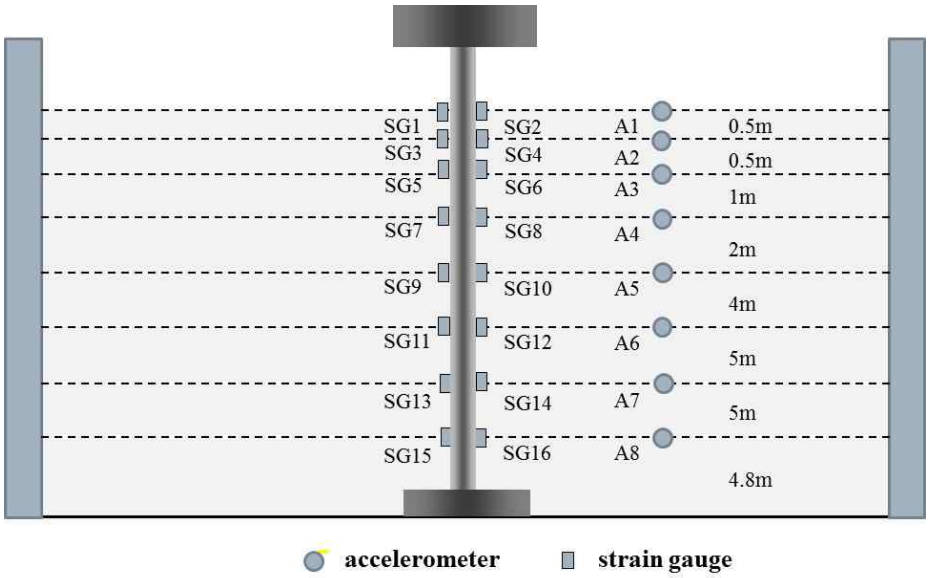

Figure 3.5 Layout of test (in prototype)

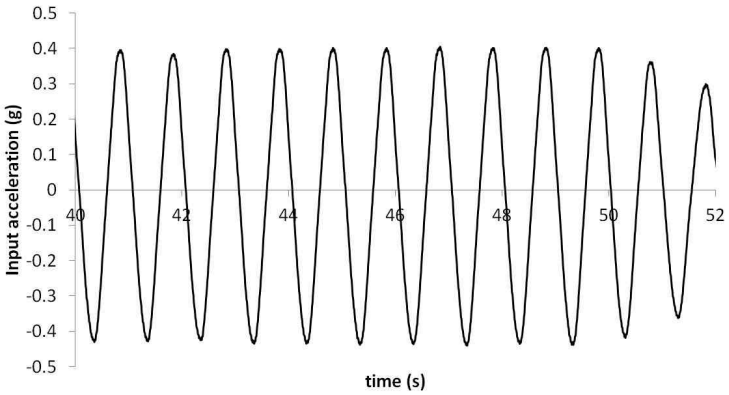

Figure 3.6 Acceleration-time history of base input for sine wave (1Hz, 0.4g)

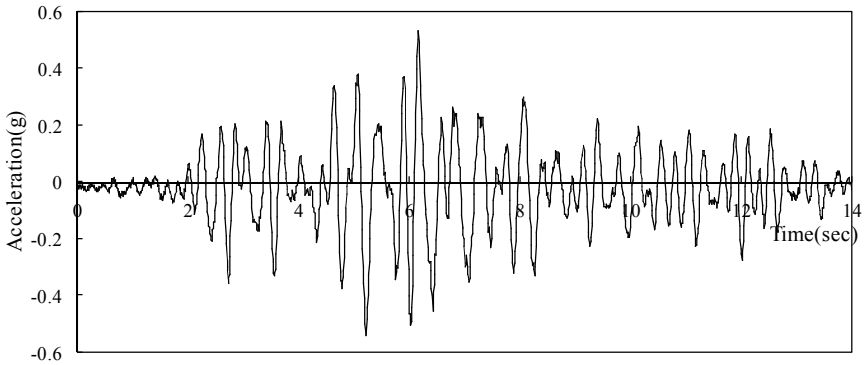

Figure 3.7 Acceleration-time history of base input for Ofunato earthquake (a_{max}=0.51g)

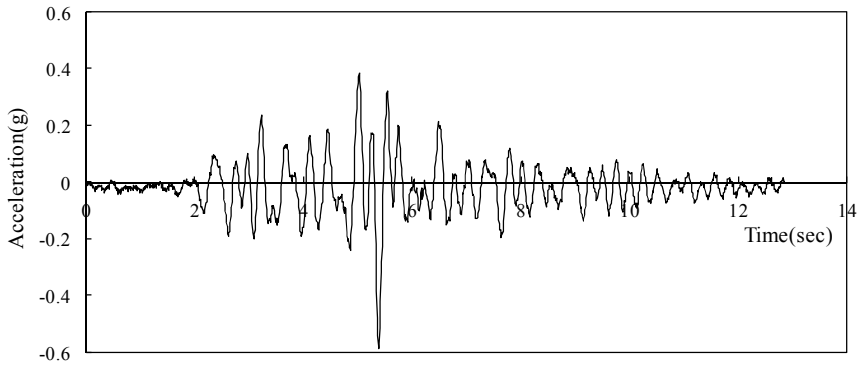

Figure 3.8 Acceleration-time history of base input for Nisqually earthquake (a_{max}=0.51g)

3.3 Modeling methodology

In this dissertation, modeling methodology evaluated for prediction of dynamic SPSI embedded in dry soil deposits is explained. As reviewed in section 2, The finite difference method has advantages for evaluation and

prediction of the dynamic soil-pile-structure interactive behavior under earthquake. Mixed discretization, commonly used in finite difference modeling, is physically more justifiable than the reduced integration scheme commonly used in finite element method. Moreover, explicit method can follow arbitrary nonlinearity in stress-strain laws in almost the same computing time as linear laws, whereas implicit method can take significantly longer time to solve nonlinear problems. In explicit calculation, no iteration process is necessary when computing stresses from strains in an element, even if, the constitutive law is wildly nonlinear. In an implicit method, every element communicates with every other element during one solution step, so several cycles of iteration are necessary before compatibility and equilibrium are obtained. Overall, explicit methods are best for ill-behaved systems such as nonlinear, large-strain, physical instability problems.

Because the finite difference method has advantages as stated above, this research utilizes the finite difference modeling to predict dynamic SPSI observed in centrifuge tests. The commercial finite difference code program, Fast Lagrangian Analysis of Continua 3D Version 3.1 which is one of the widely used numerical modeling tool in geotechnical engineering was used in this study.

3.3.1 Soil model

The Mohr-Coulomb plasticity model was used as a constitutive model in this study. This is generally used in practice, however it cannot take into

account the nonlinear behavior of soil under strong earthquake loading. Once strong earthquake occurs, soil would deform dramatically and nonlinear behavior could be observed. Therefore, nonlinearity of soil has to be properly simulated in numerical model to obtain accurate results. In this study, the hysteretic damping was applied to consider both the nonlinearity of soil modulus and the energy dissipation. If we assume an ideal soil, in which the stress depends only on the strain, not on the number of cycles, or time, incremental constitutive relation can be derived from the degradation curve. S-shape curve of modulus versus logarithm of cyclic strain can be representative by a cubic equation, with zero slope at both low strain and high strain. Thus, the secant modulus M_s can be formulated by equation 3.1

$$M_s = s^2(3 - 2s) \tag{3.1}$$

where

$$s = \frac{L_2 - L}{L_2 - L_1} \tag{3.2}$$

and L is the logarithmic strain,

$$L = \log_{10}(\gamma) \tag{3.3}$$

The parameters L_1, L_2 are the extreme value of logarithmic strain. The tangent modulus is given by equation 3.4.

$$M_t = M_s + \gamma \frac{dM_s}{d\gamma} \tag{3.4}$$

Using the chain rule,

$$\frac{dM_s}{d\gamma} = \frac{dM_s}{ds} \cdot \frac{ds}{dL} \cdot \frac{dL}{d\gamma} \tag{3.5}$$

The tangent modulus can be obtained by following equation 3.6

$$M_t = s^2(3-2s) - \frac{6s(1-s)}{L_2-L_1}\log_{10} e \quad (3.6)$$

In this study, $G/G_{m\,ax} - \gamma$ curve of Jumunjin sand was obtained from triaxial test and resonant column test. Thereafter, L_1, L_2 were determined as -3.65, 0.5 respectively by fitting calculated values to test results (Figure 3.9).

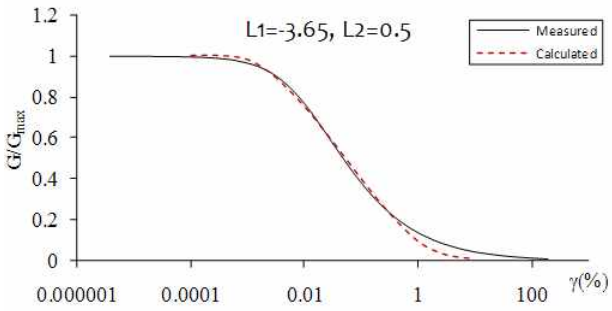

Figure 3.9 Comparison of measured and calculated $G/G_{m\,ax} - \gamma$ for L_1= -3.65 and L_2 = 0.5

Initial shear modulus ($G_{m\,ax}$) is depends on the confining pressure according to depth. In this study, initial shear modulus was determined from following formula proposed by Hardin and Drnevich (1972). Calibration of equation 3.7 was conducted, results in, empirical coefficient A, n were input as proposed by Yang (2009).

$$G_{m\,ax} = AF(e)(OCR)^k P_a^{1-n}(\sigma'_m)^n \quad (3.7)$$

Where, $F(e) = \frac{1}{0.3+0.7e^2}$, e = void ratio, *A* and *n* is coefficients, *OCR* is the overconsolidation ratio, *k* is an overconsolidation ratio exponent (see Table 3.5), σ'_m is the mean principal effective stress ($\sigma'_m = (\sigma'_1 + \sigma'_2 + \sigma'_3)/3$), and P_a is the atmospheric pressure in the same units with σ'_m. As a result of calibration, the coefficients (*A*, *n*) were determined as 247.73 and 0.567,

respectively.

Table 3.5 Overconsolidation raio exponent (Hardin and Drnevich, 1972)

Plasticity Index	k
0	0.00
20	0.18
40	0.30
60	0.41
80	0.48
≥ 100	0.50

Variation of initial shear modulus according to the depth was adopted at every elements and input by using above equation with user defined FISH function in FLAC3D. At this time, it has to be considered that soil within shallow depth can reach yield state under strong earthquake motion. Within this certain depth, a.k.a. yield depth, shear modulus of soil approaches to 25% of the initial shear modulus (Boulanger et al., 1999). Therefore, in this study, initial shear modulus within the yield depth was input as 25% of the G_{max} and maximum yield depth was estimated as 2.5 times of pile diameter by parametric study.

3.3.2 Interface model

When strong earthquake occurs, slippage and separation can be induced at the interface between soil and pile foundation. Interface model used in numerical analysis has to simulate these kinds of behavior properly. In this study, soil-pile interface model which can simulate fully contact, slippage, separation state according to the input motion was adopted. Figure 3.10 shows the concept of applied interface model and Figure 3.11 shows the components of interface model. During each timestep, the absolute normal penetration and the relative shear velocity are calculated for each interface node and its contacting target face. Both of these values are then used by the interface constitutive model to calculate a normal force and a shear-force vector. The interface constitutive model is defined by a linear Coulomb shear-strength criterion that limits the shear force acting at an interface node, normal and shear stiffnesses, tensile and shear bond strengths, and a dilation angle that causes an increase in effective normal force on the target face after the shear strength limit is reached. The Coulomb shear-strength criterion limits the shear force by the following relation.

$$F_{sm\,ax} = cA + \tan\emptyset(F_n - pA) \tag{3.8}$$

Where c is the cohesion along the interface, $\emptyset$ is the friction angle of the interface surface, and p is pore pressure.

The separation and slippage phenomenon were modeled as the linear springs in the normal and shear direction, respectively. Through the elastic relation, the relationship between normal stress and normal strain is formulated as equation 3.9.

$$\sigma_x = [K + (4/3)G]\varepsilon_x \tag{3.9}$$

where K is bulk modulus, G is shear modulus. A good rule-of-thumb is that normal and shear stiffness be set to ten times the equivalent stiffness of the stiffest neighboring zone. Resulting in, apparent normal stiffness of a zone in the normal direction is derived as equation 3.10.

$$k_n = max\left[\frac{K+(4/3)G}{\Delta z_{min}}\right] \tag{3.10}$$

where Δz_{min} is the smallest width of an adjoining zone in the normal direction (Figure 3.12). The max [ ] notation indicates that the maximum value over all zones adjacent to the interface is to be used. Adopted interface model may take into account nonlinear behavior of soil because shear modulus (G) and bulk modulus (K) in equation 3.10 is the value considering soil nonlinearity as stated in 3.3.1. Normal and shear stiffnesses were input identically according to the parametric study. Stiffness is calculated and input to be dependent on the confined pressure along depth by using FISH function.

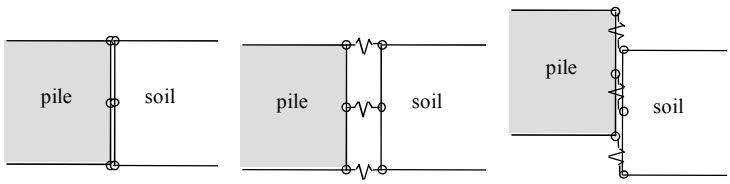

(a) no gap, no slide (b) gap, no slide (c) no gap, slide

Figure 3.10 Concept of interface model

Another input property used in interface element is interface friction angle δ. In general, from many previous researches, it is referred that interface friction is somewhat lower than maximum internal friction of far field. Kraft

(1990) suggested the interface friction angle as 70% of maximum internal friction of far field, and Reddy et al. (2000) suggested the interface friction angle as 60% of maximum internal friction of far field. In this study, according to Beringen et al. (1979) and Randolph et al. (1994), interface friction angle δ was determined by $\delta = \emptyset_{max} - 5^{\circ}$. From the expression, interface friction angle δ was determined as 37° in this study.

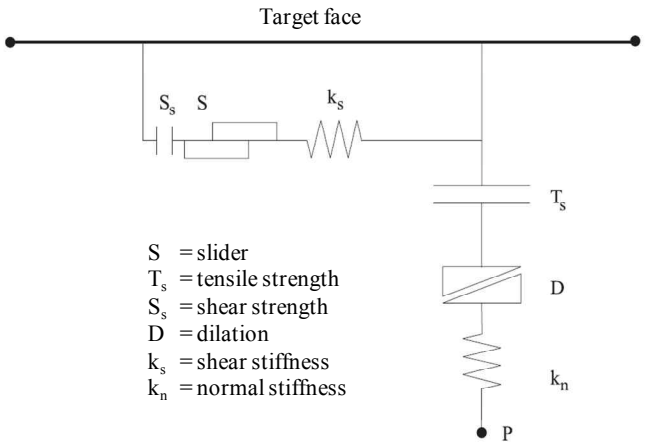

Figure 3.11 Components of interface model (Itasca, 2006)

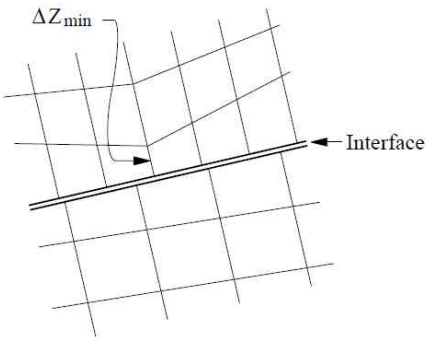

Figure 3.12 Zone dimension used in stiffness calculation (Itasca, 2006)

3.3.3 Boundary condition

One of the most important aspects of boundary condition for numerical model of dynamic SPSI is the simulation of semi-infinite boundary condition. The modeling of geomechnics problems involves media which, at the scale of analysis, are better represented as unbounded. Pile foundations are normally assumed to be surrounded by an infinite medium, while surface and near-surface structures are assumed to lie on a half-space. Numerical methods relying on the discretization of a finite region of space require that appropriate conditions be enforced at the artificial numerical boundaries. In static analysis, fixed or elastic boundaries can be realistically placed at some distance from the region of interest. In dynamic analysis, however, such boundary conditions cause the reflection of outward propagating waves back to the model, and do not allow the necessary energy radiation. The use of large model can minimize the problem, since material damping will absorb most of the energy in the waves reflected from distant boundaries. However, this solution leads to a large computational burden. The alternative is to use quiet boundaries which is viscous boundary developed by Lysmer and Kuhlemeyer (1969). The quiet boundary scheme proposed by Lysmer and Kuhlemeyer involves dashpots attached independently to the boundary in the normal and shear directions. The dashpots provide viscous normal and shear tractions as following equations.

$$t_n = -\rho C_p v_n \tag{3.10}$$

$$t_s = -\rho C_s v_s \tag{3.11}$$

where v_n and v_s are the normal and shear components of the velocity at the boundary, ρ is the mass density, C_p, C_s is the p- and s- wave velocities.

In this study, however, numerical model adopting quiet boundary condition results in large error. Therefore, simplified continuum modeling (Kim, 2011) was selected for boundary condition as alternative. In simplified continuum modeling method, meshes of far field is ignored, acceleration-time histories of far field are applied according to depth. The acceleration-time histories of the far-field area were calculated by site response analysis using FLAC3D. Figure 3.13 shows the mesh which was used in simplified continuum modeling. Distance of 10D (D : pile diameter) from the center was considered as the near field soil. To determine the distance from the pile to the far field region, the amplification ratio that refers to the maximum acceleration of the soil surface divided by the base input acceleration was calculated at various distances from the pile (Figure 3.14).

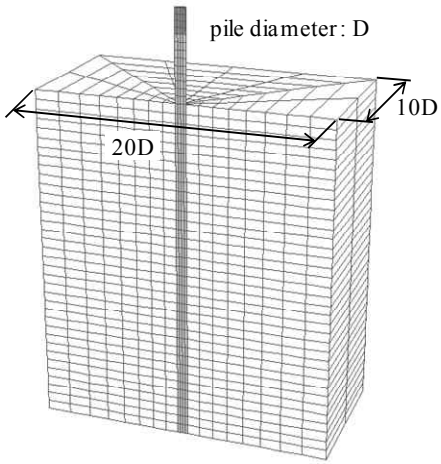

Figure 3.13 Mesh of simplified continuum modeling

Figure 3.15 illustrates that the ratio became constant when the distance from the center was further than ten times the pile diameter, meaning that the area that was more than ten times as far as the pile diameter was not affected by the soil-pile interactive behavior. The results, obtained by Remaud (1999), that there was no interaction effect between the piles when the pile spacing was over 10D supports the analysis results in this study. Accordingly, the boundary between near field and the far field was determined to be located at 10D from the pile center. Figure 3.16 shows the schematic drawing of adopted simplified continuum modeling. The system consists of the pile, near field soil which is interacts with the pile, interface element which simulate the soil-pile interaction, and the far field responses. The far field soil is substituted into the acceleration-time histories and input as the boundary condition at the boundary of the near field instead of generating meshes.

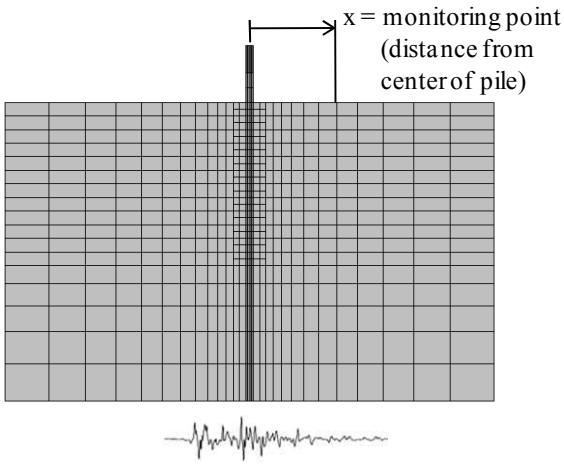

Figure 3.14 Mesh of full continuum modeling and location of monitoring point

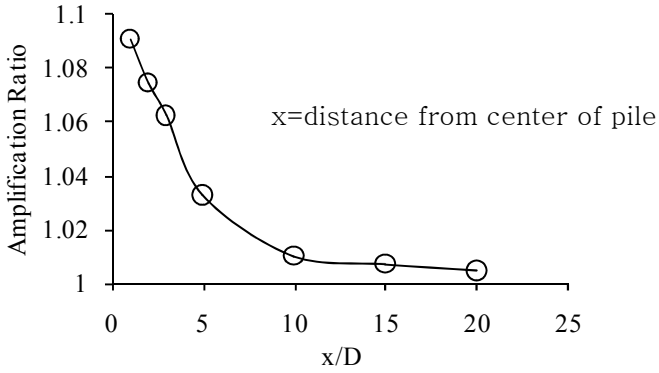

Figure 3.15 Acceleration amplification ratio of soil according to distance from pile

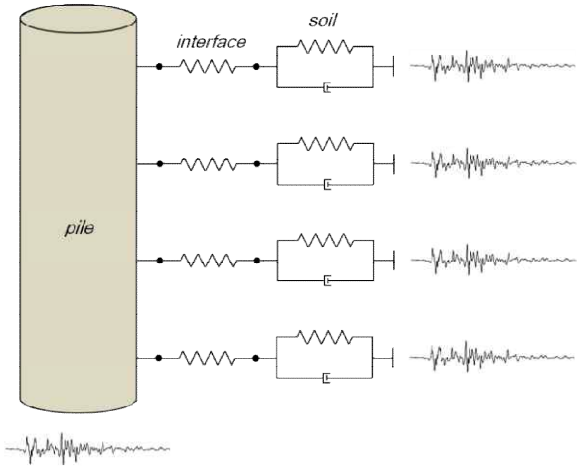

Figure 3.16 Schematic of simplified continuum modeling

3.4 Calibration and validation of the proposed method

Numerical simulation is very powerful and effective mean to predict certain behavior of material because it doesn't need many apparatus for test, labor of many persons, much time for plan and perform the test, and astronomical amount of money to operate high technological devices. However, every result obtained from numerical analysis is just approximate solution of partial difference equation, not an exact solution. Therefore, calibration of the numerical model with test results which is believed in exact solution is essential for obtaining reliability of the proposed numerical modeling method and minimizing error of numerical analysis.

In this study, many parameters used in modeling methodology were calibrated for the condition of dynamic centrifuge tests in 3.3, then results from the numerical analysis have to be calibrated with test results. Thereafter, validation of the numerical model is necessary by simulating another test case by proposed modeling method, and comparing results from numerical analysis with test results. From this procedure including calibration and validation process, applicability of proposed numerical model can be verified.

In this section, dynamic centrifuge model test in dry soil deposits conducted by Yoo (2013) was numerically simulated by proposed modeling method. For the calibration of the numerical model, the test case of pile with a diameter of 100cm, and thickness of 4cm was applied. For the validation of the numerical model, the test case of pile with a diameter of 72cm, and thickness of 4cm was applied. Pile internal responses such as bending moment and lateral displacement for various input conditions were calculated and

compared to calibrate and validate the numerical model.

3.4.1 Calibration of the proposed method

As stated above section, calibration of the numerical model was conducted using the test case of pile with a diameter of 100cm, and thickness of 4cm. A concise explanation of calibration procedure is as follows. First, every parameter used in modeling methodology was adjusted to test condition as described in section 3.3. Thereafter, results obtained from proposed numerical model was compared to those obtained from centrifuge tests. And applied parameters such as yield depth were modified to reduce discrepancy between two results repetitively. When discrepancy between two results was approached to reasonable range, modeling parameters were defaulted and numerous analyses for various input condition would be performed.

For the first case of calibration, comparison of pile internal responses using the test case which applied sinusoidal waves as a input motion was conducted to observe simulation capability of numerical model for various input frequencies and accelerations. Thereafter, comparison of pile internal responses using the test case which applied real earthquake events as input motion was performed to investigate whether proposed model could be used in practice. Table 3.6 and 3.7 shows input properties of model pile and model soil for calibration process respectively. All the values related with centrifuge test and numerical simulation described in prototype scale.

Table 3.6 Input properties of model pile for calibration of proposed method

Property	Value
Diameter (m)	1
Thickness (m)	0.04
Length (m)	27.4
Superstructure weight (kN)	960
Flexural rigidity ($N \cdot m^2$)	9.63E+9

Table 3.7 Input properties of model soil for calibration of proposed method

Property	Value
Friction angle (degree)	42
Dry density (kN/m^3)	15.80
Poisson's ratio	0.3
Void ratio	0.677
Relative density (%)	80

3.4.1.1 Pile responses to sinusoidal waves

Figure 3.17, 3.18 show measured and computed peak bending moment along depth for various input amplitudes. These results demonstrated that there was good agreement between measured and computed peak bending moment profile. As input acceleration increases, peak bending moment also increases in both results. Figure 3.19 (a), (b), (c) show measured and computed maximum values of bending moment varying input frequencies

from 1Hz to 3Hz for input acceleration of 0.13g, 0.25g, 0.45g respectively. It can be seen that results obtained from the numerical model for various input motions agree reasonably well with values recorded during the centrifuge test. Resonance occurred at 1Hz of input frequency both in numerical model and experiment results, which means natural frequency of the applied system was about 1Hz in both results. It is concluded that proposed modeling method could simulate important dynamic characteristics such as resonance due to natural frequency.

Figure 3.20 shows comparison between computed and measured peak bending moments for various input motions. In this figure, the vertical axis is calculated peak bending moment, those are results from numerical model and the horizontal axis is measured peak bending moments, those are test results. It can be seen most of the points are located nearby 1:1 line in the graph, which means calculated peak bending moments show reasonably good agreement with measured peak bending moments for various input motions.

Once similar bending moment is exerted to the pile foundation, it can be predicted that similar lateral pile displacement will be occurred. In order to confirm this phenomenon and conduct additional calibration of numerical model, comparison between measured and computed maximum lateral pile displacements were conducted. Figure 3.21, 3.22 show measured and computed maximum lateral pile displacement along depth for various input amplitudes. These results demonstrated that there was good agreement between measured and computed maximum lateral pile displacement profile similar with bending moment case. From a series of comparison process, it was concluded that proposed numerical model was capable of simulating

dynamic soil-pile-structure interactive behavior for the test case which applied sinusoidal waves as input motion.

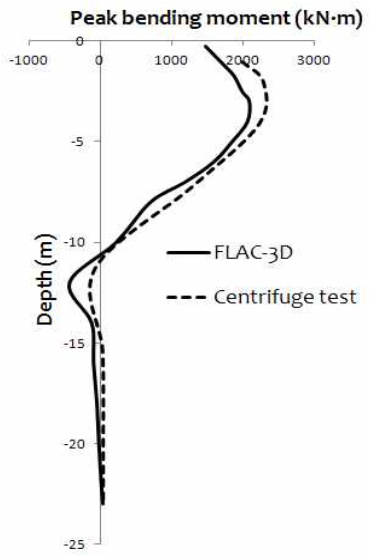

Figure 3.17 Measured and computed peak bending moment along depth (1Hz, 0.13g)

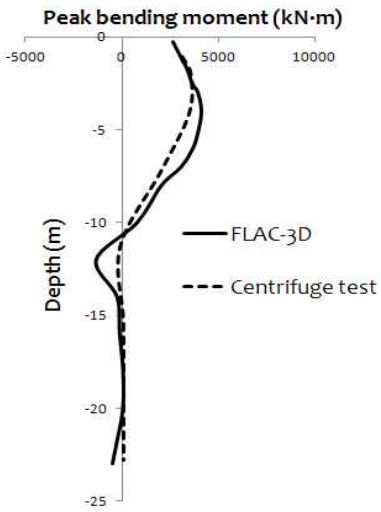

Figure 3.18 Measured and computed peak bending moment along depth (1Hz, 0.25g)

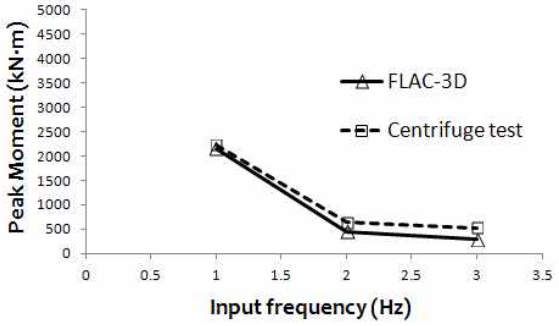

(a) Input acceleration : 0.13g

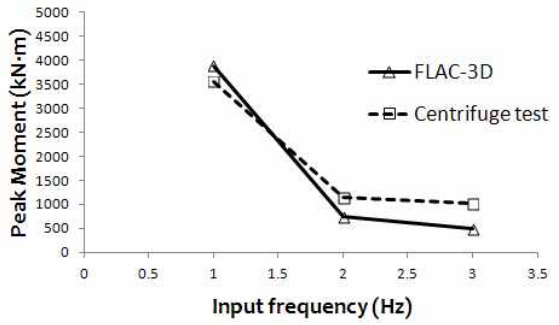

(b) Input acceleration : 0.25g

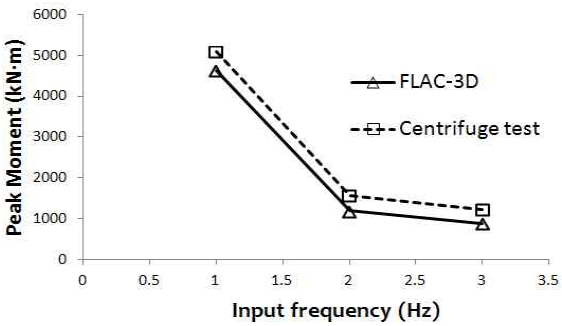

(c) Input acceleration : 0.45g

Figure 3.19 Peak bending moments for various input frequencies

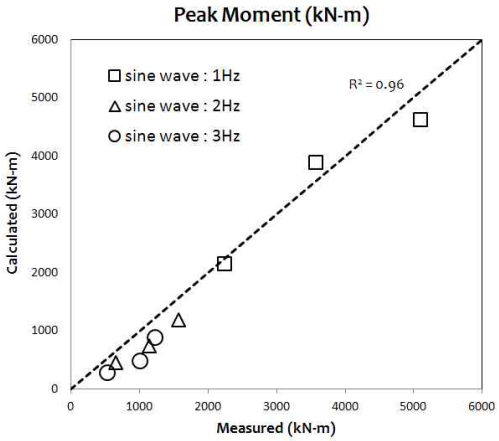

Figure 3.20 Calculated and measured peak bending moments for various input motions

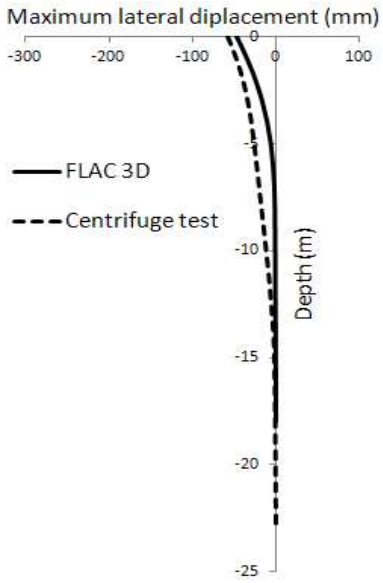

Figure 3.21 Measured and computed maximum lateral pile displacement along depth (1Hz, 0.13g)

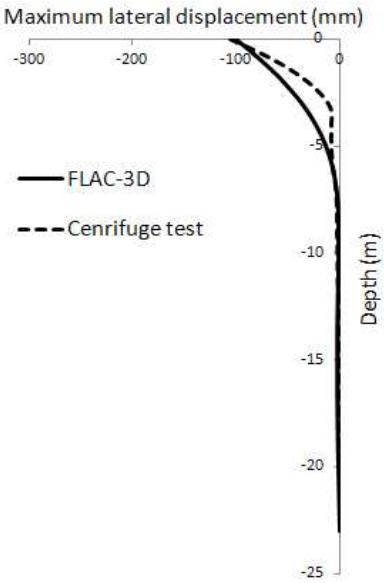

Figure 3.22 Measured and computed maximum lateral pile displacement along depth (1Hz, 0.25g)

3.4.1.2 Pile responses to real earthquake events.

Based on the calibration process to sinusoidal waves above section, additional calibration was conducted comparing pile internal responses to real earthquake events, which is meaningful in practice. Figure 3.23, 3.24 show measured and computed peak bending moment along depth to Nisqually earthquake which was scaled to 0.13g, 0.25g respectively. These results demonstrated that computed peak bending moment profiles show reasonably good agreement with test results for various input amplitudes. Figure 3.25, 3.26 show measured and computed peak bending moment along depth to Ofunato earthquake which was scaled to 0.13g, 0.25g respectively also. It can be seen that proposed numerical model predicted well dynamic response of pile for various input amplitudes.

Figure 3.27 (a), (b) show measured and computed maximum values of bending moment to Nisqually earthquake and Ofunato earthquake respectively varying input acceleration of 0.13g, 0.25g, 0.51g. It can be seen that results obtained from the numerical model for various input motions agree reasonably well with values recorded during the centrifuge test. And dynamic pile responses gradually increased as input acceleration increases both in numerical model and dynamic centrifuge test.

Figure 3.28, 3.29 show comparison between computed and measured peak bending moments to Nisqually earthquake and Ofunato earthquake respectively for various input accelerations. It can be seen that all of the points are located nearby 1:1 line in the graph for both, which means calculated peak

bending moments show reasonably good agreement with measured peak bending moments to Nisqually and Ofunato earthquake. Especially in this case, Computed results predicted well measured results in slightly conservative manner, which means proposed numerical model can predict and design seismic behavior of pile foundation in dry soil deposits on safety side economically. It is concluded that proposed numerical model can simulate dynamic SPSI observed in dynamic centrifuge tests for the case which applied both sinusoidal waves and real earthquake events. And it is identified that proposed modeling method is calibrated for dynamic centrifuge test performed for dry soil deposits

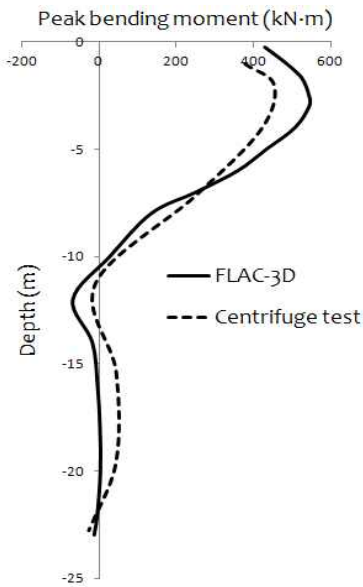

Figure 3.23 Measured and computed peak bending moment along depth (Nisqually earthquake, 0.13g)

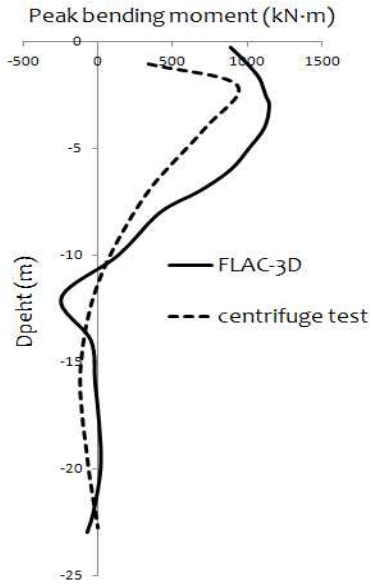

Figure 3.24 Measured and computed peak bending moment along depth (Nisqually earthquake, 0.25g)

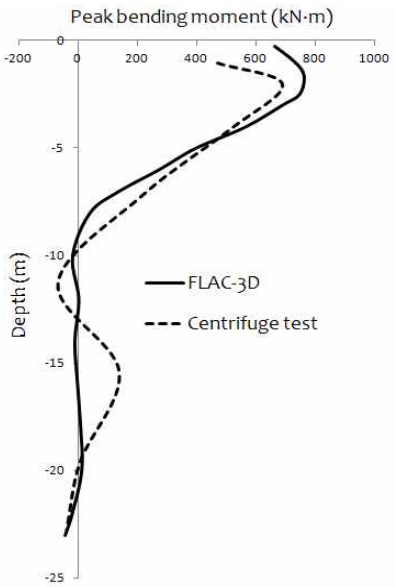

Figure 3.25 Measured and computed peak bending moment along depth (Ofunato earthquake, 0.13g)

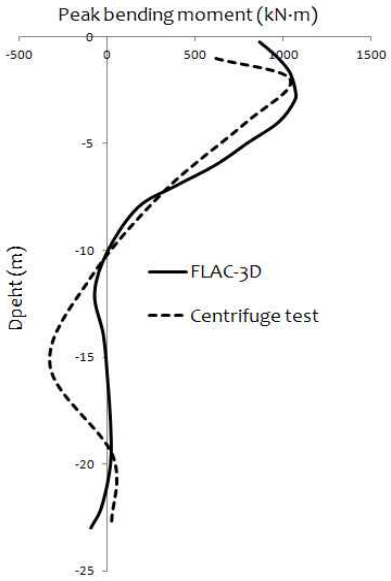

Figure 3.26 Measured and computed peak bending moment along depth
(Ofunato earthquake, 0.25g)

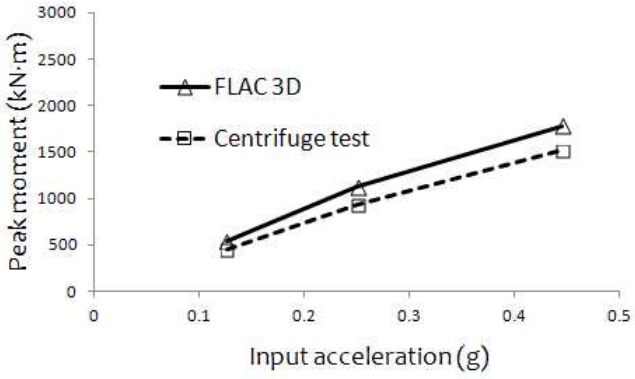

(a) Nisqually earthquake

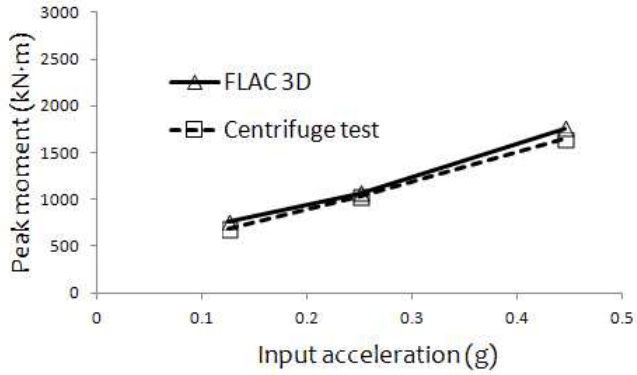

(b) Ofunato earthquake

Figure 3.27 Peak bending moments for various input accelerations

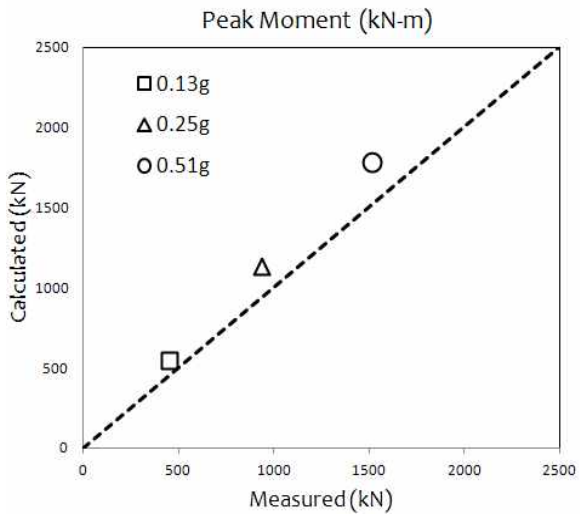

Figure 3.28 Calculated and measured peak bending moments
for various input accelerations (Nisqually earthquake)

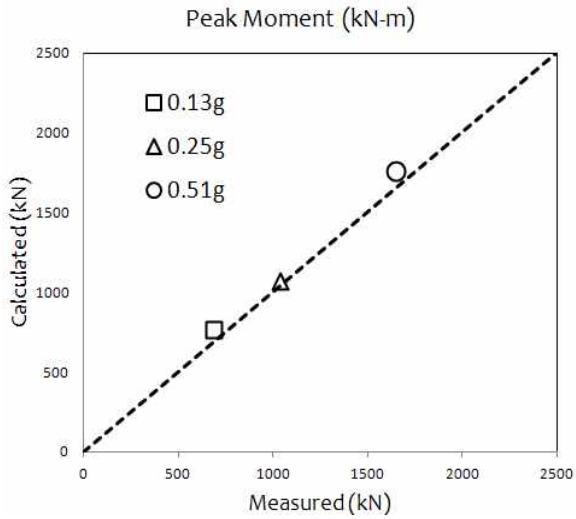

Figure 3.29 Calculated and measured peak bending moments for various input accelerations (Ofunato earthquake)

3.4.2 Validation of the proposed method

In the previous section, 3.4.1, Calibration of the proposed numerical model was conducted comparing computed pile internal responses to measured pile internal responses. Calibration results demonstrated that proposed modeling method was capable of predicting dynamic pile behavior observed in centrifuge test properly. However, Those results were for the single test case which was perform with pile with diameter of 100cm only. Additional comparison with other test case is needed to verify the applicability of numerical model for various conditions.

In this section, validation of the proposed numerical model was conducted using the test case of pile with a diameter of 72cm, and the thickness of 4cm. For the first step, comparison of pile internal responses using the test case which applied sinusoidal waves as input motion was conducted to observe simulation capability of proposed model for various frequencies and accelerations of input excitation. Thereafter, comparison of pile internal responses using the test case which applied real earthquake event, Nisqually earthquake, as input motion was performed. Table 3.7 shows input properties of model pile for validation process. Input properties of model soil were identical with those for calibration process. All the values related with centrifuge tests and numerical analysis described in prototype scale.

3.4.2.1 Pile responses to sinusoidal waves

Figure 3.30, 3.31 show measured and computed peak bending moment along depth for two different input amplitudes. These results demonstrated that there were good agreements between measured and computed peak bending moment envelopes. As input acceleration increases for identical input frequency, peak bending moment also increases both in numerical simulation and centrifuge tests. Figure 3.32 (a), (b), (c) show measured and computed maximum values of bending moment varying input frequencies from 1Hz to 3Hz for input acceleration of 0.13g, 0.25g, 0.45g respectively. It can be seen that results obtained from the proposed modeling method agree reasonably well with values recorded during the centrifuge test for various input motions. Resonance occurred at nearby 1Hz of input frequency both in numerical simulation and centrifuge test, which means the natural frequency of the applied system was about 1Hz in both. It is concluded that proposed numerical model could reproduce important dynamic characteristics for various conditions. Figure 3.33 shows comparison between computed and measured peak bending moments for various input motions. It can be seen that most of the points are located nearby 1:1 line, which identify computed peak bending moments show reasonably good agreement with measured peak bending moments for various input motions. Especially, results from numerical model were almost identical with test results for input acceleration of 0.126g which is Korean seismic design code.

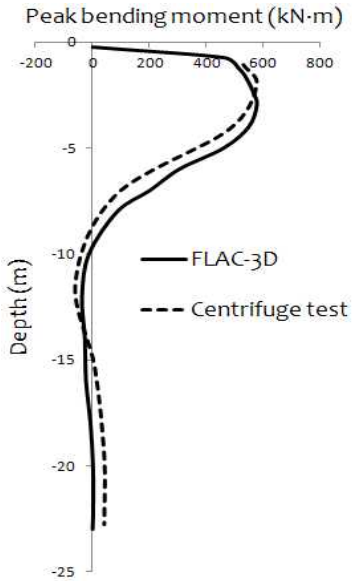

Figure 3.30 Measured and computed peak bending moment along depth (1Hz, 0.13g)

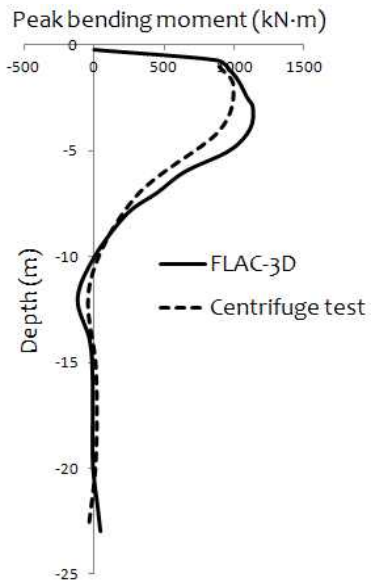

Figure 3.31 Measured and computed peak bending moment along depth (1Hz, 0.25g)

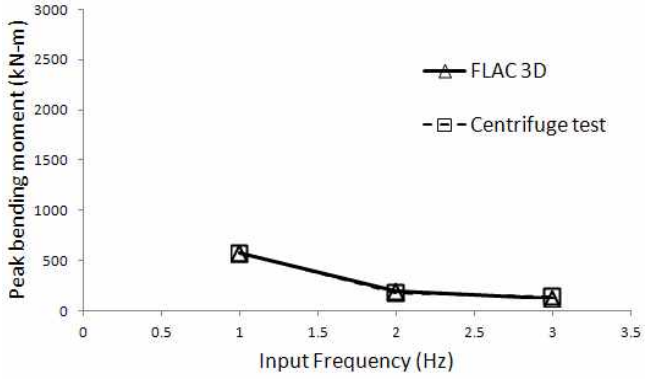

(a) Input acceleration : 0.13g

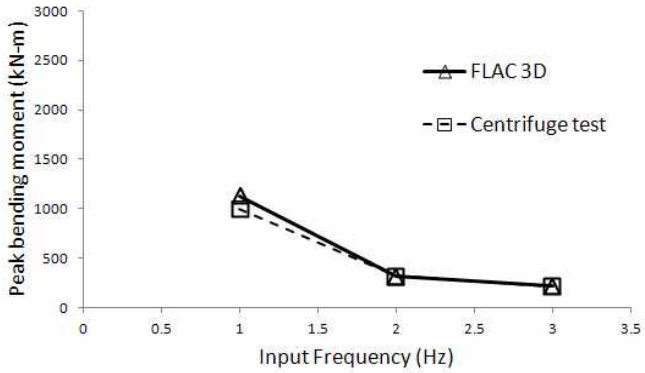

(b) Input acceleration : 0.25g

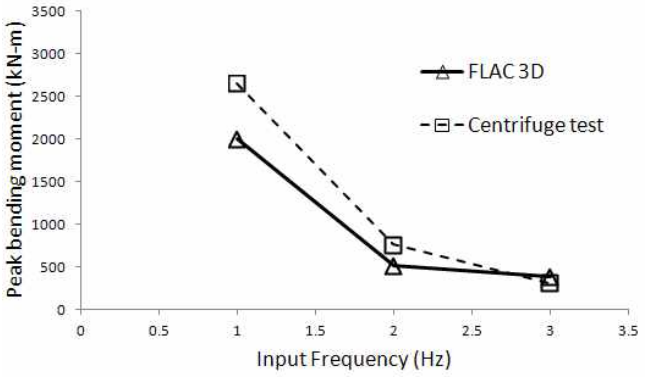

(c) Input acceleration : 0.45g

Figure 3.32 Peak bending moments for various input accelerations

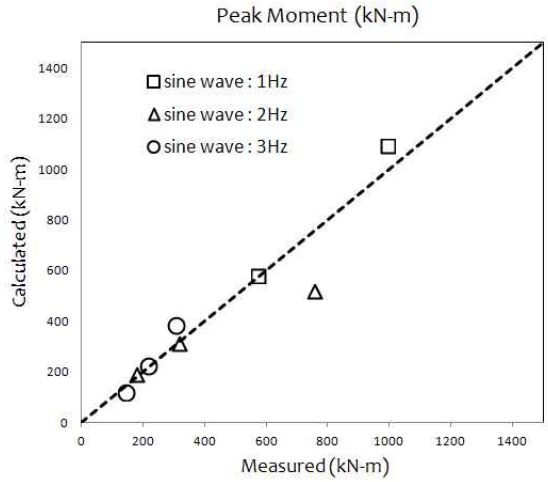

Figure 3.33 Calculated and measured peak bending moments for various input accelerations

3.4.2.2 Pile responses to real earthquake events

Additional validation process was conducted comparing pile internal responses to real earthquake event which is meaningful in practice. In this section, only Nisqually earthquake was considered because test results obtain from Ofunato earthquake showed unreasonable due to defect of measuring devices during the experiment. Figure 3.34, 3.35 show measured and computed peak bending moment along depth to Nisqually earthquake which was scaled to 0.13g, 0.25g respectively. These results demonstrated that computed bending moment envelopes show reasonably good agreement with test results for different input accelerations. Figure 3.36 shows measured and computed maximum values of bending moment for Nisqually earthquake varying input acceleration as 0.13g, 0.25g, 0.51g. It can be seen that results obtained from the numerical model for various input motions agree reasonably well with values recorded during the test. Figure 3.37 shows comparison between computed and measured peak bending moment for various input accelerations. It can be seen that computed peak bending moments were almost identical with measured peak bending moments.

Through a series of additional comparison for validation, it is confirmed that proposed numerical model was capable of simulating dynamic soil-pile-structure interactive behavior embedded in dry soil deposits. And It is identified that proposed modeling method had a applicability to predict dynamic behavior of pile foundations for various conditions

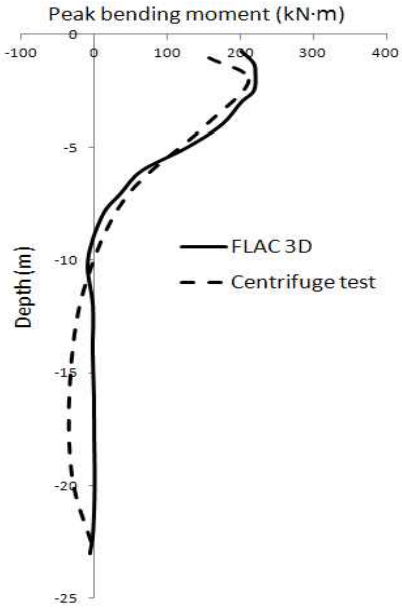

Figure 3.34 Measured and computed peak bending moment along depth (Nisqually earthquake, 0.13g)

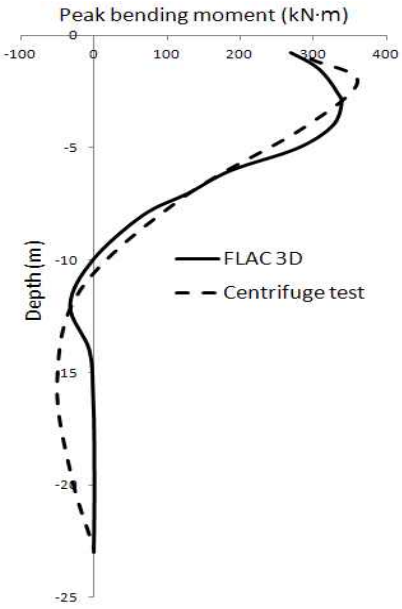

Figure 3.35 Measured and computed peak bending moment along depth (Nisqually earthquake, 0.25g)

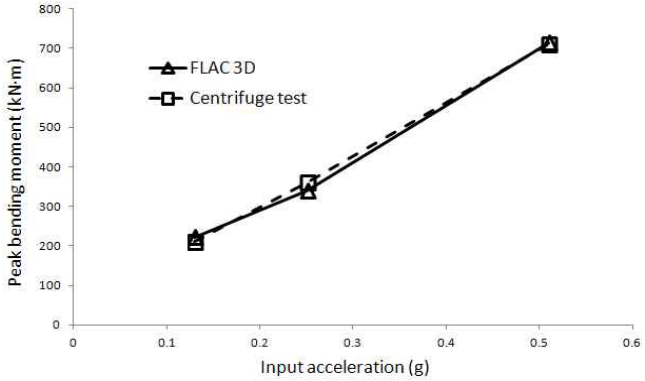

Figure 3.36 Peak bending moments for various input accelerations (Nisqually earthquake)

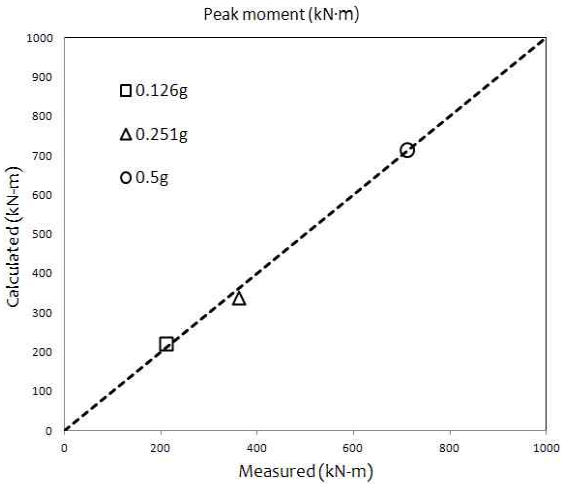

Figure 3.37 Calculated and measured peak bending moments for various input accelerations (Nisqually earthquake)

3.5 Parametric study

Based on the calibration and validation process, applicability of the proposed numerical model was verified. One of the potential advantages of numerical modeling tool is its effectiveness for utilization. Once numerical model is evaluated properly, numerous cases can be simulated and predicted conveniently by proposed numerical method. There are many parameters which affect pile behavior for dynamic problem different from static case. Each parameter sensitively affects seismic behavior of pile foundations and degree of influence of specific parameter varies significantly according to the condition of applied system. Therefore, Influence of important parameters should be identified for reliable seismic design of pile foundations.

In present section, parametric study for various conditions was carried out in order to provide better insight into the dynamic behavior of pile foundations embedded in dry soil deposits. And availability and applicability of the proposed numerical could be confirmed once again comparing with the results from previous researches. Parametric studies were performed varying weight of superstructure, pile length, relative density, and pile head fixity. Input properties of model pile used for parametric study was basically identical to the test case applied for calibration process and detailed properties were varied for applied parameters. Input properties of model soil used for parametric study are showed in Table 3.8 according to three different relative densities, 30%, 50%, 80%. Input properties of model soil were basically identical to Jumunjin sand which was used in calibration and validation of the proposed numerical model. Variation of poisson's ratio with relative density

was determined according to the study performed by Kumar et al. (2010) as shown in below table. Sinusoidal waves were used as input motion to investigate dynamic pile behavior according to various input conditions.

Table 3.8 Input properties of model soil for parametric study

Property	Value for D_r = 30%	Value for D_r = 50%	Value for D_r = 80%
Friction angle (degree)	39	40.5	42
Dry density (t/m^3)	14.2	14.8	15.8
Poisson's ratio	0.32	0.31	0.3
Void ratio	0.851	0.782	0.677

3.5.1 Effect of weight of the superstructure on pile performance

Four different model systems were investigated in this section; weight of the superstructure was 0 kN, 300 kN, 600 kN, 900 kN. Pile head was free condition for rocking and rotation, frequency of input excitation was selected to avoiding natural frequency for each model system. Maximum lateral pile displacement envelopes obtained from four different systems for input acceleration of 0.13g, 0.25g, 0.45g were presented in Figure 3.38 (a), (b), (c). It is noted that variation of weight of the superstructure significantly affects maximum lateral pile displacements. As weight of the superstructure decreases from 900 kN to 0 kN, lateral pile displacements significantly decrease by about 90%. These kinds of phenomena were observed regardless of the magnitude of input accelerations. In the analysis every condition was identical in four model systems except weight of the superstructure, which means inertial forces induced by superstructure were responsible for the observed lateral responses of pile foundations. In other words, same kinematic forces have been developed in piles regardless of weight of the superstructure. Ishihara (1997) indicated that inertial forces are the predominant forces in dry condition and mainly responsible for development of maximum bending moment near the pile head. This is confirmed by numerical model. Inertial forces induced by superstructure were dominant in dry soil deposits for various input amplitudes.

Evaluation of the relation between weight of the superstructure and lateral pile displacements was carried out. Figure 3.39 (a), (b), (c) show relationship between weight of superstructure and maximum pile lateral

displacements. As weight of the superstructure increases and acceleration of input excitation increases, maximum lateral pile displacements increase also. It is noted that weight of the superstructure and maximum lateral pile displacement show linear relation with high level of R square in every input accelerations. If this phenomenon is adopted in practice, maximum lateral pile displacements could be predicted for certain weight of the superstructure. Then lateral responses and movement of pile foundation could be predicted for any magnitude of earthquake, results in critical damage of whole structural system as well as pile foundations would be prevented properly.

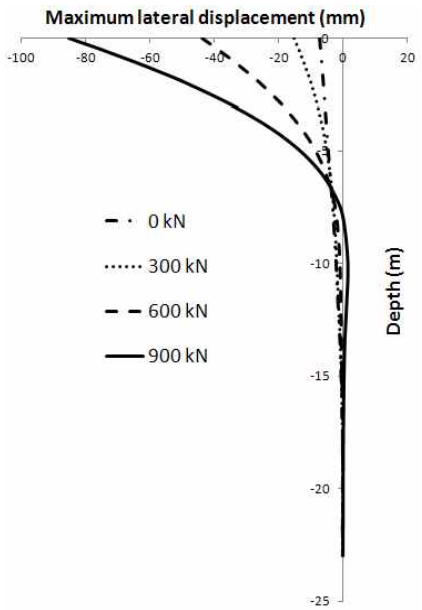

(a) Input acceleration : 0.13g

Figure 3.38 Maximum lateral pile displacement envelopes obtained from four different weight of superstructure (continue in next page)

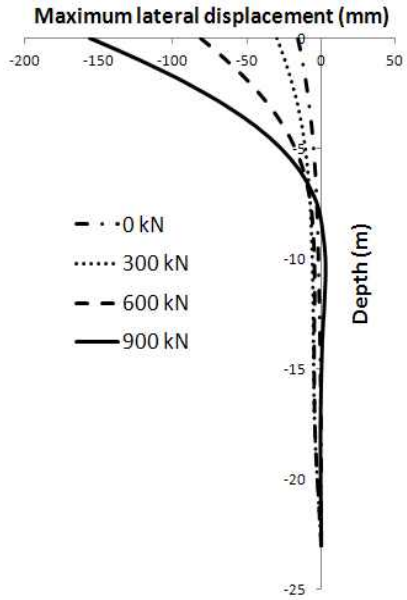

(b) Input acceleration : 0.25g

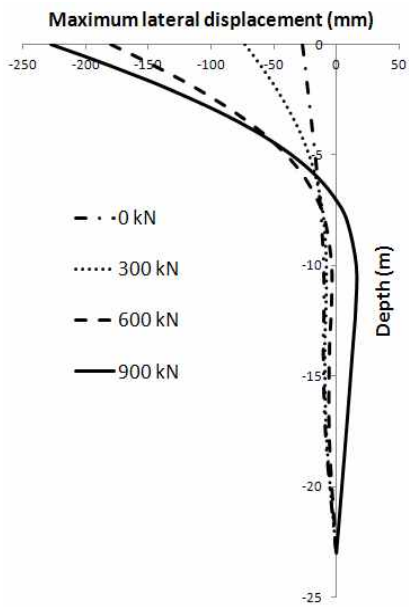

(c) Input acceleration : 0.45g

Figure 3.38 Maximum lateral pile displacement envelopes obtained from four different weight of superstructure

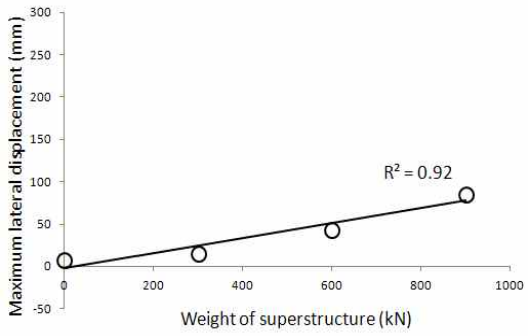

(a) Input acceleration : 0.13g

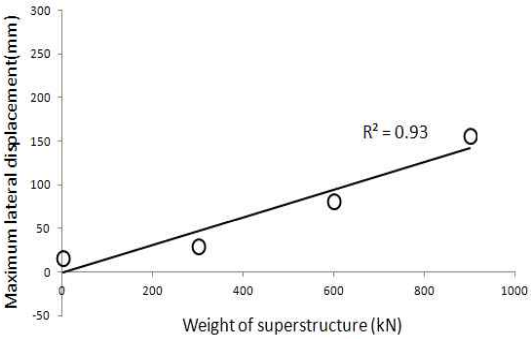

(a) Input acceleration : 0.25g

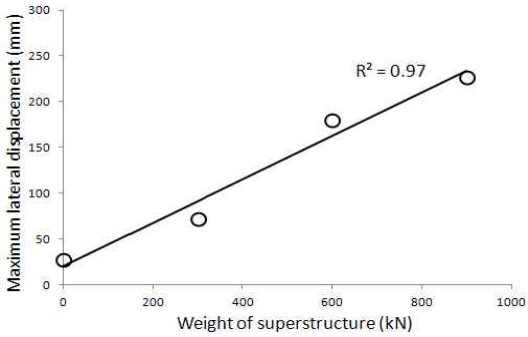

(a) Input acceleration : 0.45g

Figure 3.39 Relationship between weight of superstructure and maximum lateral pile displacement

3.5.2 Effect of relative density on pile performance

In order to investigate dynamic pile performance for different relative densities, internal pile responses obtained from repetitive analysis for three relative densities; 30%, 50%, 80% were discussed. Figure 3.40 (a), (b) show peak bending moment envelopes for three different relative densities varying input accelerations; 0.13g, 0.25g. It is observed that peak bending moments show very similar pattern for different relative densities. This kinds of phenomena occurred in maximum pile lateral displacements also (Figure 3.41). It is noted that maximum pile lateral displacements show almost identical for three different relative densities. These results were significantly different pattern with previous section which is the parametric study for weight of the superstructure. In this analysis, every condition was identical in three model systems except relative density, which means relative density induced kinematic forces were responsible for the observed dynamic responses of pile foundations. In other words, same inertial forces have been developed in piles regardless of relative density. It is concluded that effect of kinematic forces induced by soil deformation was relatively insignificant in dry soil deposits. .

According to the two kinds of parametric studies, important characteristics of dynamic soil-pile-structure interaction embedded in dry soil deposits were identified. In dry sand, inertial forces induced by superstructure were significant, while kinematic forces induced by soil deformation were relatively insignificant. This characteristic will have to be considered when seismic design of pile foundations is performed in dry condition.

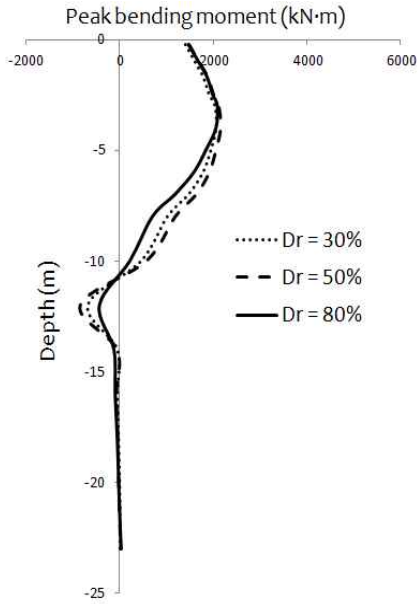

(a) Input acceleration : 0.13g

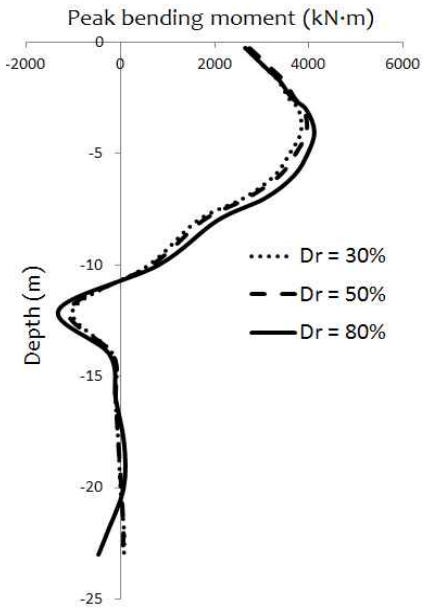

(a) Input acceleration : 0.25g

Figure 3.40 Peak bending moment envelopes obtained from three different relative densities

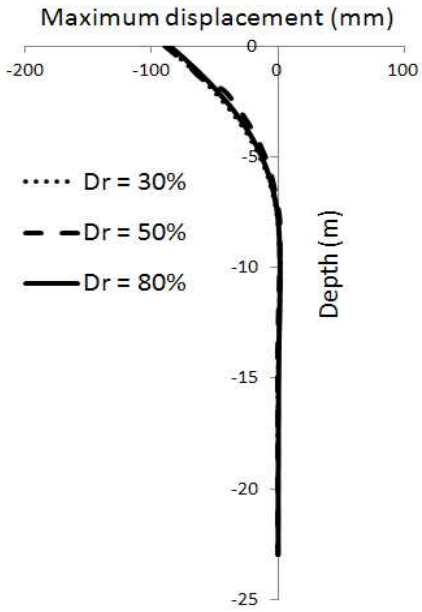

(a) Input acceleration : 0.13g

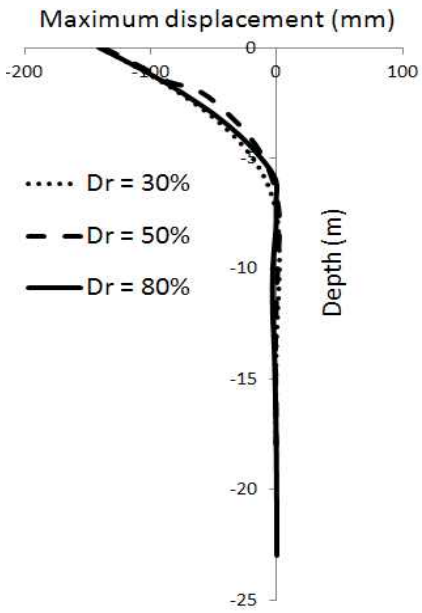

(a) Input acceleration : 0.25g

Figure 3.41 Maximum lateral pile displacement envelopes obtained from three different relative densities

3.5.3 Effect of pile length on pile performance

Prakash and Agarwal (1967) reported test data on model piles subjected to horizontal load at 5 cm above the sand surface. The pile lengths were 10, 20, 30, 40, 50, and 60 cm. It is seen that as the pile length increases, the ground deflection of a pile of constant cross section decreases at the same load. This decrease in deflection occurs first at a very rapid rate. Subsequently, this rate decreases, and, beyond a characteristic length of the pile, the deflections are not materially affected. This length L_a is defined as infinite length of the pile. This length would obviously be a function of pile stiffness EI and soil stiffness k. The greater the pile stiffness, the greater L_a, and the greater the soil stiffness, and smaller L_a. It is easy to imagine that for the deflection of the pile y_x under a given load and at any depth, x is composed of the rigid-body movement and that which is due to curvature of the pile. The latter decreases as the pile stiffness EI increases, while other things remain the same. If the pile becomes rigid enough so that its deflections, due to curvature, may be neglected as compared with its rigid-body movements, it is called a rigid pile or a pole.

From the analytical approaches performed by Matlock and Reese (1962), a quantity T, termed the relative stiffness factor was defined as equation 3.12.

$$T = \sqrt[5]{\frac{EI}{n_h}} \tag{3.12}$$

where n_h is soil reaction constant. Analytical approach showed that the pile undergoes only rigid-body deflections and that deflections caused by curvature are negligible. And the piles with L (pile length) ≤ 2T behaves as

rigid piles or poles. Further, pile length beyond 5T is not effective in altering the deflections of the pile. Therefore, solutions for long piles are applicable in this case. Infinite length of the pile applied in this study was calculated as about 9.15 m.

Broms (1964) suggested a simplified distribution of deflection and bending moment of free-head piles in a cohesionless soil. Possible deflections, bending moment distributions for 'long' and 'short (a.k.a. rigid)' piles are shown in Figure 3.42, 3.43.

In order to investigate dynamic pile performance for various pile length, internal pile responses obtained from repetitive analysis for nine different pile lengths; 2 m (T), 4 m (2 T), 5 m (3 T), 8 m (4.5 T), 9 m (5 T), 10 m (5.5 T), 12 m (7 T), 18 m (10 T), 23 m (13 T). Figure 3.44 shows maximum lateral pile displacement envelopes for various pile lengths. When pile length is longer than 5T, distribution of pile deflection show long pile behavior suggested by Broms. On the other hands, when pile length is shorter than 3T, distribution of pile deflection show short pile behavior suggested by Broms. Piles which have a length between 3T and 5T show intermediate behavior in the figure. Figure 3.45 shows peak bending moment profiles for various pile lengths. As similar with the case of deflection, when pile length is longer than 5T, distribution of bending moment show long pile behavior suggested by Broms. The boundary between short pile and intermediate pile was not clear in bending moment profiles. It is similar pattern with suggested distributions from Broms, which means distribution of bending moment for short pile and intermediate pile was not clear also in figure 3.43.

Overall, from the analysis of maximum lateral pile displacement and

peak bending moment for various pile length, long pile behavior was observed when pile length became 5.5T and short pile behavior was observed when pile length became 2T. These results were considerably coincident with the studies carried out by previous researchers. Through a series of the parametric study for pile length, it is concluded that existing studies about pile length such as infinite length are generally valid.

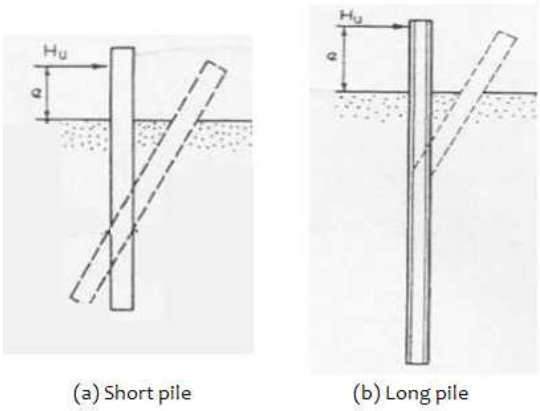

Figure 3.42 Deflection of free-head piles in a cohesionless soil (Broms, 1964)

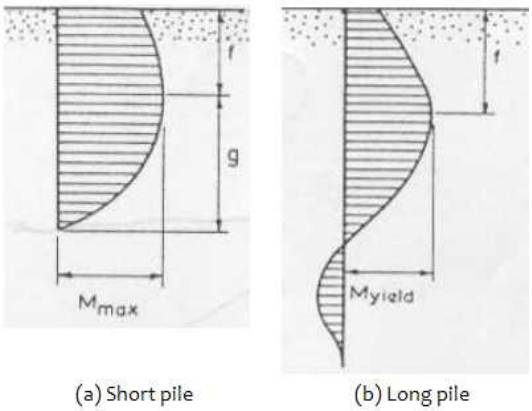

Figure 3.43 Bending moment of free-head piles in a cohesionless soil (Broms, 1964)

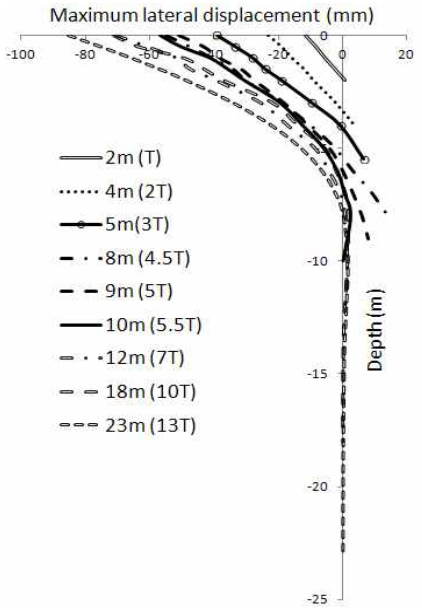

Figure 3.44 Maximum lateral pile displacements for various pile lengths (input acceleration : 0.13g)

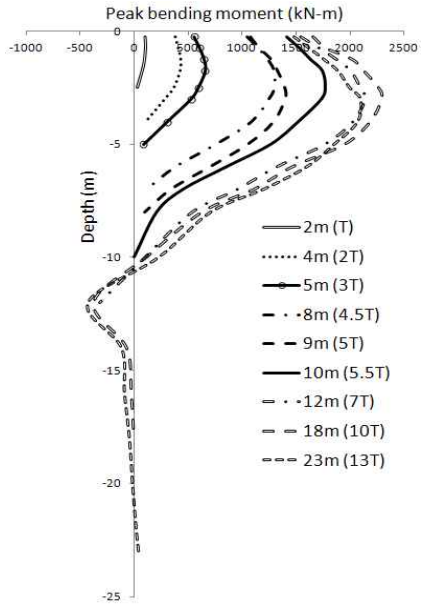

Figure 3.45 peak bending moment profiles for various pile lengths (input acceleration : 0.13g)

3.5.4 Effect of pile head fixity on pile performance

Two different pile head conditions were investigated in this section; free-head and fixed-head condition. Pile head fixity was controlled in numerical modeling tool, FLAC3D, by adjusting restrain option above the ground surface. Input acceleration of 0.13g was used in the analysis same with other cases. Peak bending moment profiles for different pile head fixity varying pile length as 23 m (13 T), 18 m (10 T), 8 m (4.5 T) are shown in Figure 3.46 (a), (b), (c). It is noted that peak bending moment occurred at different depth according to the pile head fixity. For the fixed-head pile, maximum bending moment occurred at the pile cap, while for the free-head pile, maximum bending moment occurred at about 3 m below the pile cap for every pile length. On the other hand, as shown in Figure 3.46 (c), maximum value of bending moment for fixed-head pile significantly decreased when pile length was 8 m (4.5 T). This was because relatively rigid behavior was revealed due to decrease of pile length to 4.5 T which was identified as intermediate pile length in previous section.

Rahmani and Pak (2012) carried out finite element analysis for soil-pile system, and drew the results that in saturated sand, the fixity of pile head leads to much more increase in maximum bending moment compared to that corresponding to dry soils. According to the their results, if the pile head is fixed against rotations, maximum bending moment increases about 95% ~ 130% for various analysis cases. However, in dry ground, pile head fixity leads to nearly 20% increase in maximum bending moment. In liquefying soils, when the pile head is restrained rotationally, relative lateral

displacement of pile at upper and lower regions significantly increases due to liquefaction of surrounding soil; larger relative displacements lead to larger bending moment so boundary condition of pile head has a big effect on bending moment in the cases where the ground liquefies. Coincidence with Rahmani and Pak, in this study, maximum bending moment obtain from fixed-head pile condition was very similar with the maximum bending moment obtained from free-head pile condition despite of the difference of occurred location. It is concluded that previous study for pile head fixity is confirmed by proposed numerical model, applicability is also verified.

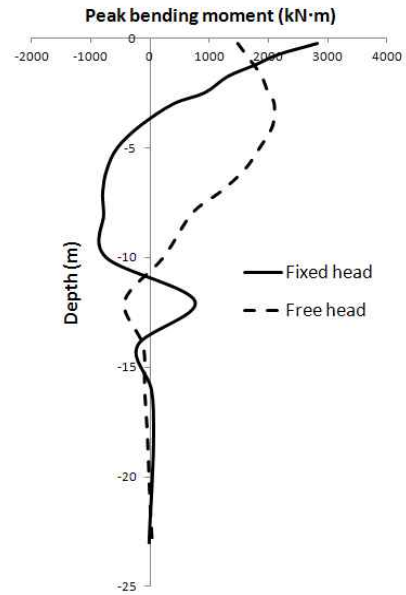

(a) Pile length : 23 m (13 T)

Figure 3.46 peak bending moment profiles for different pile head fixity (input acceleration : 0.13 g) ,(continued in next page)

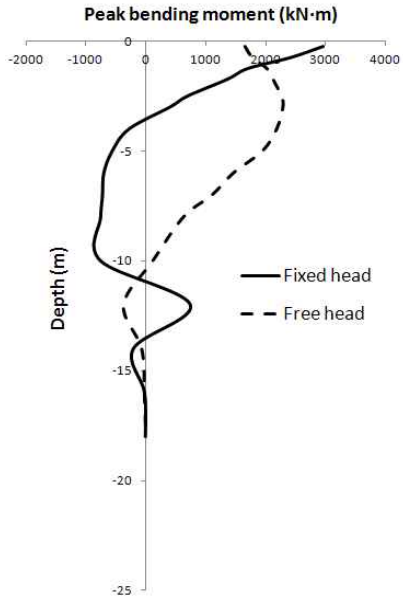

(a) Pile length : 18 m (10 T)

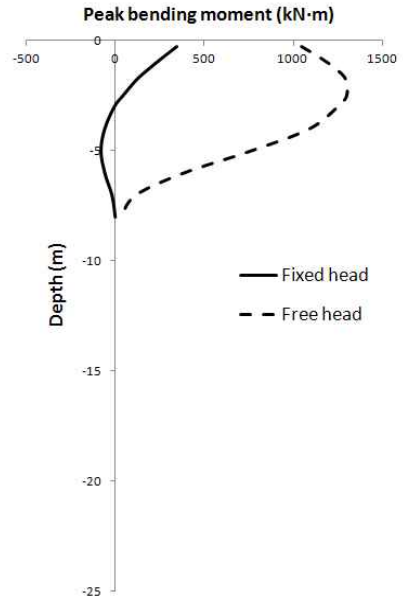

(a) Pile length : 8 m (4.5 T)

Figure 3.46 peak bending moment profiles for different pile head fixity (input acceleration : 0.13 g)

3.6 Summary and conclusions

In this chapter, three dimensional numerical simulation of dynamic soil-pile-structure interactive behavior embedded in dry soil deposits was performed. First, modeling methodology was evaluated for dry condition. Mohr-Coulomb plasticity model was applied as soil constitutive model. Hysteretic damping was adopted to consider both the nonlinearity of soil modulus and the energy dissipation. Initial shear modulus and yield depth was determined and calculated by proper empirical relations. Using user defined FISH function in FLAC3D, shear modulus of soil was continuously input according to depth. Interface model which is able to simulate fully contact, slippage, separation state according to the input motion was adopted. Interface elements consists of normal and shear spring, interface stiffness was determined by formula obtained from elastic relation of stress and strain. Applied interface model could also consider nonlinearity of soil from shear modulus and bulk modulus in stiffness equation. Interface stiffnesses were input using FISH function according to depth. Simplified continuum modeling method was used as a boundary condition to reduce analysis time and obtain accurate pile responses. Far field responses were input at the boundary of near field as acceleration-time histories. Pile was modeled by elastic.

Calibration and validation of the proposed modeling method was performed by comparing with test results. In the first step, calibration of the numerical model was conducted using the test case of pile with a diameter of 100cm, and thickness of 4cm. Pile internal responses such as peak bending

moment and maximum lateral pile displacement profile obtained from numerical simulation show good agreement with those from dynamic centrifuge tests. Thereafter, validation of the numerical model was conducted using the test case of pile with a diameter of 72cm, and thickness of 4cm. There were reasonably good agreement between measured and computed dynamic pile responses also. Based on a series of calibration and validation procedure, it is concluded that applicability of the proposed modeling method was verified.

Parametric study for various conditions was carried out. First of all, effect of weight of the superstructure on dynamic behavior of pile was investigated. It is noted that as weight of the superstructure decreases from 900 kN to 0 kN, maximum lateral pile displacement decreases about 90%. It is concluded that inertial forces induced by superstructure is dominant in dry soil deposits and it is confirmed by numerical method. Effect of relative density on dynamic behavior of pile was investigated. Peak bending moment and maximum lateral pile displacement profiles were almost identical for three different relative densities. It is confirmed that effect of kinematic forces induced by soil movement is relatively insignificant in dry condition by numerical method. Effect of pile length on dynamic behavior of pile was investigated. When pile length was longer than infinite length (5 T), long pile performance was observed. When pile length was between 2 T and 5 T, intermediate pile performance was observed. When pile length was shorter than 2T, short pile performance was observed. Overall, long pile behavior was observed when pile length became about 5 T, short pile behavior was observed when pile length became about 2 T. It is concluded that existing

studies about pile length such as infinite length are generally valid. Effect of pile head fixity on dynamic behavior of pile was investigated. Maximum bending moment occurred at different depth according to the pile head fixity. Maximum bending moment occurred at pile cap for fixed head condition, while maximum bending moment occurred at about 3m below ground surface for free head condition. On the other hands, bending moment for fixed head pile significantly decreased when pile length was 8 m (4.5 T). This is because of the relative rigid behavior of the pile foundation due to decrease of pile length to 4.5 T which was identified as intermediate pile length in previous section.

Based on the parametric studies for various conditions, the influence of several parameters on seismic behavior of soil-pill-structure system was established and availability and applicability of the proposed numerical were confirmed once again comparing with the results from previous researches.

4. Numerical Simulation for liquefiable soil deposits

4.1 Introduction

Liquefaction represents one of the biggest contributors to damage of constructed facilities during earthquakes. This phenomenon was reported as the main cause of damage to pile foundations during the major earthquakes as presented in section 2.2. However, application of the design procedure developed for evaluating pile behavior under earthquake loading involving liquefiable ground is uncertain since the performance of piles in liquefied soil layers is much more complex than that of non-liquefying soil layer. It is not only because the superstructure and the surrounding soil exert different dynamic loads on pile, but also because the stiffness and shear strength of the surrounding soil diminishes over time due to nonlinear behavior of soil and also pore water pressure generation. Moreover, prediction of seismic response of pile foundations in liquefying soil layer is difficult due to both a lack of physical data against which they can be evaluated, and the continued lack of understanding of the mechanisms involved in soil-pile-structure interaction in soft and liquefied soils. Resolving these uncertainties is an important step in current earthquake hazard remediation.

In this chapter, modeling methodology to simulate dynamic soil-pile-structure interactive behavior in liquefiable sand was presented. First, dynamic centrifuge test (Wilson, 1998) which is used as exact solution for

prototype is introduced. The finite difference code, FLAC3D was used in this study to model the dynamic soil-pile-structure interaction problem also in liquefiable soil condition. Additional soil constitutive model was applied to estimate dynamic behavior of pile embedded in liquefiable soil deposits, which can directly capture development of pore water pressure according to shear deformation of soil in real time.

Calibration and validation procedure are introduced afterward. Calibration of the proposed modeling method was performed using results from test case of upper liquefiable layer with a relative density of 55%. Development of pore water pressure according to depth and pile internal responses obtained from numerical model are compared to those of centrifuge tests. Validation of the proposed modeling method was performed using results from test case of upper liquefiable layer with a relative density of 35%. Applicability of the numerical model was estimated by comparing computed values with measured values.

Parametric study for various conditions was conducted in order to understand the effect of several variables on the dynamic pile behavior and to confirm once again the availability and applicability of the proposed numerical comparing with the results from previous researches. In this study, frequency of input excitation, thickness of liquefiable layer, relative density, weight of superstructure were considered and detailed discussions are presented.

4.2 Dynamic centrifuge tests

In this section, a series of centrifuge tests performed to evaluate the dynamic soil-pile-structure interactive behavior using the shaking table on the 9m radius The National Geotechnical Centrifuge at UC Davis is introduced (Wilson. 1998). Tests were conducted with different soil conditions and various input motions. Test apparatus, test materials, and test programs will be introduced.

4.2.1 Description of the centrifuge and model layouts (Wilson, 1998)

The National Geotechnical Centrifuge at UC Davis has a radius of 9m and is equipped with a large shaking table driven by servo-hydraulic actuators (Kutter et al. 1994). The centrifuge has a maximum model mass of about 2500 kg, an available bucket area of $4.0\,m^2$, and a maximum centrifugal acceleration of 50 g. The earthquake simulator was designed to accommodate 1.7 m long models and provide 15 g input shaking accelerations. Earthquake motions are produced by two pair of servo hydraulic actuators acting in parallel, one pair mounted on either side of the model container.

A Flexible Shear Beam (FSBI) container was designed and constructed for this project. The FSBI container has inside dimensions of 1.72 m long, 0.685 m wide, by 0.70 m deep. FSBI consists of six hollow aluminum rings separated by 12 mm thick layers of 20 durometer neoprene. The mass of each

of the upper three rings is about one-half the mass of each of the lower three rings. The combined mass of the six rings and rubber is about 25% of the soil profile mass (assuming the container is full of soil). The amount of neoprene separating the rings is varies such that the shear stiffness of the container increases with depth. The fixed base natural frequency of the empty container is about 15-20 Hz (0.5-0.67 Hz in prototype) for the larger shaking events presented herein. Vertical shear rods in the soil near the container ends provide complementary shear stresses (Divis et al. 1996). A section of a portion of the rings, neoprene layers, and shear rods at the end of the container is shown in Figure 4.1.

All the tests were performed at a centrifugal acceleration of 30 g. Note that the centrifugal acceleration varies with radial position, and thus varies from 29.2 g at the soil surface to 31.5 g at the container base. All results are presented in prototype units unless otherwise noted.

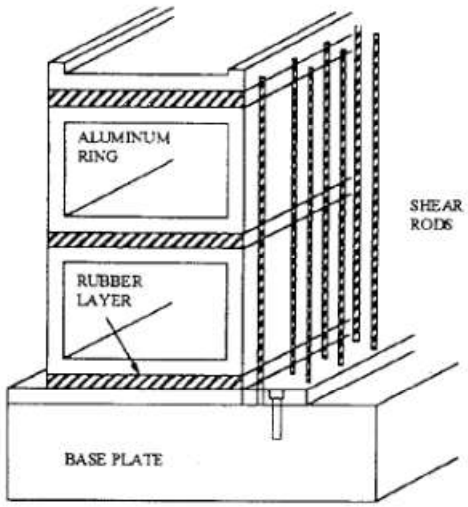

Figure 4.1 Schematic of rings and shear rods (Divis et al. 1997)

Table 4.1 Summary of soil profiles (Wilson, 1998)

Container	Soil profile		Pore fluid
	Upper layer (9 m thick)	Lower layer (11.4 m thick)	
Csp1	Sand (D_r=55%)	Sand (D_r=80%)	Water
Csp3	Sand (D_r=35-40%)	Sand (D_r=80%)	HPMC-water
Csp3	Sand (D_r=55%)	Sand (D_r=80%)	HPMC-water
Csp4 & 5	Reconstituted Bay Mud (NC)	Sand (D_r=80%)	Water

*Upper layer was only 6.1 m thick (prototype-before testing) in Csp4 & 5.

The soil profiles are summarized in Table 4.1. In all cases, the soil profile consisted of two horizontal soil layers. The lower layer for all tests was dense Nevada sand, a fine, uniform sand ($C_u = 1.5, D_{50} = 0.15$ mm). The upper layer was medium-dense Nevada sand in Csp1 and Csp3, loose Nevada sand in Csp2, and normally consolidated (NC) reconstituted Bay Mud (LL≒90, PI≒40) in Csp4 and Csp5. In all tests the sand was air pluviated, subjected to a vacuum (typically achieving≒90 kPa vacuum), flushed with carbon dioxide and then saturated under vacuum. The pore fluid was water in tests Csp1, Csp4, Csp5, and was a viscous fluid in tests Csp2 and Csp3. The viscous fluid consisted of a mixture of water and hydroxyl-propyl methyl-cellulose (HPMC) (Stewart et al. 1998). The viscosity of the pore fluid was increased to improve the simultaneous scaling of consolidation and dynamic processes. Note that dynamic time on the centrifuge is scaled as 1/n and consolidation time is

scaled as $1/n^2$, resulting in a prototype that consolidates n-times faster than desired. By increasing the pore fluid viscosity in the model the consolidation rate can be decreased. In these tests, the 10-fold increase in fluid viscosity and the $1/30^{th}$ scale modeling can be viewed as having the net result of consolidation occurring three times faster than would occur in the prototype, assuming pure water as the prototype pore fluid.

P-wave velocities were measured from top to bottom of the soil profile near the container center. Values were high enough (on the order of 1000 m/s) to indicate the sample was very close to saturated. Note it is difficult to determine the p-wave velocity in the sample with certainty, as the sampling rate required for accurate measurement is beyond the capability of the data acquisition system. Fortunately the relationship between p-wave velocity and degree of saturation is very steep as complete saturation is approached (e.g. see Gazetas 1991), so simply showing that the p-wave velocity is close to 1000 m/s was considered sufficient to ensure a high degree of saturation (i.e. > 99.5%).

The structural systems are illustrated in Figure 4.2. Detailed drawings of the highly instrumented single pile system are given in Figure 4.3. The superstructure mass was typically about 500 kN (prototype). Pile was model of a prototype steel pipe pile 0.67 m in diameter, 16.8 m long, with a 72 mm wall thickness. Pile material properties are listed in Table 3.2. To represent typical bridge fundamental periods, column heights were selected to give fundamental periods for the structural models, the pile tips were about 3.7 m above the container base (about 5.5 pile diameters); thus the end bearing of the piles should not have been significantly influenced by the container base.

Table 4.2 Pile properties (Wilson, 1998)

Material	6061-T6 Aluminum
Yield stress (Mpa)	290
Young's modulus (Mpa)	70
Outside diameter (m)	0.667
Wall thickness (mm)	72.4
Moment of inertia (m^4)	6.1×10^{-3}
Yield moment, M_y (MN-m)	5.3

Piles were driven into the sand at 1 g. Driving was done by dropping hammers from constant drop-heights onto the superstructure masses. A guide rod kept the hammer impact centered on the superstructure mass and a guide bar kept the piles aligned horizontally and vertically. Hammer blows per 2.54 cm (1 inch) of penetration were recorded. In all test the single pile structures were driven after saturation.

Each container was subjected to a series of shaking events, beginning with very low-level shaking events to characterize the low-strain response of the soil and soil-structure systems. Successive events progressed through very strong motions with peak base accelerations of up to 0.6 g. Earthquake events generally sequenced in order of increasing amplitude, with periodic repeats of smaller events. Input base motions included step displacement waves and scalar multiples of recorded earthquake motions. In this study, test cases of Csp2, Csp3 were used for numerical simulation. The earthquake motions used are summarized in Table 3.3 and acceleration-time history of Kobe earthquake scaled to 0.22g is shown in Figure 4.4. Each shaking event was separated by

an amount of time that exceeded the time required for full dissipation of any excess pore pressures.

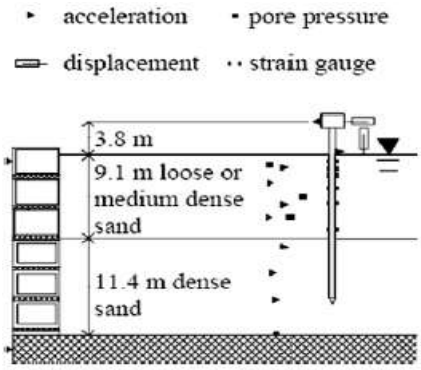

Figure 4.2 Layout of the model for centrifuge test (Wilson, 1998)

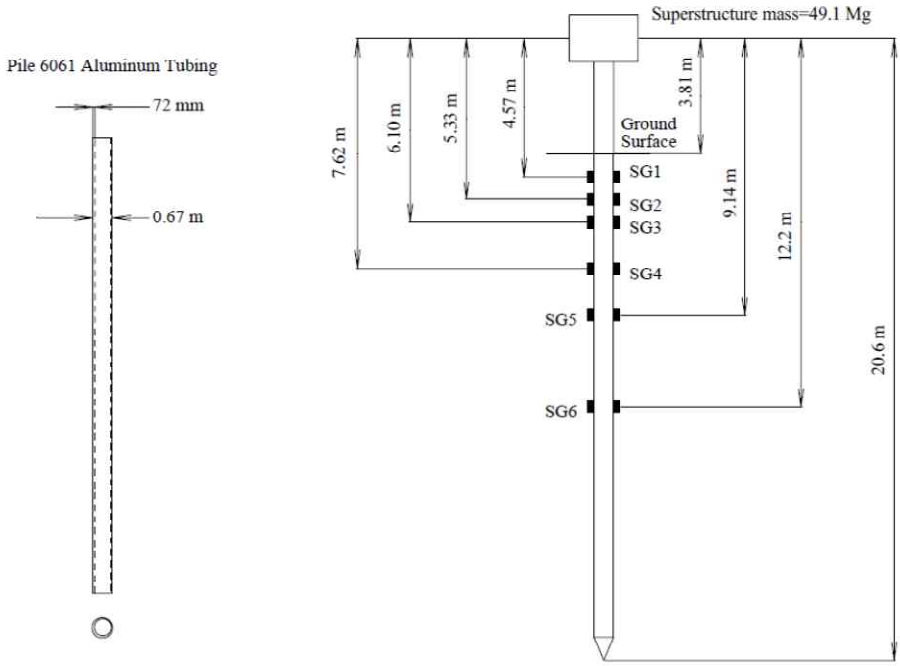

Figure 4.3 Highly instrumented single pile (Wilson, 1998)

Table 4.3 Earthquake motions used (Wilson, 1998)

Motion	Recording
Kobe	1995 Kobe earthquake – Port Island 83m depth, NS direction
Santa Cruz	1989 Loma Prieta earthquake – UCSC/Lick Lab, Ch.1-90 degrees
Santa Cruz*	Same as above, but the original time step was doubled

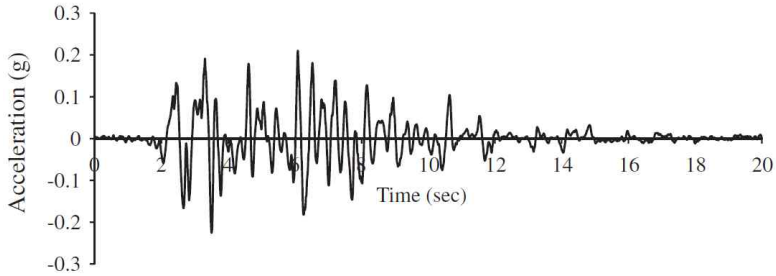

Figure 4.4 Input earthquake ground motion
(Acceleration record of Kobe (1995) earthquake scaled to 0.22g)

4.3 Modeling methodology

In this section, modeling methodology evaluated for prediction of dynamic SPSI embedded in liquefiable soil deposits is explained. FLAC3D was used same as dry case, three-dimensional continuum modeling was carried out. Based on the modeling methodology developed for dry condition, additional soil constitutive model was adopted to estimate dynamic behavior of pile embedded in liquefiable soil deposits, which can directly capture development of pore water pressure according to shear deformation of soil in real time.

First, two kinds of deformation analysis methods considering liquefaction are presented. One is total stress method, the other is effective stress method. Thereafter, theoretical background of Finn model which was adopted as additional constitutive model for numerical simulation of dynamic SPSI embedded in liquefiable sand was explained.

4.3.1 Deformation analysis considering liquefaction

4.3.1.1 Total stress method

Once earthquake occurs, shear waves which depart from the bed rock transmit to upper soil layer and cyclic shear stress is induced to soil elements (Figure 4.5). If equivalent cyclic shear stress induced by earthquake is larger than cyclic stress required to cause liquefaction, liquefaction occurs. According to the figure 4.6, zone of liquefaction can be determined. Liquefaction is similar mechanism with strain-softening which occurs when soil is sheared under undrained condition (Figure 4.7). It is a concept that undrained strength gradually decrease to the steady state as strain go through the maximum value. The strength at this state is referred to residual strength. After estimate the zone of liquefaction and residual strength after liquefaction, dynamic numerical analysis is performed by input strength parameters corresponds to the residual strength in the zone of liquefaction.

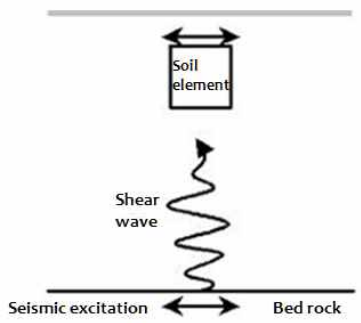

Figure 4.5 Earthquake wave transmission

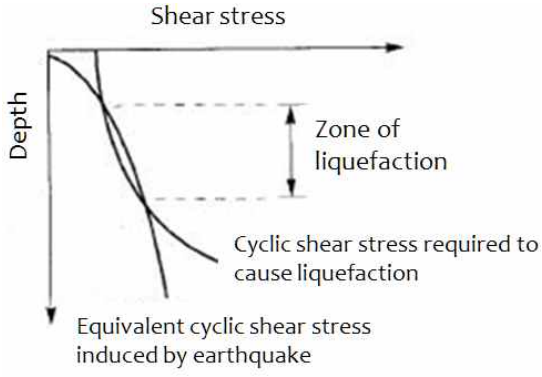

Figure 4.6 Shear stress & resistance according to depth

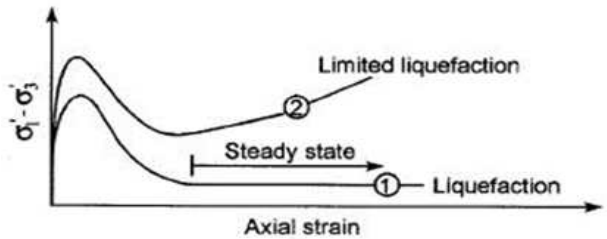

Figure 4.7 Undrained compression test of sand

4.3.1.2 Effective stress method

Total stress method stated above is such a simplified method to analyze soil behavior in the zone of liquefaction. On the other hand, effective stress method is much more complex and difficult to perform the analysis but straightforward approach. Three steps of total stress method are combined in one step. In effective stress method, development of excess pore pressure, reduction of effective stress, time of occurring liquefaction and deformation behavior after the liquefaction, etc. for any location can be directly captured in real time. Therefore, for the accurate adoption of effective stress analysis, proper model for liquefaction is necessary to reproduce liquefaction phenomena. There are several models for liquefaction which is able to adopt effective stress method such as Finn model, UBC-Sand model, DSC (Distributed State Concept) mode. In this study, Finn model was used to simulate dynamic soil-pile-structure interactive behavior in liquefiable soil deposits.

4.3.2 Theoretical background of the Finn model

When earthquake occurs, shear waves transmitted from bed rock causes shear stress to upper soil elements, shear deformation is induced (Figure 4.8). Shear stress is exerted to soil elements and volume change is induced, resulting in development of excess pore water pressure in every cycle. In

reality, pore pressure build-up is a secondary effect, although many people seem to think it is the primary response to cyclic loading. The primary effect is the irrecoverable volume contraction of the matrix of grains when a sample is taken through a complete strain cycle when the confining stress is held constant.

Martin et al. (1975) performed drained cyclic simple shear test for Crystal silica sand with relative density of 45% to formulate those kinds of aspects. Once shear deformation is induced to saturated soil elements under undrained condition, excess pore pressure is developed due to reduction of soil volume. And soil volume expands due to reduction of effective stress simultaneously. For every stage of cyclic shear deformation, compatibility condition of volume change is given as Equation 4.1.

$$\frac{\Delta u \cdot n_e}{K_w} = \Delta\varepsilon_{vd} - \frac{\Delta u}{E_r} \tag{4.1}$$

where, Δu is increment of pore pressure, $\Delta\varepsilon_{vd}$ is increment of volume decrease, E_r is tangent modulus of unloading curve, n_e is porosity, K_w is bulk modulus of water. Above expression means that increment of void ratio under undrained condition (water compression) is identical with subtraction volume increase of soil element due to pore pressure from the volume change of soil element under drained condition. Above equation can be reconstructed as Equation 4.2 which is the expression about pore water pressure.

$$\Delta u = \frac{E_r \cdot \Delta\varepsilon_{vd}}{1 + \frac{E_r \cdot n_e}{K_w}} \tag{4.2}$$

where, $K_w = 4 \times 107$ psf and E_r is about 106 psf in saturated soils. Because $\frac{E_r \cdot n_e}{K_w}$ is negligible in this condition. increment of pore water

pressure at every stage of shear deformation can be expressed by multiplication of the increment of volume decrease by tangent modulus of unloading curve.

To obtain a formula about the increment of volume decrease, undrained cyclic simple shear test under constant shear strain for Crystal silica sand with relative density of 45% was conducted. Relationship between load cycle and volume strain under constant shear strain as 0.1 %, 0.2 %, 0.3 % can be obtained. And, from this relationship, increment of volume decrease when shear strain of γ is exerted under ε_{vd} of accumulated irrecoverable volume strain can be obtained by following Equation 4.3.

$$\Delta\varepsilon_{vd} = C_1(\gamma - C_2\varepsilon_{vd}) + \frac{C_3\varepsilon_{vd}^2}{\gamma + C_4\varepsilon_{vd}} \quad (4.3)$$

where ε_{vd} is accumulated irrecoverable volume strain to N cycle, γ is shear strain at N+1 cycle, $\Delta\varepsilon_{vd}$ is increment of volume decrease at N+1 cycle, C_1, C_2, C_3, C_4 is volume change constants.

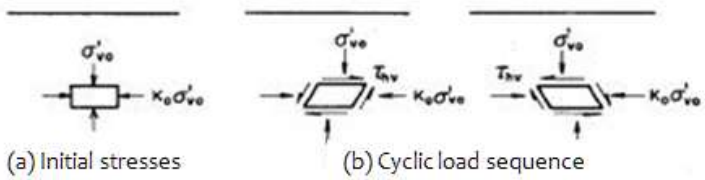

Figure 4.8 Ideal stress condition in soil

An alternative, and simpler formula is proposed by Byrne (1991):

$$\frac{\Delta\varepsilon_{vd}}{\gamma} = C_1 \exp\left(-C_2\left(\frac{\varepsilon_{vd}}{\gamma}\right)\right) \quad (4.4)$$

In many cases, $C_2 = \frac{0.4}{C_1}$. FLAC3D contains a built-in constitutive model

(named the “Finn model”) that incorporates both Equation 4.3 and Equation 4.4 into the standard Mohr-Coulomb plasticity model. As it stands, the model captures the basic mechanisms that can lead to liquefaction in sand. For Equation 4.4, Byrne (1991) noted that the constant, C_1 could be derived from relative densities as follows.

$$C_1 = 7600(D_r)^{-2.5} \tag{4.5}$$

C_2 is then calculated from $C_2 = \frac{0.4}{C_1}$, in this case. Refer to Byrne (1991) for more details.

Finn model was combined with the numerical model proposed for dry condition. Calibration of the input constants was performed for target system, resulting in input properties of model soil used in numerical simulation is given as Table 4.4.

Table 4.4 Input properties of model soil used in numerical analysis

Properties	Values for $D_r = 35\%$	Values for $D_r = 55\%$	Values for $D_r = 80\%$
Porosity	0.438	0.409	0.377
Saturated unit weight (kN/m^3)	19.38	19.87	20.41
Permeability coefficient (m/s)	7.5×10^{-5}	5.9×10^{-5}	3.7×10^{-5}
Volume change constants	$C_1 = 1.05$ $C_2 = 0.38$	$C_1 = 0.34$ $C_2 = 1.17$	$C_1 = 0.13$ $C_2 = 3.07$

4.4 Calibration and validation of proposed method

Calibration of the proposed model by comparing measured and computed values is needed to minimize error of numerical analysis and to have a reliability of results from numerical simulation. Results of a centrifuge test are used to demonstrate the capability of the model for reliable analysis of pile foundations under dynamic loading. For this purpose, dynamic centrifuge tests in liquefiable sands conducted by Wilson (1998) were numerically simulated by proposed modeling method. For the calibration of the numerical model, the test case of upper liquefiable layer with a relative density of 55% was applied. Excess pore water pressure, bending moment-time histories for various depth and pile head displacement-time history obtained from proposed numerical model were compared to those obtained from centrifuge tests. For the validation of the numerical model, the test case of upper liquefiable layer with a relative density of 35% was applied. Various dynamic pile responses calculated by numerical model were compared to those measured by centrifuge tests in order to verify the applicability of the proposed modeling method.

4.4.1 Calibration of the proposed method

As stated above, calibration of the numerical model was conducted using the test case of upper liquefiable layer with a relative density of 55%. Table 4.5 and Figure 4.9 show model soil profile and schematic drawing for calibration process. All the values related with centrifuge test and numerical simulation are described in prototype scale.

Table 4.5 Input properties of model soil for calibration of proposed method

Property	Value
D_r (upper layer)	55%
D_r (lower layer)	80%
Pore fluid	HPMC-water

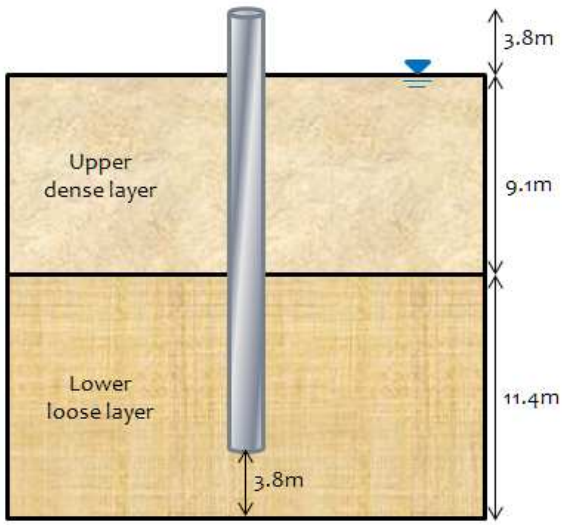

Figure 4.9 Schematic drawing of model case

Time histories of measured and computed excess pore pressure ratio at three different depths in the free field were presented in Figure 4.10. Those results demonstrated that there were good agreements between measured and computed excess pore pressure ratio. As deeper the depth, maximum values of the excess pore pressure ratio decreased due to increase of confining pressure both in numerical simulation and centrifuge tests. Excess pore pressure ratio reached 1.0 at the 1 m depth from the ground surface, which means almost 100% liquefaction occurred. Excess pore pressure ratio reached only 0.5 at the 7 m depth, however, which means liquefaction occurred partially in deeper depth.

Figure 4.11 shows the measured and computed bending moment-time histories at two different depths. It is concluded that the proposed numerical model was also capable of predicting pile bending moment values for liquefied state. Figure 4.12 shows the measured and computed displacement-time history at the pile head. It can be seen that the results obtained from the numerical simulation agree reasonably well with the values recorded during the centrifuge tests. Pile head displacement obtained from numerical model show good agreement especially at 2 ~ 5 seconds after shaking which critically affect the dynamic response of pile foundations. In the results, peak bending moment at the depth of 1m from ground surface occurred at about 3.5 second. As shown in Figure 4.10, this time corresponds to sudden increase of pore water pressure which results in the softening of surrounding soils. Also in Figure 4.12, the time 3.5 second corresponds to the peak value of pile head displacement which results in a large amount of inertial forces induced to the pile shaft. Therefore, it can be concluded that the maximum value of bending

moment measured and computed at 3.5 second was the consequence of the surrounding soil softening and the inertial forces developed at the pile head.

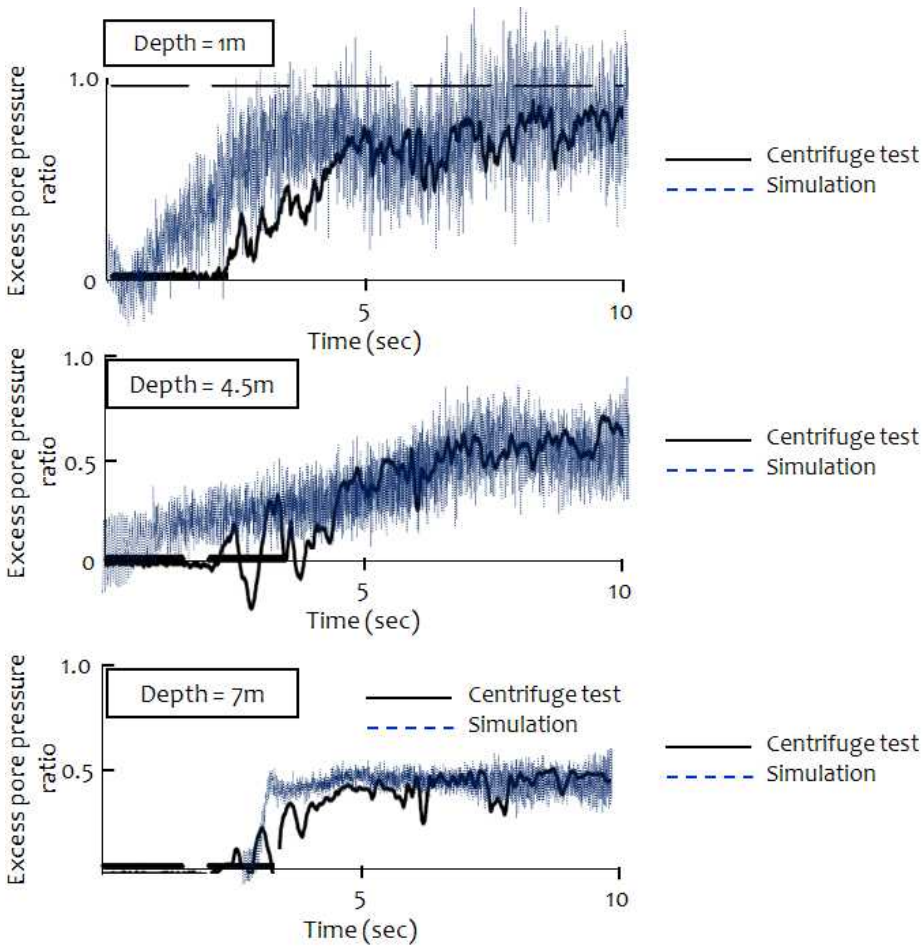

Figure 4.10 Comparison of time histories of excess pore pressure ratio in the free field at the depth of 1, 4.5, 7 m with the centrifuge test

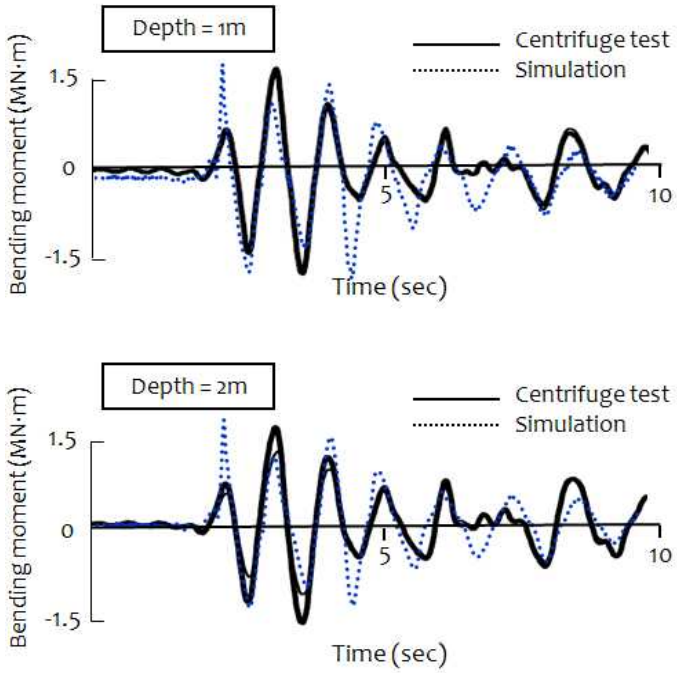

Figure 4.11 Comparison of time histories of bending moment with the centrifuge test

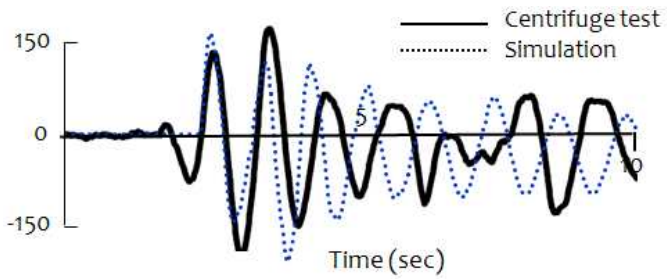

Figure 4.12 Comparison of time histories of pile head displacement with the centrifuge test

4.4.2 Validation of the proposed method

In the previous section, 4.4.1, Calibration of the proposed numerical model was conducted comparing computed excess pore pressure-time history and pile internal responses to measured values. Calibration results demonstrated that proposed modeling method was capable of predicting dynamic pile behavior observed in centrifuge test properly for liquefiable condition also. However, Those results were for the single test case which was perform with upper liquefiable layer with relative density of 55% only. Additional comparison with other test case is needed to verify the applicability of numerical model for various conditions.

In this section, validation of the proposed numerical model was conducted using the test case of upper liquefiable layer with relative density of 35%. Table 4.6 shows model soil profile and schematic drawing for validation process. Other conditions except relative density of upper sand layer was identical with the case which was used for calibration process. All the values related with centrifuge tests and numerical analysis are described in prototype scale.

Table 4.6 Input properties of model soil for validation of proposed method

Property	Value
D_r (upper layer)	35%
D_r (lower layer)	80%
Pore fluid	HPMC-water

Time histories of the measured and computed excess pore water pressure ratio at two different depths in the free field are presented in Figure 4.13. The results indicate that there is generally a good agreement between measured and computed excess pore pressure ratio. The excess pore pressure ratio-time history at depth of 4.5 m, 7 m reached 1.0, which means almost 100% liquefaction occurred both in numerical simulation and centrifuge tests. It was different phenomena with the results for calibration process. This is because that relative density of upper sand layer is lower than that for calibration process, resulting in decrease of confining pressure. Figure 4.14 depicts the measured and computed pile bending moment-time histories at two different depths. It is demonstrated that the applied method was capable of predicting the pile bending moment for various conditions in liquefiable condition. Figure 4.15 shows the measured and computed displacement-time history at pile head. Although there was a discrepancy in phase after peak value, computed pile head displacement obtained from numerical model agree generally well with the values recorded by centrifuge tests especially peak value which critically affects the dynamic pile responses in liquefied condition.

Finally it is concluded that proposed numerical model could simulate dynamic soil-pile-structure interactive behavior in liquefiable soil deposits for various conditions and its applicability was verified.

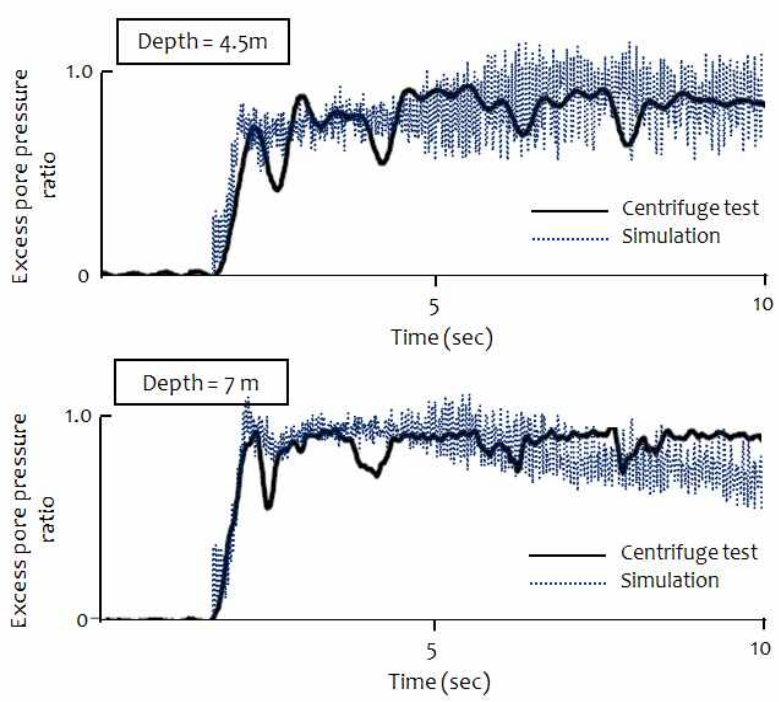

Figure 4.13 Comparison of time histories of excess pore pressure ratio in the free field at the depth of 4.5, 7 m with the centrifuge test (Validation)

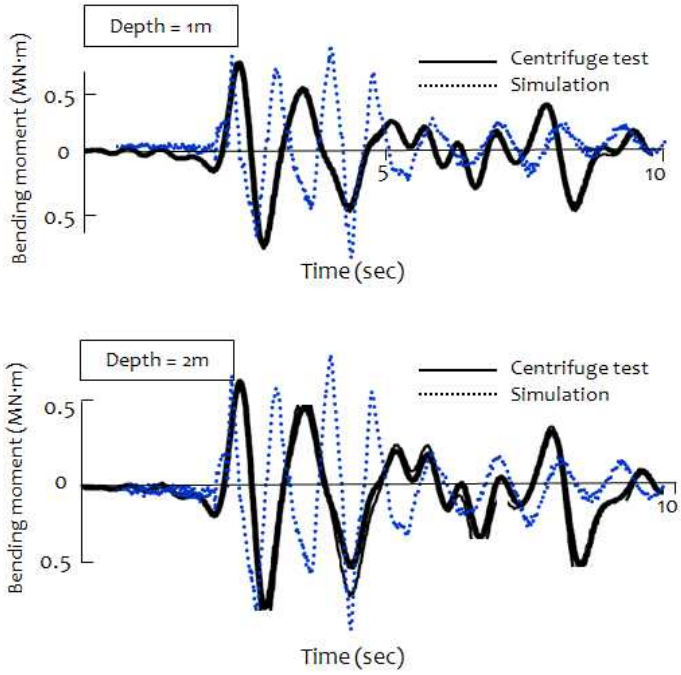

Figure 4.14 Comparison of time histories of bending moment with the centrifuge test (Validation)

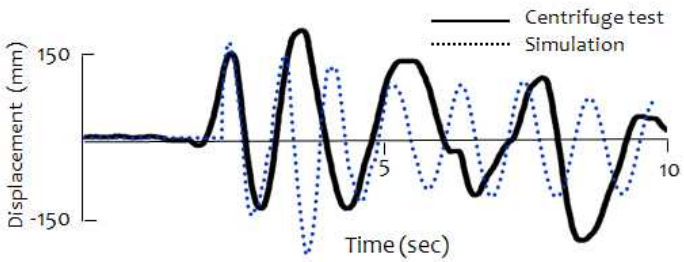

Figure 4.15 Comparison of time histories of pile head displacement with the centrifuge test (Validation)

4.5 Parametric study

Based on the calibration and validation process, applicability of the proposed numerical model was verified. In present section, parametric study for various conditions was carried out in order to provide better insight into the dynamic behavior of pile foundations embedded in liquefiable soil deposits. Parametric studies were performed varying frequency of input excitation, thickness of liquefiable layer, relative density, weight of the superstructure. Input properties of model pile used for parametric study was basically identical to the test case applied for calibration process and detailed properties were varied for each applied parameter. Input properties of model soil used for parametric study are shown in Table 4.7 according to three different relative densities, 30%, 50%, 80%. Input properties of model soil were basically identical to Nevada sand which was used in calibration and validation of the proposed numerical model. Sinusoidal waves were used as input motion to investigate dynamic pile behavior according to various input conditions. All the results were obtained in liquefied state.

Table 4.7 Input properties of model soil for parametric study

Properties	Values for D_r = 30%	Values for D_r = 50%	Values for D_r = 80%
Porosity (n)	0.445	0.415	0.377
Saturated unit density (kN/m^3)	19.27	19.75	20.41
Volume change constants	C_1=1.54 C_2=0.26	C_1=0.43 C_2=0.93	C_1=0.13 C_2=3.07

4.5.1 Effect of input frequency on pile performance

Peak bending moment and maximum lateral pile displacement along depth obtained for various input frequencies of 1 Hz, 2 Hz, 3 Hz are presented in Figure 4.16, 4.17. Acceleration of input excitation was 0.13g for all cases. It is noted that the frequency of input excitation had a significant effect on dynamic responses of pile foundation. As frequency of input excitation increases from 1 Hz to 3 Hz, peak bending moment and maximum lateral pile displacement decrease about 70%, 90% respectively. Since acceleration of input excitation was the same in all analysis, frequency of input excitation was responsible for the observed behavior. This was similar results with Rahmani and Pak (2012). In Rahmani and Pak (2012), by increasing the frequency from 3 Hz to 10 Hz, maximum lateral pile displacement, maximum bending moment and settlement decreased about 75 %, 90 %, and 70 %, respectively. These kinds of phenomena were effect of natural frequency which induces resonance of the system. The natural frequency of the corresponding system was seen to be about 1 Hz. It is concluded that it is important to prevent resonance of the system by considering effect of frequency of input excitation when seismic design of pile foundations embedded in liquefiable soil deposits is carried out.

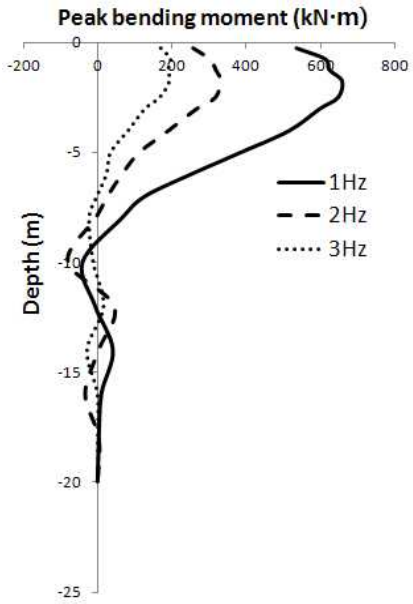

Figure 4.16 Peak bending moment along depth for different input frequencies (Input acceleration : 0.13g)

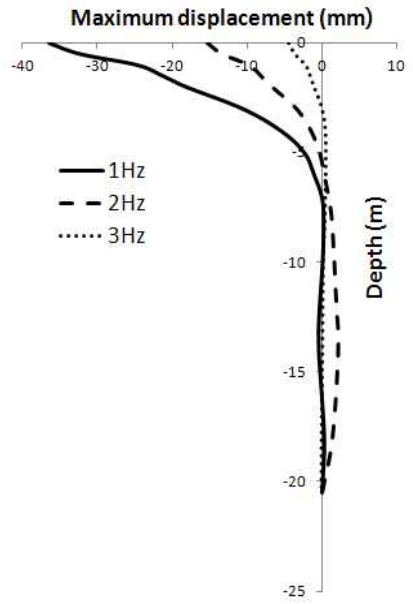

Figure 4.17 Maximum lateral pile displacement along depth for different input frequencies (Input acceleration : 0.13g)

4.5.2 Effect of thickness of liquefiable layer on pile performance

In this section, pile responses obtained from repetitive analysis for thickness of liquefiable soil layers of 3 m, 6 m, 9 m were discussed. Figure 4.18 (a), (b), (c) show schematic drawing of soil profiles with three different thicknesses of liquefiable layer. In each case, relative density of liquefiable soil layer was 30%, and that of non-liquefiable soil layer was 80%. Figure 4.19 shows maximum lateral pile displacement for various thicknesses of liquefiable layers. It is concluded that the thickness of liquefiable layer has a significant effect on maximum lateral pile displacement. According to the results, as thickness of liquefiable layer decreased from 9 m to 3 m, maximum lateral pile displacement decreased by about 90%. If liquefaction occurs, piles are intensely under the control of the surrounding liquefied soil, so thicker liquefiable soil layer significantly affects pile lateral displacement which is very important in performance-based design approaches.

Figure 4.20 shows peak bending moment envelopes for three different thicknesses of liquefiable layers of 3 m, 6 m, 9 m. In all cases, the maximum bending moment developed at the interface between liquefiable and non-liquefiable soil layers. Finn (2002) indicated that critical design section with the maximum bending moment is the interface between liquefied and non-liquefied regions. This was confirmed by proposed numerical model. Furthermore, it is concluded that pattern of peak bending moment envelopes caused significant difference of lateral pile displacement for different thickness of liquefiable layers.

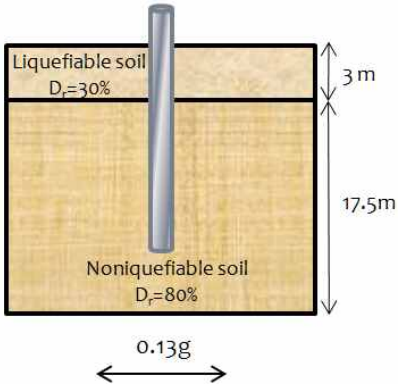

(a) Thickness of liquefiable layer : 3 m

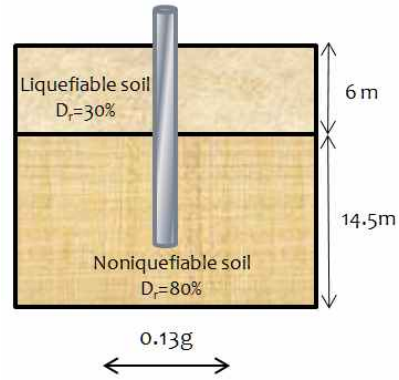

(b) Thickness of liquefiable layer : 6 m

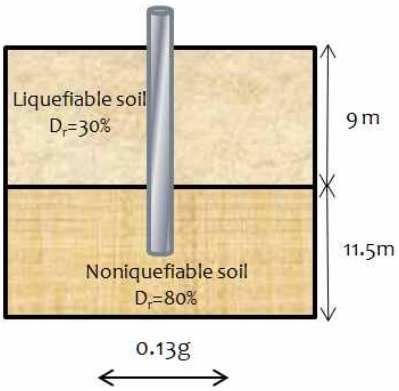

(c) Thickness of liquefiable layer : 9 m

Figure 4.18 Schematic drawing of soil profiles for different thickness of liquefiable layer

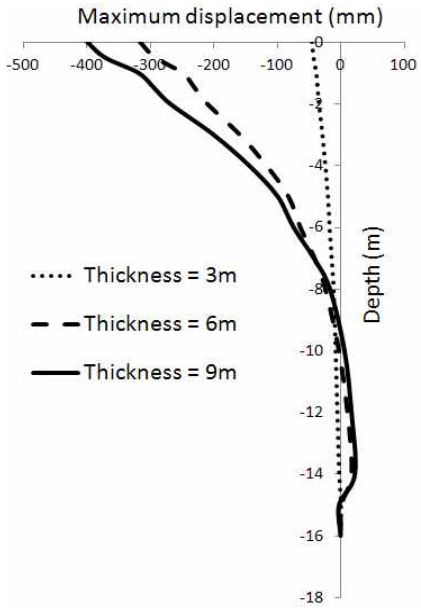

Figure 4.19 Maximum pile lateral displacement along depth for different thickness of liquefiable layer (input acceleration : 0.13g)

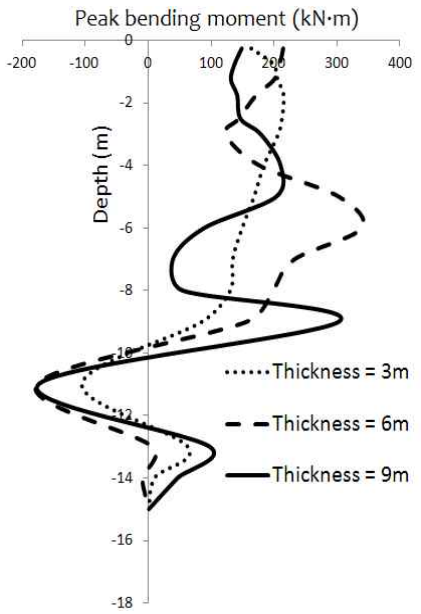

Figure 4.20 Peak bending moment along depth for different thickness of liquefiable layer (input acceleration : 0.13g)

4.5.3 Effect of relative density on pile performance

In order to investigate pile performance for different relative densities, results obtained from repetitive analysis for two different relative densities of 30%, 50% were discussed. Figure 4.21, 4.22 show peak bending moment and maximum lateral pile displacement envelopes for different relative densities. Acceleration of input excitation was 0.13g in all cases. In these two figures, the lower relative density of liquefiable soil deposits, the larger dynamic pile responses. It is observed that as relative density increased from 30% to 50%, maximum value of peak bending moment and lateral pile displacement decreased 45%, 40% respectively. This was due to the increase of the liquefiable soil stiffness and relatively smaller values of soil displacement. These kinds of behavior were wholly different from pile performance embedded in dry soil deposits. Figure 4.23, 4.24 show peak bending moment and maximum lateral pile displacement envelopes for different relative densities embedded in dry sand, which was discussed in 3.5.2. Acceleration of input excitation was same to 0.13g with that for liquefiable sand case. It can be seen that peak bending moment and maximum lateral pile displacement envelopes show almost identical values for different relative densities in dry condition. It was concluded that kinematic forces induced by soil movement is dominant in liquefiable sand than in dry sand. It was notable that dynamic pile performance was significantly different in dry and liquefiable soil conditions.

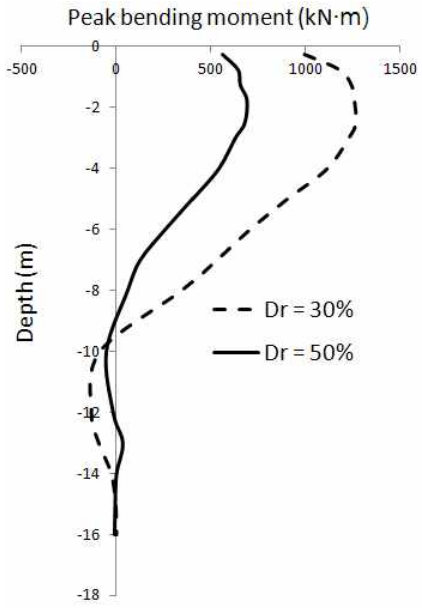

Figure 4.21 Peak bending moment along depth for different relative density (input acceleration : 0.13g)

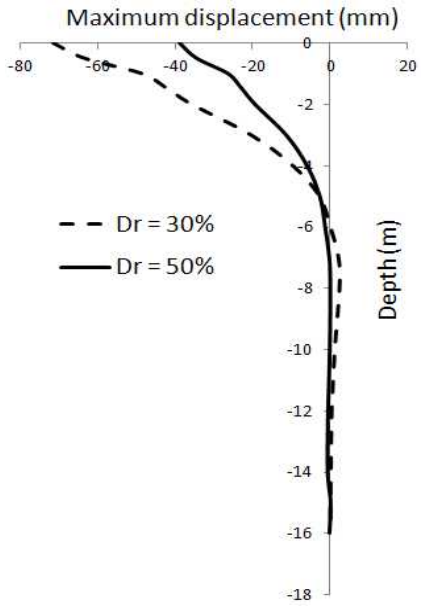

Figure 4.22 Maximum lateral displacement along depth for different relative density (input acceleration : 0.13g)

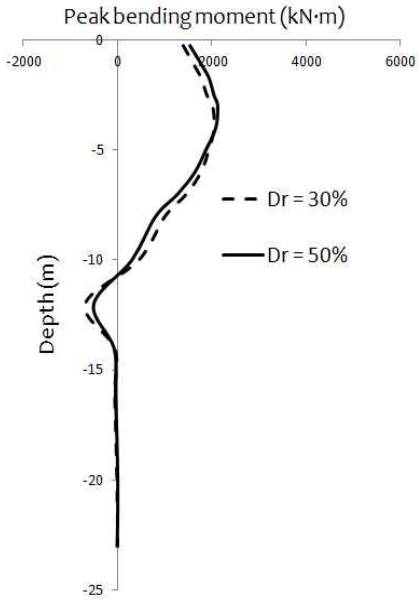

Figure 4.23 Peak bending moment along depth for different relative density in dry condition (input acceleration : 0.13g)

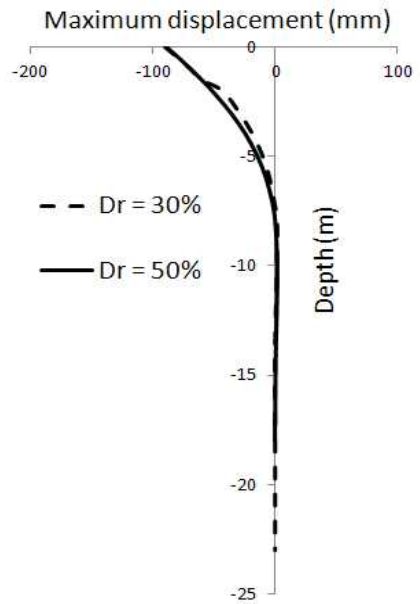

Figure 4.24 Maximum lateral displacement along depth for different relative density in dry condition (input acceleration : 0.13g)

4.5.4 Effect of weight of the superstructure on pile performance

Four different model systems were investigated in this section; weight of the superstructure was 0 kN, 300 kN, 600 kN, 900 kN. Maximum lateral pile displacement envelopes obtained from four different systems for input acceleration of 0.13g, 0.25g were presented in Figure 4.25 (a), (b). It is noted that variation of weight of the superstructure rarely affects maximum lateral pile displacements. As weight of the superstructure decreased from 900 kN to 0 kN, lateral pile responses were almost identical in four cases. These kinds of phenomena were observed regardless of the magnitude of input accelerations. Figure 4.26 (a), (b) show maximum lateral displacement envelopes for four different weight of the superstructure embedded in dry sand which was discussed in 3.5.1. Acceleration of input excitation was same with the case of liquefiable condition as 0.13g, 0.25g. It is noted that lateral pile displacements were remarkably varied for different weight of the superstructure in dry condition different from liquefiable condition. Table 4.8 shows detailed variation of dynamic pile responses for different weight of the superstructure. It is identified that maximum values of lateral pile displacement decreased to 92% when weight of the superstructure decreased from 900 kN to 0 kN for dry condition. Maximum values of lateral pile displacement, however, decreased only 26% when weight of the superstructure decreased from 900 kN to 0 kN for liquefiable condition. It is concluded that effect of inertial forces induced by superstructure is relatively insignificant in liquefiable soil deposits compared to dry soil deposits.

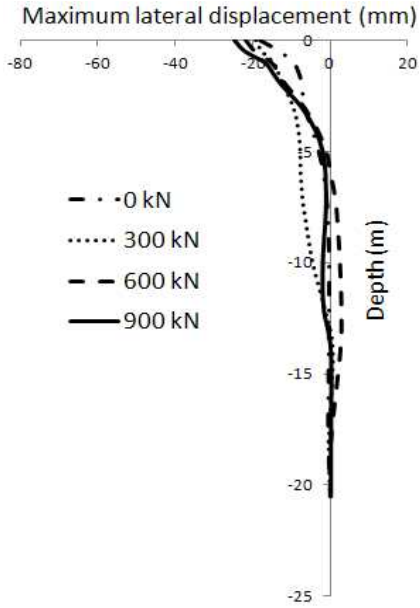

(a) Input acceleration : 0.13g

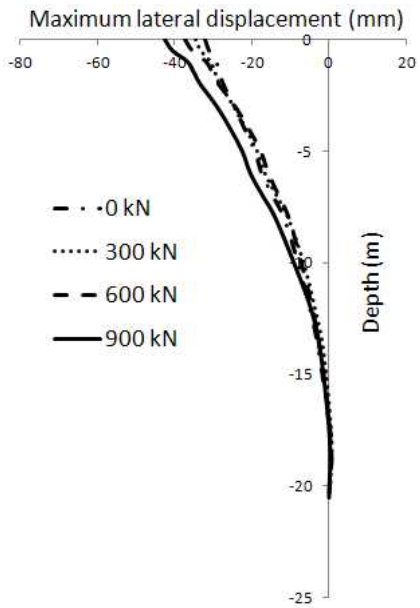

(b) input acceleration : 0.25g

Figure 4.25 Maximum lateral displacement along depth for different weight of superstructure

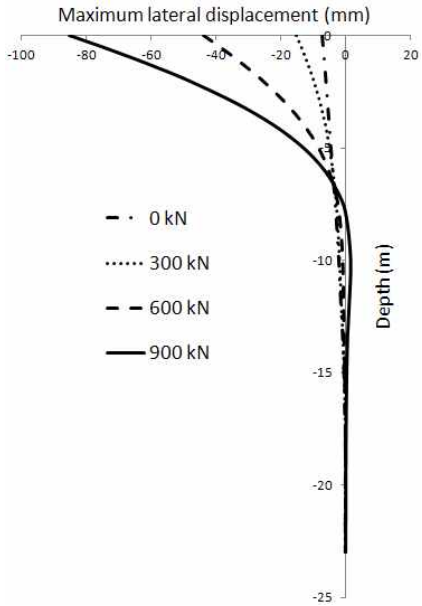

(a) Input acceleration : 0.13g

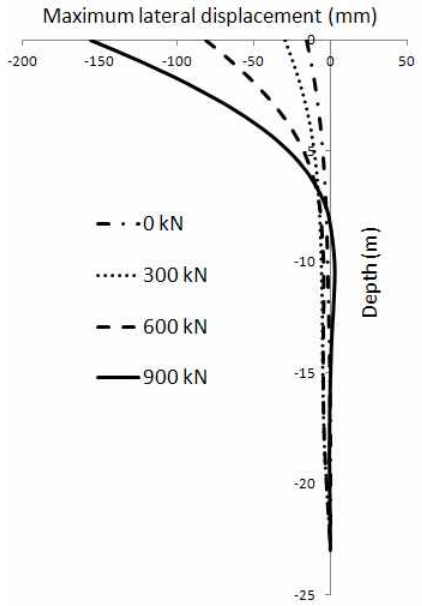

(b) input acceleration : 0.25g

Figure 4.26 Maximum lateral displacement along depth for different weight of superstructure in dry condition

Table 4.8 Variation of pile responses for different weight of superstructure

Input motion	Response ratio compared to 900 kN		
	600 kN	300 kN	0 kN
	Dry condition		
0.13g	48 %	82%	92%
0.25g	48%	81%	90%
	Liquefiable condition		
0.13g	12 %	19 %	25 %
0.25g	11 %	22 %	26 %

4.6 Summary and conclusions

In this chapter, three-dimensional continuum modeling of soil-pile-structure interactive behavior in liquefiable soil deposits was carried out. First of all, numerical simulation of dynamic SPSI observed in dynamic centrifuge tests was performed. As a modeling methodology, Finn model was adopted to estimate dynamic behavior of soil and pile foundation embedded in liquefiable soil deposits. By using Finn model, development of pore water pressure according to the shear deformation of soil can be directly captured in real time. Adopted Finn model was combined with standard Mohr-Coulomb criteria used in dry condition.

Calibration and validation of the proposed numerical model was performed by comparing with test results. For calibration of the numerical model, the test case of upper liquefiable layer with relative density of 55% was applied. Excess pore water pressure-time histories, pile bending moment-time histories for various depths and pile head displacement-time history obtained from proposed numerical model show reasonably good agreement with those obtained from dynamic centrifuge test performed by Wilson (1998). For validation of the numerical model, the test case of upper liquefiable layer with relative density of 35% was applied. Although there was a discrepancy in phase after peak value, excess pore water pressure-time histories, pile bending moment-time histories for various depths and pile head displacement-time history obtained from proposed numerical model show generally good agreement with those obtained from dynamic centrifuge tests. Finally it is concluded that proposed numerical model could simulate dynamic soil-pile-

structure interactive behavior in liquefiable soil deposits for various conditions and its applicability was verified.

Parametric study for various conditions was carried out to provide better insight into the dynamic behavior of pile embedded in liquefiable soil deposits. First, effect of frequency of excitation on pile performance was investigated. By increasing the input frequency from 1 Hz to 3 Hz, peak bending moment and maximum lateral pile displacement decreased 70 % and 90% respectively. Frequency of input excitation had significant effect also in liquefiable condition, therefore, proper seismic design should be performed considering effect of input frequency such as resonance induced by natural frequency. Effect of thickness of liquefiable soil layer on pile performance was investigated. As thickness of liquefiable layer decreased from 9 m to 3 m, maximum lateral pile displacement decreased about 90 %. Peak bending moment developed at the interface between liquefied and non-liquefied layers for every model case. It is concluded that critical design section is the interface between the liquefied and non-liquefied regions, which was confirmed by numerical model. Effect of relative density on pile performance was investigated. Increase of relative density from 30% to 50% caused 40% decrease in peak bending moment and 45% decrease in maximum lateral pile displacement. It is identified that effect of kinematic forces induced by soil movement is dominant in liquefiable condition. Effect of weight of the superstructure on pile performance was investigated. Maximum lateral pile displacements were similar regardless of weight of the superstructure. It is concluded that effect of inertial forces induced by superstructure is relatively insignificant in liquefiable sand, which was confirmed by numerical model.

5. Conclusions and Recommendations

5.1 Conclusions

The objectives of this dissertation are to establish a modeling methodology and validate by comparing the internal pile responses both in dry and liquefiable soil deposits, and to investigate the dynamic behavior of piles for various conditions by means of parametric studies. The numerical simulation of dynamic soil-pile-structure interactive behavior for the dry and liquefiable conditions observed in dynamic centrifuge tests was carried out. For calibration and validation of the proposed numerical model in the dry condition, the results obtained from the centrifuge test performed by Yoo, (2013) were used; for those in the liquefiable condition, the results obtained from the centrifuge test performed by Wilson (1998) were used. Based on the verification of the applicability of the proposed modeling method, parametric studies for various conditions were carried out to provide better insight into the dynamic behavior of pile foundations. And availability and applicability of the proposed numerical were confirmed once again comparing with the results from previous researches. For the dry soil condition, parametric studies were performed while varying the weight of the superstructure, pile length, relative density, and pile head fixity. For the liquefiable soil condition, parametric studies were performed while varying the frequency of input excitation, thickness of the liquefiable layer, relative density, and weight of the superstructure.

5.1.1 Numerical simulation for dry soil deposits

A three-dimensional numerical simulation of the dynamic soil-pile-structure interactive behavior in dry soil deposits was performed. First, the modeling methodology was evaluated for the dry condition. A Mohr-Coulomb plasticity criterion was applied as the soil constitutive model. Hysteretic damping was adopted to consider both the nonlinearity of the soil modulus and the energy dissipation. The initial shear modulus and yield depth were determined and calculated using proper empirical relations. Using the user-defined FISH function in FLAC3D, the shear modulus of the soil was continuously updated according to depth. An interface model which was able to simulate fully contact, slippage, and the separation state according to the input motion was adopted. The interface elements consisting of normal and shear spring and interface stiffness were determined using a formula obtained from the elastic relation between stress and strain. The applied interface model was also able to take into account the nonlinearity of the soil from the shear modulus and the bulk modulus in the stiffness equation. The interface stiffnesses were entered using the FISH function according to depth. A simplified continuum modeling method was used as a boundary condition to reduce the analysis time and obtain accurate pile responses. Far-field responses were input at the near-field boundary as acceleration-time histories. The piles were modeled by elastic.

The dynamic centrifuge model test conducted by Yoo, (2013) was used as an exact solution for the prototype. Centrifuge tests were performed using the KOCED Centrifuge at the Korea Advanced Institute of Science and

Technology (KAIST) using a centrifugal acceleration of 40 g. Jumunjin sand, a typical type of sand in Korea, with a relative density of 80% was used in the dry condition. Sinusoidal waves and real earthquake events for various input amplitudes were applied as input motion in order to estimate the dynamic pile behavior under various input conditions.

Calibration and validation of the proposed modeling method was performed by comparing with test results. In the first step, calibration of the numerical model was conducted using the test case of a pile with a diameter of 100 cm and a thickness of 4 cm. Internal pile responses such as the peak bending moment and the maximum lateral pile displacement profile obtained from a numerical simulation show good agreement with those obtained from dynamic centrifuge tests. Thereafter, validation of the numerical model was conducted using the test case of a pile with a diameter of 72 cm and a thickness of 4 cm, resulting in reasonably good agreement between the measured and computed dynamic pile responses as well. Based on The results of the calibration and validation procedures, it is concluded that the applicability of the proposed modeling method was verified.

Parametric studies for various conditions were then carried out. First, the effect of the weight of the superstructure on the dynamic behavior of the piles was investigated. It is noted that as the weight of the superstructure decreased from 900 kN to 0 kN, the maximum lateral pile displacement decreased by about 90%. It is concluded that inertial forces induced by the superstructure are dominant in dry soil deposits, which is confirmed by the numerical method. The effect of the relative density on the dynamic behavior of the piles was investigated. The peak bending moment and maximum lateral pile

displacement profiles were almost identical for the three different relative densities. It is confirmed by means of the numerical method that the effect of the kinematic forces induced by soil movement is relatively insignificant in the dry condition. The effect of pile length on the dynamic behavior of the piles was investigated. When the pile length was made infinite (longer than 5 T), long pile performance was observed. When the pile length was between 2 T and 5 T, intermediate pile performance was observed. When the pile length was shorter than 2 T, short pile performance was observed. Overall, long pile behavior was observed when the pile length exceeded about 5 T and short pile behavior was observed when the pile length became about 2 T. It is concluded that existing studies about pile length such as the effects of increasing the pile length towards infinite are generally valid. The effect of pile head fixity on the dynamic behavior of the piles was investigated. The maximum bending moment occurred at different depths according to the pile head fixity. The maximum bending moment occurred at the pile cap for the fixed head condition, while the maximum bending moment occurred at about 3 m below the surface of the ground for the free head condition. On the other hand, the bending moment for the fixed head pile decreased significantly when pile length was 8 m (4.5 T). This is because of the relatively rigid behavior of the pile due to the decrease of the pile length to 4.5 T, which was identified as the intermediate pile length. Through the parametric studies for various conditions, influence of many parameters on seismic behavior of pile foundations embedded in dry soil deposits was established and availability and applicability of the proposed numerical were confirmed once again comparing with the results from previous researches.

5.1.2 Numerical simulation for liquefiable soil deposits

Three-dimensional continuum modeling of soil-pile-structure interactive behavior in liquefiable soil deposits was carried out. First, a numerical simulation of the dynamic SPSI observed in dynamic centrifuge tests was performed. As a modeling methodology, the Finn model was adopted to estimate the dynamic behavior of the soil and a pile foundation embedded in liquefiable soil deposits. By using the Finn model, the development of pore water pressure according to the shear deformation of soil can be directly captured in real time. The Finn model was combined with the standard Mohr-Coulomb criteria used in the dry condition.

The dynamic centrifuge model test conducted by Wilson (1998) was used as an exact solution of the prototype. Centrifuge tests were performed at the National Geotechnical Centrifuge at the University of California, Davis using a centrifugal acceleration of 30 g. Nevada sand was used with the saturated condition and hydroxypropyl methylcellulose HPMC-water was used as a pore fluid. The Kobe earthquake scaled to 0.22 g was applied as the input earthquake motion.

Calibration and validation of the proposed numerical model was performed by comparing the results of the numerical modeling with test results. For the calibration of the numerical model, the test case of an upper liquefiable layer with a relative density of 55% was applied. The excess pore water pressure-time histories, pile bending moment-time histories for various depths and pile head displacement-time history obtained from the proposed numerical model show reasonably good agreement with those obtained from

the dynamic centrifuge test performed by Wilson (1998). For the validation of the numerical model, the test case of an upper liquefiable layer with a relative density of 35% was applied. Although there was a discrepancy in the phase after peak value, the excess pore water pressure-time histories, pile bending moment-time histories for various depths and pile head displacement-time history obtained from the proposed numerical model show generally good agreement with those obtained from the dynamic centrifuge tests. Thus it is concluded that the proposed numerical model could simulate dynamic soil-pile-structure interactive behavior in liquefiable soil deposits for various conditions and the applicability was verified.

Parametric study for various conditions was carried out to provide better insight into the dynamic behavior of piles embedded in liquefiable soil deposits. First, the effect of frequency of excitation on pile performance was investigated. By increasing the input frequency from 1 Hz to 3 Hz, the peak bending moment and maximum lateral pile displacement decreased by 70 % and 90 % respectively. The frequency of input excitation also had a significant effect in the liquefiable condition; proper seismic design should be performed considering the effect of input frequency such as the resonance induced by natural frequencies. The effect of the thickness of the liquefiable soil layer on pile performance was investigated. As the thickness of the liquefiable layer decreased from 9 m to 3 m, the maximum lateral pile displacement decreased by about 90%. The peak bending moment developed at the interface between the liquefied and non-liquefied layers for every model case. It is concluded that the critical design section is the interface between the liquefied and non-liquefied regions, which was confirmed by the numerical model. The effect of

relative density on pile performance was investigated. Increasing the relative density from 30 % to 50 % caused a 40 % decrease in the peak bending moment and a 45 % decrease in the maximum lateral pile displacement. It is identified that the effect of kinematic forces induced by soil movement is dominant as compared to the dry condition. The effect of the weight of the superstructure on pile performance was investigated. Maximum lateral pile displacements were similar regardless of the weight of the superstructure. It is concluded that the effect of the inertial forces induced by the superstructure is relatively insignificant in liquefiable sand, which was confirmed by the numerical model. Through the parametric studies for various conditions, influence of many parameters on seismic behavior of pile foundations embedded in liquefiable soil deposits was established and availability and applicability of the proposed numerical were confirmed once again comparing with the results from previous researches.

5.2 Recommendations

The following engineering contributions are presented, as well as recommendations for future studies to clarify the problems discussed.

I. The proposed numerical model was capable of predicting the seismic behavior of piles embedded in dry soil deposits quantitatively. Discrepancies between the results of the numerical simulation and centrifuge tests were within a reasonable enough range to allow them to be applied to the practical seismic design of pile foundations embedded in dry sand. The applicability of the proposed model was reliable because dynamic centrifuge tests which could reproduce field-confining pressure were used as an exact solution of the prototype. The proposed modeling methodology could be used to predict the seismic behavior of pile foundations in dry sand quantitatively.

II. The proposed numerical modeling method was able to simulate the dynamic behavior of piles embedded in liquefiable soil deposits quantitatively. Although there were slight phase differences after the peak response occurred, the peak values and soil strength reduction phenomenon according to depth obtained from the numerical model generally matched the test results. The reliability of the results obtained from the proposed model was gained by comparing the proposed model results with those obtained from centrifuge tests

(Wilson, 1998) often cited by other researchers.

III. Parametric study for various conditions in dry soil deposits provided better insight into the dynamic behavior of piles embedded in dry sand. A series of parametric studies employing the numerical model confirmed that, in the dry condition, the effect of inertial forces is significant and that the effect of kinematic forces is relatively insignificant. It is identified that existing theory treating pile length such as infinite length of pile was generally valid and that pile head fixity had a significant effect on the location of the peak bending moment. The emphasis on the seismic design of pile foundations embedded in dry soil deposits could be established by the proposed model. Moreover, the proposed numerical model could be used to estimate the influence of numerous other parameters which affect the dynamic performance of piles in the field.

IV. The influence of many parameters on the seismic behavior of pile foundations embedded in liquefiable soil deposits was established by parametric study for various conditions. It is confirmed that the effect of the kinematic forces was significant and that the effect of the inertial forces was relatively insignificant in the liquefied condition. It was identified that critical design section of piles to be used in liquefiable sand is the interface between the liquefied and non-liquefied regions. The principal point for the seismic design of piles embedded in a liquefiable soil layer could be established using the

numerical model.

V. Proposed numerical model was originally evaluated for dynamic loading condition but it can be applied for static loading condition also in convenience. Detailed consideration for various modeling parameters in this study would be helpful to carry out accurate and proper analysis for static case. Simple adjustment of loading command would be enough to convert from dynamic mode to static mode. Finally, numerical model proposed in this study can be used to predict pile behavior under vertical or horizontal static loading condition as well as dynamic soil-pile-structure interactive behavior under earthquake.

VI. Additional validation would be needed for general application of the proposed modeling procedure in the field. The proposed numerical model and aforementioned recommendations were established using experimental results conducted under particular conditions. Although numerous values were tested for conditions such as the base input motion (acceleration and frequency) and pile diameter, there was little variability in other conditions tested such as soil type. The application of the proposed numerical model to the group pile would be meaningful in practice. Overall, generalized results are necessary to establish a more applicable numerical model.

References

Abdoun, T, Dobry, R. (2002). “Evaluation of Pile Foundation Response to Lateral Spreading,” Soil Dynamics and Earthquake Engineering, 22, pp.1051–8.

Beringen, F. L., Windle, D., & Van Hooydonk, W. R. (1979). “Results of loading tests on driven piles in sand,” Fugro.

Bhattacharya, S, Madabhushi, PG, Bolton, MD. (2004). “An alternative mechanism of pile failure in liquefiable deposits during earthquakes,” Geotechnique, 3, 203–13

Blaney, G., Kausel, E., and Roesset, J. (1976). “Dynamic Stiffness of Piles,” In Proceeding: 2nd International Conference on Numerical Methods in Geomechanics, Blacksburg, Vol. 2, pp. 1001-1012

Boulanger, R.W. and Curras, C.J. (1999), “Seismic Soil-Pile-Structure Interaction Experiments and Analyses,” Journal of Geotechnical and Geoenvironmental Engineering, American Society of Civil Engineers, Vol. 125, No. 9, pp. 750-759

Broms, B. B. (1965), “Design of Laterally Loaded Piles,” In Proceeding: ASCE Journal of Soil Mechanics and Foundation Div., 91, pp.79-99.

Brown, D. A. and Shie, C. F. (1991). “Some numerical experiments with a three-dimensional finite element model of laterally loaded piles,” Computers and Geotechnics 12, pp. 149-162

Byrne, P. (1991), “A Cyclic Shear-Volume Coupling and Pore-Pressure Model for Sand,” in Proceedings: Second International Conference on Recent Advances in Geotechnical Earthquake Engineering and Soil Dynamics, St. Louis, Missouri, March, 1;24, pp. 47-55.

Cai, Y., Gould, P., and Desai, C. (1995). “Numerical Implementation of a 3-D Nonlinear Seismic S-P-S-I Methodology,” in Seismic Analysis and Design for Soil-Pile-Structure Interactions, Geotech. Spec. Pub. 70, ASCE, pp. 96-110

Chang, DW, Lin, BS, Cheng, SH. (2007), “Dynamic pile behaviors affecting by liquefaction from EQWEAP analysis,” In Proceedings: 4th International conference on earthquake geotechnical engineering, Thessaloniki, Greece; pp. 1336.

Chen, L. T. and Poulos, H. G. (1997). “Piles subjected to lateral soil movements,” Journal of Geotechnical and Geoenvironmental Engineering, ASCE, 123(9), pp. 802-811

Cheng, Z. h., Jeremic, B. (2009), “Numerical modeling and simulation of pile in liquefiable soil,” Soil Dynamics and Earthquake Engineering, 29, pp. 1404–16

Comodromos, E. (2003), “Response prediction of horizontally loaded pile groups,” Geotechnical Engineering Journal, 34(2), pp. 123–133

Comodromos, E. M., Papadopoulou, M. C., Rentzepris, I. K. (2009), “Pile foundation analysis and design using experimental data and 3-D numerical analysis,” Computers and Geotechnics, 36, pp. 819–36

Desai, C. S., Abel, J. F., & Marcal, P. V. (1973), “Introduction to the Finite-Element Method,” Journal of Applied Mechanics, 40, pp. 404.

Divis, C. J., Kutter, B. L., Idriss, I. M., Goto, Y., and Matsuda, T. (1996). "Uniformity of specimen and response of liquefiable sand model in a large centrifuge shaker." In Proceedings: Sixth Japan-U.S. Workshop on Earthquake Resistant Design of Lifeline Facilities and Countermeasures Against Soil Liquefaction, Hamada and O’Rourke, Eds., NCEER-96-0012, SUNY, Buffalo, pp. 259-273

Dobry, R., Vicente, E., O’Rourke, M., and Roesset, J. (1982). “Horizontal Stiffness and Damping of Single Piles,” J. Geotech. Eng., ASCE, 108(3), pp. 439-458

Dungca, J. R., Kuwano, J., Takahashi, A., Saruwatari, T., Izawa, J., Suzuki, H., et al. (2006), “Shaking table tests on the lateral response of a pile buried in liquefied sand,” Soil Dyn Earthquake Eng, 26, pp. 287–95

Finn, W. D. L, Fujita, N. (2002), “Pile in liquefiable soils: seismic analysis and design issues,” Soil Dyn Earthquake Eng, 22, pp. 731–42.

Fujii, S., Isemoto, N., Satou, Y., and Kaneko, O. (1998). “Investigation and analysis of a pile foundation damaged by liquefaction during the 1995 Hyogoken-Nambu earthquake,” Soils and Foundations, Special issue on geotechnical aspects of the 17 January 1995 Hyogoken-Nambu Earthquake, No. 2, pp 179–192

Gazetas, G. (1991). "Foundation Vibrations," Chapter 15 in Foundation Engineering Handbook, H.Y. Fang, Ed., Van Nostrand Reinhold, New York.

Gazetas, G. and Mylonakis, G. (1998). “Seismic Soil-Structure Interaction: New Evidence and Emerging Issues,” In Proceedings: 3rd Conf. Geotechnical Earthquake Engineering and Soil Dynamics, ASCE, Seattle, pp. 1119-1174

Gazetas, G., Fan, K., Tazoh, T., and Shimizu, K. (1993). “Seismic Response of the Pile Foundation of Ohba-Ohashi Bridge,” Proc. 3rd Intl. Conf. on Case Histories in Geotech. Eng., St. Louis, Vol. 3, pp. 1803-1809

Hamada M. (1992), “Large ground deformation and their effects on lifelines: 1983 Nihokai-Chubu earthquake,” In: Hamada M, O’Rourke T, editors. Case studies of liquefaction and lifeline performance during past earthquake, (I): Japanese case studies, vol. 4-1; 1992. p. 4–85 [chapter 4]

Han, J. T. (2006). “Evaluation of Seismic Behavior of Piles in Liquefiable Ground by Shaking Table Tests,” Ph. D. Dissertation, Seoul National University, South Korea

Hardin, B. O. and Drnevich, V. P. (1972). “Shear Modulus and Damping in Soils: Design Equations and Curves,” Journal of the Soil Mechanics and Foundations Division, ASCE, Vol. 98, No. SM7, July 1972, pp. 667-692

Ishihara K. (1997), “Terzaghi oration: geotechnical aspects of the 1995 Kobe earthquake,” In Proceedings: ICSMFE, Hamburg, 1997, pp. 2047–2073.

Ishihara, K., & Cubrinovski, M. (2004). “Case studies of pile foundations undergoing lateral spreading in liquefied deposits,” In Proceedings: Fifth International Conference on Case Histories in Geotechnical Engineering, New York, NY, April 13-17

Itasca Consulting Group (2006): FLAC3D (Fast Lagrangian Analysis of Continua in 3Dimensions) User's Guide, Minnesota, USA

Kagawa, T. and Kraft, L. (1981). “Lateral Pile Response During Earthquakes,” J. Geotech. Eng., ASCE, 107(12), pp. 1713-1731

Kagawa, T. (1992), “Lateral pile response in liquefying sand,” In Proceedings: The 10th world conference on earthquake engineering, Madrid, Spain, Paper No. 1761

Kavvadas, M. and Gazetas, G. (1993). “Kinematic seismic response of end bearing of free-head piles in layered soil,” Geotechnique 43(2), pp. 207-222

Kaynia, A. and Kausel, E. (1982). “Dynamic behavior of pile groups,” 2nd Int. Conf. on Numerical Methods in Offshore Piling, Austin, Texas, pp. 509-532

Kim, S. H. (2011). “Numerical Simulation of Pile Behavior Observed in 1g Shaking Table Tests and Centrifuge Tests,” Ph. D. Dissertation, Seoul National University, South Korea

Kim, S. H., Kwon, S. Y., Kim, M. M., Han, J. T., (2012), “3D Numerical Simulation of a Soil-Pile System Under Dynamic Loading,” Marine Georesources & Geotechnology, 30(4), pp. 347-361.

Kim, D. S., Lee, S. H., Choo, Y. W., & Perdriat, J. (2013). “Self-balanced earthquake simulator on centrifuge and dynamic performance verification,” KSCE Journal of Civil Engineering, 17(4), pp. 651-661.

Klar, A. and Frydman, S. (2002). “Three-Dimensional Analysis of Lateral Pile Response using Two-Dimensional Explicit Numerical Scheme,” Journal of Geotechnical and Geoenvironmental Engineering, Vol. 128 (9), pp. 775-784

Klar, A., Baker, R., & Frydman, S. (2004), “Seismic soil–pile interaction in liquefiable soil,” Soil Dynamics and Earthquake Engineering, 24(8), pp. 551-564.

Kuhlemeyer, R. L. (1979). "Vertical vibration of piles," Journal of Geotechnical Engineering, ASCE, Vol. 105 No. GT2, pp. 273-288

Kumar, J., & Madhusudhan, B. N. (2010), “Effect of relative density and confining pressure on Poisson ratio from bender and extender elements tests,” Geotechnique, 60(7), pp. 561-567.

Kutter, B. L., Idriss, I. M., Kohnke, T., Lakeland, J., Li, X. S., Sluis, W., Zeng, X., Tauscher, R., Goto, Y., and Kubodera, I. (1994), "Design of a large earthquake simulator at UC Davis." In Proceedings: Centrifuge 94, Leung, Lee, and Tan, Eds., Balkema, Rotterdam, pp. 169-175.

Kraft Jr, L. M. (1990), “Computing axial pile capacity in sands for offshore conditions,” Marine Georesources & Geotechnology, 9(1), pp.61-92.

Lee, S. H., Choo, Y. W., and Kim, D. S. (2011) "Performance evaluation of Equivalent Shear Beam (ESB) model container for dynamic geotechnical centrifuge tests", In Proceedings: 2011 Pan-Am CGS geotechnical conference.

Lewis, K. and Gonzalez, L. (1985). “Finite Element Analysis of Laterally Loaded Drilled Piers in Clay,” Proc. 12th Intl. Conf. Soil Mechanics Fdn. Eng., Rio de Janiero, Vol. 2, pp. 1201-1204

Liyanapathirana, D. S., & Poulos, H. G. (2005), “Seismic lateral response of piles in liquefying soil,” Journal of geotechnical and geoenvironmental engineering, 131(12), pp. 1466-1479.

Liyanapathirana, D. S., & Poulos, H. G. (2010), "Analysis of pile behaviour in liquefying sloping ground," Computers and Geotechnics, 37(1), pp. 115-124.

Lysmer, J., & Kuemyer, R. L. (1969), "Finite dynamic model for infinite media," J Eng Mech Div, ASCE, 95, pp. 877-895.

Makris, N., and Gazetas, G. (1992). "Dynamic Pile-Soil-Pile Interaction - Part II: Lateral and Seismic Response," Earthquake Eng. Struct. Dyn., 21(2), pp. 145-162

Marti, J. and Cundall, P. A. (1982). "Mixed discretization procedure for accurate modelling of plastic collapse," Int. J. for Num. and Anal. Meth. in Geomech, 6, pp. 129-139

Martin, G. R. and Chen, C. Y. (2005). "Response of piles due to lateral slope movement", Computers and Structures, Vol. 83, pp. 588-598

Martin, G. R., Finn, W. D. L. and Seed, H. B. (1975), "Fundamentals of Liquefaction under Cyclic Loading," J. Geotech., Div. ASCE, 101(GT5), pp. 423-438

Matlock, H., & Reese, L. C. (1962), "Generalized solutions for laterally loaded piles," Transactions of the American Society of Civil Engineers, 127(1), pp. 1220-1247

Matlock, H., Foo, S. H., and Bryant, L. L. (1978). "Simulation of lateral pile behavior," Proceedings, Earthquake Engineering and Soil Dynamics, ASCE, pp. 600-619

Miwa, S., Ikeda, T., & Sato, T. (2006), “Damage process of pile foundation in liquefied ground during strong ground motion,” Soil Dynamics and Earthquake Engineering, 26(2), pp. 325-336

Mori S, Namuta A, Miwa S. (1994), “Feature of liquefaction damage during the 1993 Hokkaido Nanseioki earthquake,” In Proceedings: The 29th annual conference of Japanese Society of soil mechanics and foundation engineering, pp. 1005–08

Nogami, T., Otani, J., Konagai, K., and Chen, H. (1992). “Nonlinear Soil-Pile Interaction Model for Dynamic Lateral Motion,” J. Geotech. Eng., ASCE, 118(1), pp. 89-106

Novak, M. and Aboul-Ella, F. (1978). “Impedance functions of piles in layered media,” Journal of the Engineering Mechanics Division, ASCE, 104(EM3), pp. 643-661

Novak, M. and Sheta, M. (1980). “Approximate Approach to Contact Effects of Piles,” in Dynamic Response of Pile Foundations: Analytical Aspects, ASCE, pp. 53-79

Oka F., Lu C. W., Uzuoka R., Zhang F. (2004), “Numerical study of structure-soil-group pile foundations using an effective stress based liquefaction analysis method,” In Proceedings: 13th World conference on earthquake engineering. Canada, Vancouver, p. 3338.

Onishi K., Namba S., Sento N., Horii K., Tatsumi Y., Oh-Oka H. (1996), “Investigation of failure and deformation modes of piles throughout overall length,” Tsuchi to Kiso, 45, pp. 24–6

Poulos, H. G. (1994). “An approximate analysis of pile–raft interaction,” International Journal for Numerical and Analytical Methods in Geomechanics, 18, pp. 73-92

Prakash, S., & Agarwal, S. L. (1967). “Effect of Pile Embedment on Natural Frequency of Foundations,” Journal Article-unidentified

Priestley, M. J. N., Singh, J., Youd, T., and Rollins, K. (1991). “Costa Rica Earthquake of April 22, 1991 Reconnaissance Report,” Publications 91-02, Earthquake Engineering Research Institute, pp. 59-91

Rahmani, A., & Pak, A. (2012), “Dynamic behavior of pile foundations under cyclic loading in liquefiable soils,” Computers and Geotechnics, 40, pp. 114-126.

Randolph, M. F., Dolwin, R., & Beck, R. (1994), “Design of driven piles in sand,” Geotechnique, 44(3), pp. 427-448.

Reddy, E. S., Chapman, D. N., & Sastry, V. V. (2000), “Direct shear interface test for shaft capacity of piles in sand,” Geotechnical Testing Journal, 23(2)

Reese, L. C. (1977). “Laterally Loaded Piles: Program Documentation,” Journal of the Geotechnical Engineering Division, ASCE, 103, GT4, pp. 287-306

Remaud, D. (1999), “Piles under Lateral Forces: Experimental Study of Piles Group,” University of Nantes, France

Shamoto Y., Sato M., Futaki M., Shimazu S. (1996), “Site investigation of post liquefaction lateral displacement of pile foundation in reclaimed land,” Tsuchi to Kiso, 44(3). Pp. 25–7

Stewart, D. P., Chen, Y. R.., and Kutter, B. L. (1998), "Experience with the use of methylcellulose as a viscous pore fluid in centrifuge models," Geotechnical Testing Journal, GTJODJ, 21(4), December, pp. 365-369

Suzuki H, Tokimatsu K, Sato M, Abe A. (2005), “Factor affecting horizontal subgrade reaction of piles during soil liquefaction and lateral spreading,” Geotechnical SP No.145, ASCE, pp. 1–9.

Tachikawa H., Fujii S., Onishi K., Suzuki Y., Isemoto N., Shirahama M. (1998), “Investigation and analysis of pile foundation located on Kobe Port Island,” In Proceedings: 33rd Japan national conference on geotechnology engineering, Vol. 1, pp. 811–2.

Tahghighi, H., & Konagai, K. (2007), “Numerical analysis of nonlinear soil–pile group interaction under lateral loads,” Soil Dynamics and Earthquake Engineering, 27(5), pp. 463-474.

Tamura S., Tokimatsu K. (2005), “Seismic earth pressure acting on embedded footing based on large-scale shaking table tests,” Geotechnical SP No.145, ASCE, pp. 83–95

Trochanis, A. M., Bielak, J., and Christiano, P. (1988). “A three-dimensional nonlinear study of piles leading to the development of a simplified model,” Technical Report of Research Sponsored by the National Science Foundation, Grant ECE-86/1060, Carnegie Mellon University, Washington, D.C

Uzuoka R., Sento N., Kazama M. (2007), “Three-dimensional numerical simulation of earthquake damage to group-piles in a liquefied ground,” Soil Dyn Earthquake Eng, 27, pp. 395–413

Wilson, D. W. (1998). “Soil-pile-superstructure interaction in liquefying sand and soft clay,” Doctoral dissertation, University of California, Davis

Wong, P., Kulhawy, F., and Ingraffea, A. (1989). “Numerical Modeling of Interface Behavior for Drilled Shaft Foundations Under Generalized Loading,” in Foundation Eng.: Current Principles and Practices, ASCE, Vol. 1, pp. 565-579

Wu, G. and Finn, W. (1997a). “Dynamic Elastic Analysis of Pile Foundations Using Finite Element Method in the Frequency Domain,” Can. Geotech. J., 34(1), 34-43

Wu, G. and Finn, W. (1997b). “Dynamic Nonlinear Analysis of Pile Foundations Using Finite Element Method in the Time Domain,” Can. Geotech. J., 34(1), 44-52

Yang, E. K. (2009). “Evaluation of Dynamic p-y curves for a Pile in Sand from 1g Shaking Table Tests,” Ph. D. Dissertation, Seoul National University, South Korea

Yang, E. K., Choi, J. I., Kwon, S. Y., & Kim, M. M. (2011). “Development of dynamic p y backbone curves for a single pile in dense sand by 1g shaking table tests,” KSCE Journal of Civil Engineering, 15(5), pp. 813-821.

Yao S, Nogami T. (1994), “Lateral cyclic response of piles in viscoelastic Winkler subgrade,” J Eng Mech, 120(4), pp. 758–75

Yao S., Kobayashi K., Yoshida N., Matsuo H. (2004) “Interactive behavior of soil–pile-superstructure system in transient state to liquefaction by means of large shake table tests,” Soil Dyn Earthquake Eng, 24, pp. 397–409

Yoo, M. T. (2013). “Evaluation of dynamic pile behavior by centrifuge tests considering kinematic load effect,” Ph. D. Dissertation, Seoul National University, South Korea

Zhang, Y., Conte, J. P., Yang, Z., Elgamal, A., Bielak, J., and Acero, G. (2008), “Two-dimensional nonlinear earthquake response analysis of a bridge-foundation-ground system,” Earthquake Spectra, 24(2), pp. 343-386

초 록

많은 토목구조물의 기초로써 사용되는 말뚝 기초의 동적 거동을 예측하는 것은 매우 중요한데, 이는 말뚝 기초의 동적 거동이 그 자체의 거동뿐 아니라 구조물 전체의 거동에 커다란 영향을 미치기 때문이다. 이러한 말뚝 기초의 동적 거동을 평가하기 위한 방법은 크게 현장 조사, 실내 모형시험, 수치 모델링의 세 가지로 나누어볼 수 있다. 이 중 현장 조사는 지진에 의한 피해가 일어난 후에 수행되는 소극적 형태의 접근법이며, 최근 들어 실내 모형시험의 절차적, 경제적, 시간적인 한계점들로 인하여 수치 모델링 기법의 효율성이 더욱 중요시되고 있는 상황이다.

수치 모델링 기법을 적용하여 말뚝 기초의 동적 거동을 예측하고자 한 선행 연구들은 대부분 단순화 접근법을 이용하였다. 단순화 접근법은 절차가 비교적 간단하고 해석이 간편하다는 장점이 있으나 단순화 과정에서 발생하는 여러 가지 가정조건들로 인하여 정확하고 신뢰성 있는 결과를 기대하기 힘들다는 한계점을 가진다. 이에 대해 2차원 혹은 3차원 연속체 모델링은 계산 과정이 복잡하고 해석 시간이 오래 걸린다는 단점에도 불구하고 가장 직접적인 접근법이며, 적절한 모델링이 수행된다면 가장 정확하고 신뢰성 있는 결과를 얻을 수 있다. 따라서 본 연구에서는 3차원 연속체 모델링 기법을 사용하여 지진 시 지반-말뚝-구조물 동적 상호작용을 평가하고자 하였다.

원심모형시험 (Yoo, 2013) 에서 관측된 건조토 조건에서의 지반-말뚝-구조물 동적 상호작용을 모사하기 위하여 유한 차분법에 기초한 3차원 동적 수치 모델링이 수행되었다. 제안된 3차원 모델은 지반의 비선형

거동을 적절히 모사하기 위해 상용 유한 차분 프로그램인 FLAC3D를 이용하여 시간 영역에서 해석이 수행되었다. 모델링 방법론으로써 지반 구성 모델은 Mohr-Coulomb 모델을 적용하였으며 이력 감쇠 모델을 적용하여 지반의 비선형 거동을 모사하고자 하였다. 진동 중 지반과 말뚝 간의 미끄러짐 및 분리 현상을 모사할 수 있는 인터페이스 모델을 적용하였으며 인터페이스 강성은 탄성이론에 기초하여 결정되어, 내장 함수인 FISH를 통해 깊이 별로 입력되었다. 경계 조건의 경우에는 지반-말뚝 상호작용의 영향을 받는 근역 지반만 메쉬를 생성하고 근역 지반의 경계부에 원역 지반의 가속도-시간 이력을 입력하는 방식인 단순화 연속체 모델링 기법 (Kim, 2011)을 적용함으로써 해석 시간을 감소시키고자 하였다.

수치 해석의 오차를 최소화하고 결과의 신뢰성을 확보하기 위해, 원심모형시험 결과와 수치 해석 결과와의 비교를 통한 제안된 기법의 캘리브레이션이 수행되었다. 제안된 수치 모델로부터 계산된 말뚝 최대 휨 모멘트와 횡 방향 말뚝 최대 변위의 깊이 별 분포가 다양한 입력 하중 조건에서 실험 결과와 잘 일치하는 것을 확인하였다. 제안된 수치 모델의 적용성 평가를 위해 다른 실험 케이스의 결과와 수치 해석 결과와의 추가적인 비교가 수행되었다. 수치 해석으로부터 계산된 다양한 말뚝의 동적 응답이 다양한 입력 하중 조건에서 실험 결과를 적절히 모사하고 있는 것으로 나타났다. 이를 통하여 다양한 조건에서 제안된 수치 모델링 기법의 적용성이 검증되었다고 판단하였다. 제안된 수치 해석 기법의 적용성 평가를 토대로 다양한 조건에서의 말뚝 동적 거동을 조사하기 위하여 제안된 수치 모델을 이용한 매개변수 연구를 수행하였다. 이를 통하여 건조토 지반에 근입된 말뚝 기초의 동적 거동에 미치는 다양한 변수들의 영향을 평가하였으며, 기존의 연구결과와 매개변수 연구 결과를 비교함으로써 제안된 수치 모델링 기법의 적용성 및 신뢰성을 확인하였다.

원심모형시험 (Wilson, 1998) 에서 관측된 액상화 가능한 지반 조건에서의 지반-말뚝-구조물 동적 상호작용을 모사하기 위해 3차원 수치 모델링이 수행되었다. 액상화 시, 지반의 전단 변형으로 인해 야기되는 간극 수압의 발달을 모사하기 위해 Finn 모델을 적용하였다. Finn 모델은 유효응력 해석법을 이용한 액상화 모델의 하나로써 임의의 지점에서의 다양한 액상화 거동을 실시간으로 파악할 수 있다. Finn 모델은 건조토 조건에서 사용된 기존의 구성 모델에 결합되어 해석이 수행되었다.

건조토 조건에서와 마찬가지로 실험 결과와 수치 해석 결과와의 비교를 통한 제안된 기법의 캘리브레이션이 수행되었다. 수치 모델로부터 계산된 과잉 간극수압 비, 말뚝 휨 모멘트, 말뚝 두부 변위의 시간 이력이 실험 결과를 적절히 모사하고 있는 것으로 나타났다. 제안된 수치 모델의 적용성 평가를 위해 다른 실험 케이스와의 추가적인 비교를 수행한 결과, 수치 해석으로부터 계산된 다양한 말뚝의 동적 응답이 실험 결과를 대체로 잘 모사하고 있는 것으로 나타났다. 이를 통하여 제안된 수치 모델링 기법의 적용성이 검증되었다고 판단하였다. 다양한 조건에서의 말뚝의 동적 거동을 조사하기 위하여 제안된 기법을 이용한 매개변수 연구를 수행하였다. 이를 통하여 액상화 지반에 근입된 말뚝의 동적 거동에 미치는 여러 변수들의 영향을 평가하였으며 기존의 연구결과와 매개변수 연구 결과를 비교함으로써 제안된 수치 모델링 기법의 적용성 및 신뢰성을 다시 한번 확인하였다. 또한 건조토 조건에서의 결과와 비교 분석함으로써 다양한 조건에 알맞은 말뚝 기초 내진 설계의 방향을 제시하였다.

주요어: 수치 모델링, 지반-말뚝-구조물 동적 상호작용, 원심모형시험, 유한차분해석방법, 액상화

감사의 글

꿈에 그리던 대학생이 된다는 설렘을 안고 세상 물정 모르던 약관의 철부지가 상경하여 관악에 보금자리를 마련한지 10년, 드디어 박사 졸업이라는 열매를 맺으며 유종의 미를 거두게 되었다고 생각하니 감회가 새롭습니다. 저의 20대를 오롯이 함께한 관악이니만큼 이곳을 떠날 때가 다가왔다는 사실이 실감이 나지 않습니다. 서울대학교에 입학하여 새내기 생활을 하고 학사 졸업, 대학원 입학, 석, 박사 통합 과정으로 박사 졸업에 이르기까지 생각해보면 참 많은 일들이 있었고 많은 좋은 사람들과 함께 했기에 돌이켜보면 정말 행복했던 시간이었던 것 같습니다. 특별히 잘난 구석도 없는 제가 이렇게 무사히 학위 과정을 밟고, 박사 졸업에 이를 수 있었던 데에는 무엇보다 그 과정에서 만나게 되었던 많은 사람들의 도움이 있었기 때문이라고 생각합니다. 제 졸업 논문의 마지막 페이지는 이와 같은 고마운 분들에 대한 마음을 전하는 것으로 할애하고자 합니다.

가장 먼저 부모님께 감사 드리는 마음을 전하고 싶습니다. 어려서부터 밖에서 뛰어 놀기 좋아하고 책상 앞 보다는 운동장을 즐겨 찾던 저를 물심양면으로 지원해주시고 아낌 없는 사랑을 주셔서 정말 감사합니다. 제가 표현이 서툰 무뚝뚝한 아들이라 직접적으로 마음을 전한 기억이 드물지만 언제나 부모님에 대한 감사의 마음을 갖고 있습니다. 언제나 제 편인 부모님께서 든든히 계시기에 학업에 집중할 수 있었고 행복한 졸업을 맞이할 수 있는 것 같습니다. 아버지, 어머니, 사랑합니다. 그리고 내 동생들 선준이와 선우. 둘 다 공부도 열심히, 놀 때도 열심히 해서 나중에 삼형제가 지금까지 받은 부모님의 사랑을 조금이라도 갚을 수 있는 든든한 아들들이 되었으면 한다. 모두 파이팅.

다음으로 학부 및 대학원 생활 동안 큰 가르침을 주신 교수님들께

감사 드리는 마음을 전하고 싶습니다. 먼저 저의 지도교수님이시자, 지반연구실의 큰 어른이신 김명모 교수님께 감사 드립니다. 학부 수업을 통해서도 물론이고, 대학원 생활 6년을 관통하여 학업적으로 그리고 인간적으로 너무도 많은 가르침을 받았고 교수님의 박사 제자가 된 것을 큰 영광으로 생각합니다. 앞으로 더욱 노력하여 자랑스러운 제자가 되도록 최선을 다하겠습니다. 늘 세심한 관심과 배려로 연구실 원들을 살뜰히 챙기시는 정충기 교수님께도 감사 드립니다. 어느 지도교수님의 학생이건 관계 없이 관심 가져주시고 가깝게 지내려고 노력하시며 연구에 있어서는 따끔한 조언도 아끼지 않으시는 모습, 본받도록 노력하겠습니다. 참신한 주제와 창의적인 시각으로 연구실 원들의 시야를 넓혀주시는 박준범 교수님께도 감사 드립니다. 학생들이 수업에 적극적으로 참여하게 함으로써 활기찬 수업 분위기를 만들어 주시고 늘 현재와 미래의 이슈에 주목하시어 연구에 대한 새로운 시각을 갖게 해주시며 회식 자리에서는 뛰어난 위트와 입담으로 즐겁게 해주셨습니다. 사회에 나가서도 세 분 교수님께 감사 드리는 마음 잊지 않고 늘 가슴에 새기도록 하겠습니다. 더불어 바쁘신 가운데서도 제 학위 논문 심사를 맡아 신경 많이 써주신 삼성 물산의 황대진 상무님께도 정말 감사드립니다.

다음으로 동고동락했던 많은 연구실 선후배 및 동기들에게 감사한다는 말 전하고 싶습니다. 학교 정문에 '두 딸의 아버지' 라는 타이틀을 잠시 걸어두고 까마득한 후배들과 친구처럼 지내시는 진태형, 때로는 엄하게 때로는 자상하게 후배들을 챙기시는 성준형, 저의 첫 사수로서 박사과정이 연구에 임해야 하는 태도를 알게 해준 의규형, 연구실의 살림꾼으로 후배들이 항상 의지하게 되는 정인형, 마지막 사수이자 논문 심사위원이신 잘돼서 정말 보기 좋은, 광헌형이랑 같이 술 한잔 해야 하는 김사무관 성환형, 여자 좋아하고 술 좋아하고 철없는 형이지만 연구에 있어서

만큼은 진지한 면모를 보이는 민택형, 언제나 티격태격하지만 가장 편한 친구고 앞으로 열심히 해서 무사히 졸업할거라고 믿는 석중, 군인이시지만 언제나 편하게 대해주셨던 기상형, 언제나 연구에 대한 열정이 샘솟는 듯한 현욱형, 본인 결혼식의 축가를 멋들어지게 불렀던 호덕형, 04학번 최고의 성실 모범남으로 앞으로 결혼 생활은 물론이고 유학 생활도 잘 할거라고 믿어 의심치 않는 선홍, 해군 에이스로 지반 연구실의 미들 필드를 휘저으셨던 태양형, 언제나 취해있는 것 같았던 오바쿠스 만교형, 첫 후배 성헌, 연구실와서 진정한 상남자가 된 석형형, 불곰같은 외모로 시크릿 춤을 귀엽게 추던 세환형, 얼굴로 사기치는 합창단 기린 인우형, 김교수님 쪽 마지막 석사로서 많은 즐거운 시간들을 함께했던 도스크 은수 모두 감사합니다.

어리 바리했던 석사 신입생 시절 39동에서 아마 많이 답답하셨을 천틀러 성호형, 서현 누나, 용성형, 술 많이 사주셨던 상인형, 타짜 태균형, 왁스 바르고 음미대 갔던 진현형, 가장 신세 많이 졌고 지금 이순간 가장 보고 싶은 광헌형, 엄격하게 후배들을 이끌어주셨던 성수형, 418의 중흥기를 함께 했던 의룡형, 졸업 준비하며 여러모로 힘이 많이 되었던 윤식형 감사합니다. 모래알 같은 조직력을 자랑하지만 은근히 의지하며 지낸 04학번 박사과정 동기들 준영, 가현, 한샘, 희수, 현진, 고생들 많이 했지만 결국 다 잘된 후배이자 형 혹은 친구들인 준현형, 승호형, 은협형, 의석형, 병곤형, 진우형, 용우, 승훈형, 재욱형, 희수, 남규, 소피아, 아마라, 지영이, 418 스타를 이끌었던 noun을 참 좋아하는 참뜻, 같은 방에서 석사 2년을 보낸 418의 마스코트 양덕, 불굴의 다이어트로 날씬녀가 된 지영, 감사합니다.

현재 그리고 미래의 지반연구실을 이끌어갈 기둥인 연구실 재학생 후배들에게도 고맙다는 말 전하고 싶습니다. 한 때 GMO를 먹여살렸던

각종 게임에 강한 민기, 불의를 참지 못하는 알고 보니 호구왕 태영, 먹방의 왕이지만 이젠 건강을 위해 다이어트가 필요할 것 같은 승환, 본의 아니게 멸망의 금요일을 함께하게 돼 미안한 상래, 깐족의 왕이지만 의외로 지고지순한 정준, 힘들었던 대학원 적응기를 마치고 연구실에서 일과 th卜랑 th卜랑과 일을 모두 쟁취한 성하, 눈치 없다고 구박받지만 은근히 속 깊은 종찬, 여러모로 많이 챙겨준 고마운 슬기에게도 감사하다는 말 전하고 싶습니다. 바쁜 회사 생활 가운데서도 학위 하시고 후배들도 잊지 않고 챙겨주시는 파트 타임 기훈형, 주형형, 경석형, 승우형, 윤섭형, 명준형, 재현형, 창원형, 진철형, 허건형님께도 감사드립니다.

자주는 못 보지만 가끔 만날 때마다 정말 반가운 지환시 04 C반 동기들, 서고 동기동창 민석, 형민, 우현, 순형, 세진, 성수, 철호 올 연말에도 뭉치자. 중학교부터 함께한 오랜 벗 승백, 성복, 재현 등 갈마중 친구들, 우리도 곧 봐야지? 이외에 실험 관련해서 많은 도움을 줬던 카이스트의 세현형, 남룡형, 성배, 수린이, 정곤이, 재현이, 형익이에게도 감사한다는 말 전하고 싶습니다. 모두 정말 감사드립니다.